
CONTENTS

Declaration	i
Acknowledgements	iii
Abstract	xiv
1 Introduction	1
2 Mathematical preliminaries	7
2.1 Continuous-time dynamical systems	7
2.1.1 Stability of dynamical systems	8
2.1.2 Lyapunov function	11
2.2 Reproduction threshold	13
2.2.1 Next generation operator method	14
2.3 Bifurcations	16
2.3.1 Backward bifurcation	16
2.3.2 Hopf bifurcation	18
2.4 Discrete-time dynamical systems	20
2.4.1 Jury stability criterion	22
2.5 Nonstandard finite difference method	23

3	SIS Model	25
3.1	Introduction	25
3.2	SIS model without time delay	27
3.3	SIS model with discrete time delay	32
3.3.1	Basic properties of continuous-time delayed system . .	32
3.4	Towards the construction of NSFD scheme for delayed SIS model	45
3.4.1	Main setting	45
3.4.2	Combined exact and theta-NSFD schemes	49
3.4.3	Dynamic consistency of the NSFD scheme	57
3.4.4	Numerical simulations	68
3.4.5	NSFD scheme for SIS delay model	71
4	Modeling transmission dynamics of BTB-MTB in human- buffalo population	79
4.1	Introduction	79
4.2	Basic SEIR model for TB	81
4.3	A model for TB with exogenous reinfection	84
4.4	A model for TB with exogenous reinfection and two stage exposed classes	85
4.5	The model of tuberculosis in human-African buffalo population	87
4.5.1	Model formulation	87
4.5.2	Analysis of buffalo-only model	96
4.5.3	Asymptotic stability of disease free equilibrium (DFE)	99
4.5.3.1	Local asymptotic stability	99
4.5.3.2	Global asymptotic stability of the DFE	108
4.5.4	Existence of endemic equilibria: Special case	110
4.5.4.1	Global asymptotic stability of endemic equi- librium	111
4.5.5	Sensitivity and uncertainty analyses	115
4.6	Analysis of the BTB-MTB model	121
4.6.1	Local stability of DFE	121
4.6.2	Global asymptotic stability of DFE	123
4.6.3	Numerical simulations	125
4.6.3.1	Effect of BTB on MTB	126

4.6.3.2	Effect of MTB on BTB	126
5	Conclusion and Future Work	131
5.1	Contributions of the thesis	132
5.1.1	Nonstandard finite difference for SIS delay model . . .	132
5.1.2	Mathematical modeling of BTB-MTB dynamics	133
5.2	Future work	136
	Bibliography	137

LIST OF FIGURES

2.1	Backward bifurcation diagram.	17
3.1	Schematic diagram of an SIS model.	28
3.2	Approximation of the delay term $x(t_n - \tau)$	52
3.3	Simulations of the NSFD scheme (3.4.26) for $A = -0.7$, $B = -1.3$, $\tau = 2$, in (a) $\theta = 0$ and (b) $\theta = 1/2$, while in (c) NSFD (3.4.26) and (d) Euler schemes, without delay.	70
3.4	Simulations with values of $A = -0.7$, $B = -1.3$ and $\tau = 2$: (a) Euler scheme and (b) Trapezoidal rule.	71
3.5	Simulations with $A = -13$, $B = 7$, $\tau = 10$; of (a) Combined exact-NSFD scheme (3.4.26), with $\Delta t = 10$, $\theta = 0$ (b) Euler scheme, $\Delta t = 0.11$ (c) the NSFD scheme (3.4.26), illustrating positivity of solution (Theorem 3.4.7).	72
3.6	Simulations showing the roots of the characteristic polynomial for (3.4.32) within unit circles corresponding to values of $m = 0, 1, 2, \dots, 1000$ (different values of Δt), $\tau = 2$, $A = -1.3$, $B = -1.7$ in (a) $\theta = 0$, (b) $\theta = 1/2$	73

3.7	Simulations showing the roots of the characteristic polynomial for (3.4.32) within unit circles corresponding to values of $m = 0, 1, 2, \dots, 1000$ (different values of Δt), $\tau = 0.54$, $A = 1.3$, $B = -1.7$ in (c) $\theta = 0$, (d) $\theta = 1/2$	73
3.8	Simulations showing the roots of the characteristic polynomial for (3.4.32) within unit circles corresponding to values of $m = 0, 1, 2, \dots, 1000$ (different values of Δt), $\theta = 1$, in (a) $\tau = 0.54$, $A = 1.3$, $B = -1.7$ in (b) $\tau = 2$, $A = -1.3$, $B = -1.7$	74
3.9	Simulations for NSFD scheme (3.4.41) using $\tau = 5.1$, $B = 0.31$; in (a) $\theta = 0$ (b) $\theta = 1/2$	75
3.10	Numerical simulations For $\tau = 5.1$ and $B = 0.31$: using (a) the Euler scheme (b) Trapezoidal rule.	75
3.11	Simulations for NSFD scheme (3.4.48) in (a) $h = 4$, $\beta = 0.021$ (b) $h = 12$, $\beta = 0.17$ for Endemic fixed point.	77
3.12	Simulations of NSFD scheme (3.4.48) for (a) $h = 4$, $\beta = 0.014$, (b) $h = 12$, $\beta = 0.16$	78
4.1	Demographic map of Kruger National Park and African buffaloes [89].	82
4.2	Schematic diagram of the BTB-MTB model (4.5.3).	93
4.3	Data fit of the simulation of the buffalo-only model (4.5.4), using data obtained from South Africa's Kruger National Park (Table 4.4) [28]. Parameter values used are as given in Table 4.3.	100
4.4	Simulations of the buffalo-only model (4.5.7), showing the total number of infected buffaloes with clinical symptoms of BTB ($I_{BB}(t)$) at time t as a function of time. Parameter values used are as given in Table 4.3 with (A) $\beta_B = 0.00733$ (so that, $\mathcal{R}_0 = 0.7036 < 1$) and (B) $\beta_B = 0.0733$, $\delta_B = 0$ (so that, $\tilde{\mathcal{R}}_0 = 8.6050 > 1$).	102
4.5	Box plot of \mathcal{R}_0 as a function of the number of LHS runs carried out for the buffalo-only model (4.5.4), using parameter values and ranges given in Table 3.	116

4.6	PRCC values of the parameters of the buffalo-only model (4.5.4), using \mathcal{R}_0 as the output function. Parameter values used are as given in Table 4.3.	117
4.7	Box plot of the total number of symptomatic buffalos ($I_{BB} + I_{MB}$) as a function of the number of LHS runs for the buffalo-only model (4.5.4), using parameter values and ranges given in Table 3.	119
4.8	PRCC values of the parameters of the buffalo-only model (4.5.4), using total number of symptomatic buffalos ($I_{BB} + I_{MB}$) as the output function. Parameter values used are as given in Table 4.3.	120
4.9	Cumulative number of new cases of (A) MTB infection in humans. (B) BTB infection in buffalos. Parameter values used are as given in Table 4.3, with various values of θ_{MM} (A) or θ_{HH} (B).	127

LIST OF TABLES

4.1	Description of the variables of the BTB-MTB model (4.5.3). . .	94
4.2	Description of parameters of the BTB-MTB model (4.5.3). . .	128
4.3	Ranges and baseline values for parameters of the BTB-MTB model (4.5.3).	129
4.4	Number of symptomatic buffalos with BTB at Kruger Na- tional Park [28].	130

Glossary

Abbreviation	Meaning
BTB	Bovine tuberculosis
DDE	Delay differential equation
DFE	Disease-free equilibrium
CE	Christian era
EE	Endemic equilibrium
GAS	Globally asymptotically stable
LAS	Locally asymptotically stable
LDDE	Linear delay differential equation
LHS	Latin hypercube sampling
MTB	Mycobacterium tuberculosis
MSEIR	Maternal susceptible exposed infective recovered
MSEIRS	Maternal susceptible exposed infective recovered susceptible
MSEIS	Maternal susceptible exposed infective susceptible
NSFD	Nonstandard finite difference
ODE	Ordinary differential equation
PRCC	Partial correlation coefficient
SEIR	Susceptible exposed infective recovered
SEIT	Susceptible exposed infective treated
SIS	Susceptible infective susceptible
TB	Tuberculosis

Title	Dynamics and reliable numerics for some epidemic models with and without delay
Name	Adamu Shitu Hassan
Supervisor	Prof. Jean M.-S. Lubuma
Co-Supervisors	Dr. Salisu M. Garba and Prof. Abba B. Gumel
Department	Mathematics and Applied Mathematics
Degree	Philosophiae Doctor

Abstract

The thesis addresses two main problems. The first is that of designing reliable numerical method for approximating an SIS (susceptible-infected-susceptible) disease transmission model with discrete time delay. This is achieved by using the theory and methodology of nonstandard finite difference discretization which leads to a novel and robust numerical methods which, unlike many other standard numerical integrators, were shown to be dynamically consistent with the continuous delay SIS model.

The second problem is the mathematical modeling of the transmission dynamics of *bovine* and *mycobacterium* tuberculosis in a human-buffalo population. The buffalo-only component of the resulting deterministic model undergo the phenomenon of backward bifurcation, due to the re-infection of exposed and recovered buffalos. Furthermore, this sub-model has a unique endemic equilibrium point which is shown to be globally asymptotically stable for a special case, whenever the associated reproduction number exceeds unity. Uncertainty and sensitivity analyses, using data relevant to the dynamics of the two diseases in the Kruger National Park, South Africa, show that the distribution of the associated reproduction number is less than unity (hence, the diseases would not persist in the community). Crucial parameters that influence the dynamics of the two diseases are also identified. The human-buffalo model exhibit the same qualitative dynamics as the sub-model with respect to the local and global asymptotic stability of their respective disease free equilibrium, as well as the backward bifurcation phenomenon.



Numerical simulations for the human-buffalo model show that the cumulative number of mycobacterium tuberculosis cases in humans (buffalos) decreases with increasing number of bovine tuberculosis infections in humans (buffalos).

CHAPTER 1

INTRODUCTION

Epidemics of infectious diseases have historically, induced devastating public health and socio-economic burden on human populations. For instance, between 1345 - 1351 CE, the Black Death (bubonic (plague)) struck Central Asia and Europe, killing one-third of the population (24 million) and 40 million people worldwide [85]. Furthermore, since its inception in the 1980s, the Human Immunodeficiency Virus (HIV), the causative agent of Acquired Immune Deficiency Syndrome (AIDS), caused over 39 million fatalities (and about 35 million currently live with the disease globally). Most of the AIDS-related fatalities are in low- and middle-income countries, particularly in sub-saharan Africa [88]. Several other infectious diseases, such as Tuberculosis (TB), Malaria, Ebola and Cholera, have emerged and reemerged causing severe socio-economic and public health burden in affected areas/regions. In order to get deep insight into the types, spread and possible control strategies of infectious diseases, Epidemiologists conduct scientific experiments, sometimes with controlled settings using self-experimentation. However, designing such controlled experiments is often difficult or impossible based on ethical issues and possible erroneous data collection [17, 85]. These reasons motivate the possibility of using mathematical modeling and analysis as tools to substantiate the perception of disease transmission, testing theories, and

suggesting better intervention strategies.

The concept of modeling for infectious diseases dates back to work of Daniel Bernoulli, a public health physician who used statistical modeling to analyze the potential impact of Smallpox vaccine in the 18th century [94]. Subsequently, the framework for epidemic modeling was developed in the 20th century by other public health physicians such as Sir Ronald Ross, Hamer and Kermack-Mckendrick [3, 55, 56, 68]. In particular, the Kermack-Mckendrick compartmental modeling approach [68] laid the foundation for modeling the spread of infectious diseases was amongst the early models that excel in mathematical epidemiology. In such Kermack-Mckendrick type compartmental models, the population being studied is mainly sub-divided into three mutually-exclusive compartments (classes), based on disease status: susceptible, S ; infective (infectious), I ; and removed (recovered), R ; individuals. The transition between these compartments is governed by the development of infection and the assumed waiting times in each compartment.

As observed by Hale [51], in many applications, one assumes that the system under consideration is governed by a principle of causality. That is, the future state of the system is independent of the past states, and is determined solely by the present. However, under closer scrutiny, it becomes apparent that the principle of causality is often only a first approximation to the true situation and that a more realistic model would include some of the past states of the system [51]. An example is the case of the predator-prey models studied by Volterra in 1930, using the concepts of delay differential equations (DDE) [112]. This is also the case for biological systems in general, and infectious diseases in particular, as they (typically) exhibit time lapse (delay) in both transmission and progression of the disease. To be more explicit, time delay can be used to describe any of the following three situations [61]:

- (a) **Delay as latent or incubation period:** This is a time delay in which individual exposed to certain infectious disease can be infective but become fully infectious after the elapse of the time as considered in [25, 59, 77, 104].

- (b) **Delay as maturation time:** Maturation delay is the time lapse associated with stage development of an organism before it can spread diseases, for instance, in vector-borne diseases, see [23, 37, 86].
- (c) **Delay as waning time of immunity:** The delay in this case is the time from the loss of immunity by recovered individual to the time of re-infection, as studied in [101, 114].

In epidemiology, time delay can be considered in two different forms. The first approach is to introduce an additional exposed compartment in which individuals stay before becoming infectious. In its simplest form, the second approach is to assume that there is constant waiting time τ for an individual to become infectious at time t from the past history $t - \tau$. Based on this transition, several epidemiological models have been formulated by adding other compartments such as infants passive (maternal) immunity M and exposed E classes resulting in Kermack-Mckendrick models of type SIRS, MSEIS, MSEIR, MSEIRS etc [55].

This thesis focuses on the two ways of introducing delay. The first is associated with the formulation, analysis and numerical discretization of the SIS model with (discrete) time delay. Although this model seems to be simple, its explicit solution cannot be determined. Furthermore, finding effective/efficient numerical solutions for systems of differential equations with time delay is quite challenging as noted in [9, 35, 76]. Thus, the objectives of this thesis in this direction are:

- (1) To carry out a rigorous qualitative and quantitative analysis of the SIS model with discrete time delay, a study which is highly relevant considering the fact that results are scattered in the literature [58, 59, 91, 108].
- (2) To design and analyze novel and reliable nonstandard finite difference (NSFD) scheme which replicate the realistic dynamical behaviour of linear delay differential equations and SIS models with delay.

Another main objective is to design models for the transmission dynamics of bovine tuberculosis (BTB) and mycobacterium tuberculosis (MTB) in a

human-buffalo population. More precisely, detailed quantitative, qualitative and statistical analyses of the resulting BTB-MTB will be carried out. Our models are gradually built up from the standard SEIR model in the following steps:

- (3) Considering the recovered/removed compartment (R) as a class of treated individuals (T), the spread of the BTB disease in African Buffalos is modeled using simple SEIT system [20, 46].
- (4) The SEIT model in (3) is extended to include the reinfection of exposed buffalos [38].
- (5) The extended SEIT model with reinfection is further extended to include the dynamics of early and advanced exposed buffalos [2, 20].
- (6) The model in (5) above is further refined to allow for the transmission of both diseases (BTB and MTB) in the buffalo-human population.

The results in Item (2) above are new and published in [44]. The models in Items (5) and (6) are new, as reported in [52].

The rest of the thesis is organized as follows: In Chapter 2, the main mathematical theories and techniques used in the thesis are briefly described. For instance fixed-point theorems, as presented in [51, 102], are applied to establish the well-posedness of the models designed in the thesis. This, together with Gronwall inequality [102], and the method of integrating factor, are employed to prove positivity and boundedness of solutions on associated initial data. The Hartman-Grobman theorem [116], together with its extension in [11, 24] for DDE and the next generation method [107], are used to prove the local asymptotic stability (LAS) property of associated equilibria for the disease transmission models presented in the thesis. Furthermore, the LaSalle's Invariance Principle [70], in conjunction with Lyapunov function theory [116], are employed to prove global asymptotic stability (GAS) of some equilibria.

Lagrange interpolation polynomials are used to approximate the delay term, and the Jury's condition is used to prove the local stability of the fixed points of the associated finite difference schemes. Furthermore, we use the

NSFD method to reliably replicate the dynamics of the continuous-time delay differential equation system, based on the following Mickens' Rules [80]:

- (i) The standard denominator, $\Delta t > 0$, of the discrete derivatives, is replaced by a more general function $\phi(\Delta t)$, which satisfies the requirement $\phi(\Delta t) = \Delta t + \mathcal{O}(\Delta t^2)$.
- (ii) Nonlinear terms in the right-hand sides of the model equation are approximated in a non-local manner, by using multiple mesh points.

For instance, in the linear delay model and the SIS model considered, these rules are implemented for approximating the involved variables at discrete time $t_n = n\Delta t$, where $n \in \mathbb{N}$ and Δt is the time-step as follows:

- The derivative $\frac{dI(t)}{dt}$ is approximated by $\frac{I_{n+1}-I_n}{\phi(\Delta t)}$ instead of $\frac{I_{n+1}-I_n}{\Delta t}$, where the denominator function $\phi(\Delta t)$ captures the dynamics of the model, and $I_n = I(t_n)$.
- The delay term, $I(t_n - \tau)$, is approximated by $P(t_n - \tau)$, where $P(t)$ is the Lagrange interpolation polynomial of degree 1 at suitable node points.
- The nonlinear term, $S(t_n)I(t_n)$, is approximated by $S_{n+1}I_n$, instead of S_nI_n .

Chapter 3 deals with the qualitative analysis, and construction of reliable numerical method, for the SIS model with discrete time delay. First, the basic dynamical properties, and NSFD schemes for the SIS non-delayed model, are reviewed [73, 83, 119]. The well-posedness and asymptotic stability of the associated equilibria of the SIS delay model are established. Using an innovative strategy of approximating the delay term via the Lagrange interpolation polynomial, robust NSFD schemes that replicates the basic properties of the continuous model are gradually constructed and discussed. The dynamical consistency of the NSFD scheme is established by combining both the rigorous approach (see Theorem 3.4.5, Theorem 3.4.6 and Theorem 3.4.7) and the numerical simulations. The new theoretical results obtained are illustrated numerically (using appropriate parameter and initial values). The NSFD

schemes developed in this chapter constitute a major contribution to the numerical solution of DDE which is reported to be challenging in [9, 35, 76].

Chapter 4 addresses the problem of modeling the dynamics of bovine and mycobacterium tuberculosis in a human-buffalo population. A novel model is constructed for this purpose. It is shown that both the BTB-only and the BTB-MTB model exhibit the same qualitative dynamics with respect to the local and global asymptotic stability of their respective disease-free equilibria. More importantly, unlike other BTB, MTB models, these two new models are shown to exhibit the phenomenon of backward bifurcation (which play a major role on the persistence or effective control of the two diseases, when the associated reproduction number is less than unity). Similarly, the two models have unique endemic equilibria, which are globally asymptotically stable for special cases, when the reproduction number exceeds unity. Using relevant data from Kruger National Park, South Africa, uncertainty and sensitivity analyses are carried out to determine the dominant parameters that affect the transmission dynamics of both diseases. Numerical simulations, using MATLAB ODE45, are conducted to illustrate the theoretical results obtained in the thesis, as well as to assess the burden of the two diseases in the buffalo-human population.

The main contributions of the thesis (in terms of modeling, mathematical analysis and contributions to public health), as well as directions for future work, are summarized in Chapter 5.

CHAPTER 2

MATHEMATICAL PRELIMINARIES

This chapter presents the main concepts used in the thesis which are mostly taken from [102] and [116], in accordance with the presentations in the theses [66, 95, 103].

2.1 Continuous-time dynamical systems

Consider the following p -dimensional initial value problem (IVP)

$$\frac{dx}{dt} = x' = f(x), \quad x(0) = x_0 \in \mathbb{R}^p, \quad (2.1.1)$$

where $x = x(t)$, $f \in C(\mathbb{R}^p, \mathbb{R}^p)$ and $x(0) = x_0$ is a vector of initial conditions. Furthermore, let the subset $\Omega \subseteq \mathbb{R}^p$.

Definition 2.1.1 *System (2.1.1) is said to define a dynamical system on a set $\Omega \subseteq \mathbb{R}^p$ if, for every $x_0 \in \Omega$, there exists a unique solution of (2.1.1) which is defined for all $t \in [0, \infty)$ and remaining in Ω for all $t \in [0, \infty)$.*

Definition 2.1.2 *A function $f : \mathbb{R}^p \rightarrow \mathbb{R}^p$ is said to be Lipschitz on $\Omega \subset \mathbb{R}^p$ with lipschitz constant $L \geq 0$ if*

$$\|f(x) - f(y)\| \leq L\|x - y\| \quad \forall x, y \in \Omega.$$

Here, $||\cdot||$ denotes the Euclidean norm in \mathbb{R}^p . If f is lipschitz on \mathbb{R}^p , then f is said to be globally lipschitz. While if f is lipschitz on every bounded subset of \mathbb{R}^p , then f is said to be locally lipschitz. When $0 \leq L < 1$, f is called a contraction and there is exactly one equilibrium point $x \in \Omega$ such that $x = f(x)$.

Theorem 2.1.1 *Let f be globally Lipschitz. Then (2.1.1) defines a dynamical system on \mathbb{R}^p .*

Realistically, when f is locally Lipschitz, a global existence result can be obtained under some a priori estimate as stated in the following classical result.

Theorem 2.1.2 *Let $f : \mathbb{R}^p \rightarrow \mathbb{R}^p$ be Lipschitz on the ϵ -neighborhood $N(\Omega, \epsilon)$, where $\Omega \subset \mathbb{R}^p$ is bounded. If for any $x_0 \in \Omega$, the solution $x(t)$ of (2.1.1) satisfies $x(t) \in \Omega$ for each $t \geq 0$ where the solution exists, then (2.1.1) defines a dynamical system on Ω .*

The Gronwall Lemma is used, among other things, to show that a given dynamical system is continuous with respect to the associated initial data.

Theorem 2.1.3 (Gronwall Lemma) *Let $z(t)$ satisfy*

$$z_t \leq az + b, \quad z(0) = z_0,$$

for constants a, b . Then for $t \geq 0$

$$z(t) \leq e^{at} z_0 + \frac{b}{a}(e^{at} - 1), \quad a \neq 0$$

and

$$z(t) \leq z_0 + bt, \quad a = 0.$$

2.1.1 Stability of dynamical systems

Definition 2.1.3 (Evolution Semigroup) *For a dynamical system on Ω , we define its evolution semigroup operator (solution map or flow map) to be the map $\Phi_t : \Omega \rightarrow \Omega$ such that the solution of the system (2.1.1) $u(t) = \Phi_t u_0$ or $\Phi_t(u_0) = x(t; u_0)$. That is, Φ_t maps the initial data u_0 to the solution at time t .*

The terminology semigroup for the evolution operator Φ is motivated by the following properties:

- (a) For any $s, t > 0$, $\Phi_{(t+s)} = \Phi_t \Phi_s = \Phi_s \Phi_t$,
- (b) For $t = 0$, $\Phi(0) = I$, the identity operator.

Definition 2.1.4 A point $\bar{x} \in \mathbb{R}^p$ such that $f(\bar{x}) = 0$ is called an equilibrium point (steady-state solution or critical point) of equation (2.1.1).

Definition 2.1.5 An equilibrium point \bar{x} of the dynamical system (2.1.1) is said to be:

- (1.) Stable if for any $\epsilon > 0$ there exists $\delta = \delta(\epsilon) > 0$ such that if $x(0) \in \Omega(\bar{x}, \delta)$ then $x(t) \in \Omega(\bar{x}, \epsilon)$ for all $t \geq 0$.
Equivalently, for all $x(0) \in \mathbb{R}^p$ if

$$\|x(0) - \bar{x}\| \leq \delta \text{ then } \|x(t) - \bar{x}\| \leq \epsilon \text{ for all } t \geq 0$$

.

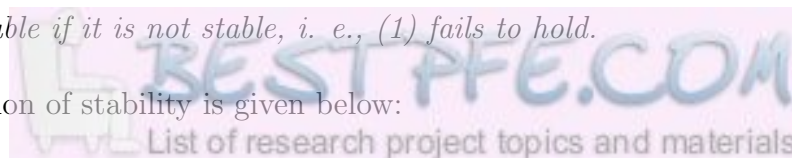
- (2.) Locally attractive if $\|x(t) - \bar{x}\| \rightarrow 0$ as $t \rightarrow \infty$ for all $\|x(0) - \bar{x}\|$ sufficiently small.
- (3.) LAS if \bar{x} is stable and locally attractive. For an asymptotically stable equilibrium point \bar{x} of (2.1.1), the set of all initial data $x(0) = x_0$ such that

$$\lim_{t \rightarrow \infty} \Phi_t(x_0) = \bar{x}$$

is said to be the basin of attraction of \bar{x} .

- (4.) Globally attractive if (2) holds for any $x(0) \in \Omega$ i.e. the basin of attraction of \bar{x} is Ω .
- (5.) GAS if (1) and (4) hold.
- (6.) Unstable if it is not stable, i. e., (1) fails to hold.

Interpretation of stability is given below:



Remark 2.1.1 *An equilibrium point \bar{x} is stable if the dynamical system can be forced to remain in any neighbourhood of \bar{x} by appropriate choice of initial condition. It is asymptotically stable if, in addition, any solution starting near the steady state approaches it as $t \rightarrow \infty$. Thus, the basin of attraction of an asymptotically stable equilibrium point includes a neighbourhood of the equilibrium.*

Definition 2.1.6 *A function $p(t) \in C^1(\mathbb{R}, \mathbb{R}^p)$ is a periodic solution of (2.1.1) with period T if $p_t = f(p(t))$, $p(t) = p(t + T)$ for all $t \in \mathbb{R}$, and $p(t) \neq p(t + s)$ for all $s \in (0, T)$.*

Theorem 2.1.4 *(Stability for Linear Ordinary Differential Equations) Consider the differential equation*

$$x' = Ax, \quad (2.1.2)$$

where A is a $p \times p$ matrix and prime, represents differentiation with respect to time. Let A have eigenvalues $\{\lambda_i\}_{i=1}^l$, $l \leq p$. Then

- (i) *The origin is asymptotically stable if and only if $\text{Re}(\lambda_i) < 0$ for all i .*
- (ii) *If $\text{Re}(\lambda_i) \leq 0$ for all i , and those eigenvalues with $\text{Re}(\lambda_i) = 0$ are non-defective (λ has multiplicity $k \leq 1$, $k = 0, 1, \dots$), then the origin is stable.*

Definitions 2.1.5 cannot easily be used in practice. Fortunately, the method of linearization permits to reduce the analysis to the user-friendly Theorem 2.1.4. The simplest natural way to proceed would have been to replace the system (2.1.1) by its linearized system. The starting point is the following definition :

Definition 2.1.7 *Let $x = \bar{x}$, $x \in \mathbb{R}^p$. Then \bar{x} is called a hyperbolic equilibrium point if none of the eigenvalues of $Jf(\bar{x})$ (the Jacobian matrix of f at \bar{x}) have zero real part.*

The linearized form of (2.1.1), near \bar{x} , is given by

$$u' = Ju, \quad (2.1.3)$$

where f is assumed to be of class C^1 .

Theorem 2.1.5 (*Hartman-Grobman Theorem*) Assume that f in (2.1.1) is of class C^1 and consider a hyperbolic equilibrium point \bar{x} of the dynamical system defined by (2.1.1). Then, there exist $\delta > 0$, a neighborhood $N \in \mathbb{R}^p$ of the origin and a homeomorphism h from the ball $\mathcal{B} = \{x \in \mathbb{R}^p : \|x - \bar{x}\| < \delta\}$ onto N such that

$$u(t) := h(x(t)) \text{ solves (2.1.3) if and only if } x(t) \text{ solves (2.1.1).}$$

Theorem 2.1.5 states that the behavior as $t \rightarrow \infty$ of solution $x(t)$ of (2.1.1) near an equilibrium point \bar{x} is the same as the behavior of solution $u(t)$ of its linearization $Jf(\bar{x})$ near the origin. This observation leads us to the following result.

2.1.2 Lyapunov function

Definition 2.1.8 Let the system (2.1.1) define a dynamical system on an open subset $\Omega \subset \mathbb{R}^p$ and $\bar{x} \in \Omega$ an equilibrium point. A function $V \in C^1(\Omega, \mathbb{R})$ is called a Lyapunov function of the system (2.1.1) for \bar{x} on a neighborhood $\mathcal{B} \subset \Omega$ of \bar{x} provided that

$$\dot{V}(x) := \lim_{h \rightarrow 0} \frac{V(x + hf(x)) - V(x)}{h} = \nabla V(x) \cdot f(x) \leq 0, \quad \forall x \in \mathcal{B}, \quad (2.1.4)$$

where $\dot{V}(x)$ is the directional derivative of V in the direction of f . If in addition, $V(\bar{x}) = 0$ and $V(x) > 0$ for all $x \in \mathcal{B} \setminus \{\bar{x}\}$, then V is said to be a positive definite Lyapunov function at \bar{x} .

If $x = x(t)$ is a solution of (2.1.1), applying the chain rule on $V(x(t))$, we have

$$\begin{aligned} \frac{d}{dt} V(x(t)) &= \sum_{i=1}^p \frac{\partial V(x(t))}{\partial x_i} \cdot \frac{dx_i(t)}{dt}, \\ &= \nabla V \cdot f(x), \\ &= \dot{V}(x(t)). \end{aligned} \quad (2.1.5)$$

The Equation (2.1.5) reveals the reason why \dot{V} is sometimes called “the derivative along the trajectories” and one can get information about V without prior knowledge about the solutions.

The method of Lyapunov can be applied whenever the linearization approach is not conclusive, i.e. when some eigenvalues are purely imaginary.

Theorem 2.1.6 *If there exists a positive definite Lyapunov function V of the dynamical system (2.1.1) on a neighborhood \mathcal{B} of an equilibrium point \bar{x} then \bar{x} is stable. If in addition, $\dot{V}(\bar{x}) < 0$, $\forall x \in \mathcal{B} \setminus \{\bar{x}\}$, then \bar{x} is asymptotically stable and unstable if $\dot{V}(\bar{x}) > 0$, $\forall x \in \mathcal{B} \setminus \{\bar{x}\}$.*

Global asymptotic stability using Lyapunov function theory, is determined in conjunction with LaSalle's Invariance Principle, first we consider the following definition.

Definition 2.1.9 ([116]) *Let $\mathbb{S} \subset \mathbb{R}^p$ be a set, then \mathbb{S} is said to be invariant under the system (2.1.1) if for any $x(0) \in \mathbb{S}$ we have $x(t, 0, x(0)) \in \mathbb{S}$ for all $t \in \mathbb{R}$. If we restrict ourselves to positive times (i.e. $t > 0$ then, we refer to \mathbb{S} as a positively invariant set and, for a negative time, as a negatively invariant set.*

Definition 2.1.10 *A dynamical system on $\Omega \subset \mathbb{R}^p$ is said to be dissipative if there exists a bounded, positively invariant set \mathbb{S} with the property that for any bounded set $\mathcal{B} \subseteq \mathbb{R}^p$, there exists a time $t^* = t^*(\mathbb{S}, \mathcal{B}) \geq 0$ such that $\Phi_t \mathcal{B} \subseteq \mathbb{S}$ for all $t > t^*$. The set \mathbb{S} is called an absorbing set.*

Theorem 2.1.7 (LaSalle's Invariance Principle ([70])). *Let \bar{x} be an equilibrium point of a dissipative dynamical system on Ω define by (2.1.1). Let V be a positive definite Lyapunov function for \bar{x} on the set Ω . Furthermore, let $\mathcal{U} = \{x \in \bar{\Omega} : \dot{V}(x) = 0\}$. If \mathbb{M} is the largest invariant set of \mathcal{U} such that $\mathbb{M} \subset \Omega$, then \bar{x} is globally asymptotically stable on Ω if and only if it is globally asymptotically stable for the system restricted to \mathbb{M} .*

The Comparison theorem [100], stated below is applied to prove global stability of equilibria for a monotone dynamical system on the space of related system of ODEs by comparing their solutions. A monotone dynamical system is the dynamical system on an ordered metric space which has the property that ordered initial states lead to ordered subsequent states. Consider the nonautonomous system

$$x' = g(t, x), \text{ where } g : \mathcal{D} \rightarrow \mathbb{R}^p, \mathcal{D} \subset \mathbb{R}^p, \quad (2.1.6)$$

with the solutions of the differential inequality system

$$z' \leq g(t, z), \quad (2.1.7)$$

or,

$$y' \geq g(t, y), \quad (2.1.8)$$

on an interval. This method requires that the solution of the dynamical system (2.1.6) to be unique.

Theorem 2.1.8 ([100, Comparison Theorem, pp 86]) *Let g be monotone continuous and Lipschitz on \mathcal{D} , $x(t)$ be a solution of (2.1.6) defined on $[a, b]$. If $z(t)$ is a continuous function on $[a, b]$ satisfying (2.1.7) on (a, b) with $z(a) \leq x(a)$, then $z(t) \leq x(t)$ for all t in $[a, b]$. If $y(t)$ is continuous on $[a, b]$ satisfying (2.1.8) on (a, b) with $y(a) \geq x(a)$, then $y(t) \geq x(t)$ for all t in $[a, b]$.*

2.2 Reproduction threshold

In epidemiology, the existence of thresholds forms an underlying concept in determining the spread or decline of a disease in a community. The basic reproduction number, denoted by \mathcal{R}_0 , is the average number of secondary cases generated by a single infected individual during its entire period of infectiousness when introduced into a completely susceptible population [4, 32, 53]. The threshold quantity, \mathcal{R}_0 , typically, determines whether disease will invade a community, if $\mathcal{R}_0 > 1$ or will not invade if $\mathcal{R}_0 < 1$. This corresponds to the qualitative property of epidemic models that if $\mathcal{R}_0 < 1$, there is a DFE which is asymptotically stable, and the infection dies out. If $\mathcal{R}_0 > 1$, the usual situation is that there is an EE which is asymptotically stable, and the infection persists [16]. This exchange of stability between the DFE and an EE occur at $\mathcal{R}_0 = 1$, and is referred as *forward bifurcation* (or transcritical bifurcation).

For simple models, the basic reproduction number is the product of the infection rate and the duration of infectiousness.

2.2.1 Next generation operator method

The next generation operator method is typically employed to determine the basic reproduction number, \mathcal{R}_0 , of a disease transmission model and to subsequently, establish the local asymptotic stability of the associated disease-free equilibrium. The method is described below using the formulation and notations in [107].

Let $x = (x_1, \dots, x_n)$, be the number of individuals in each compartment with each $x_i \geq 0$ and the first m compartments correspond to infected individuals. Define \mathbf{X}_s to be the set of all disease-free states. That is,

$$\mathbf{X}_s = \{x \geq 0 \mid x_i = 0, i = 1, \dots, m\}.$$

The disease transmission model consists of nonnegative initial conditions together with the following system of equations:

$$\dot{x}_i = f_i(x) = \mathcal{F}_i(x) - \mathcal{V}_i(x), \quad i = 1, \dots, n, \quad (2.2.1)$$

where $\mathcal{V}_i(x) = \mathcal{V}_i^-(x) - \mathcal{V}_i^+(x)$, $\mathcal{F}_i(x)$ be the rate of appearance of new infections in compartment i , $\mathcal{V}_i^+(x)$ be the rate of transfer of individuals into compartment i by all other means and $\mathcal{V}_i^-(x)$ be the rate of transfer of individuals out of compartment i . The functions are differentiable at least twice and satisfy assumptions (A1)-(A5) described below

- (A1) if $x \geq 0$, then $\mathcal{F}_i, \mathcal{V}_i^+, \mathcal{V}_i^- \geq 0$ for $i = 1, \dots, n$.
- (A2) if $x_i = 0$ then $\mathcal{V}_i^+ = 0$. In particular, if $x \in \mathbf{X}_s$ then $\mathcal{V}_i^+ = 0$ for $i = 1, \dots, m$.
- (A3) $\mathcal{F}_i = 0$ if $i > m$.
- (A4) if $x \in \mathbf{X}_s$ then $\mathcal{F}_i(x) = 0$ and $\mathcal{V}_i^+(x) = 0$ for $i = 1, \dots, m$.
- (A5) If $\mathcal{F}(x) = 0$ is set to zero, then all eigenvalues of $Df(x_0)$ have negative real parts, where $Df(x_0)$ is the derivative $[\partial f_i / \partial f_j]$ evaluated at the DFE, x_0 (i.e., the Jacobian matrix).

Let A be a square matrix with nonpositive off-diagonal and nonnegative diagonal entries as shown below

$$A = \begin{bmatrix} a_{11} & -a_{12} & -a_{13} & \cdots \\ -a_{21} & a_{22} & -a_{23} & \cdots \\ -a_{31} & -a_{32} & a_{33} & \cdots \\ \vdots & \vdots & \vdots & \ddots \end{bmatrix},$$

where the a_{ij} are nonnegative. Furthermore, let A be expressed as

$$A = sI - B, \quad s > 0, \quad B \geq 0. \quad (2.2.2)$$

Definition 2.2.1 (*M-Matrix [12]*) Any matrix A of the form (2.2.2) for which $s \geq \rho(B)$, (where $\rho(B)$ is the spectral radius of B), is called an *M-matrix*.

Lemma 2.2.1 If x_0 is a DFE of (2.2.1) and $f_i(x)$ satisfies (A1)-(A5), then the derivatives $D\mathcal{F}(x_0)$ and $D\mathcal{V}(x_0)$ are partitioned as

$$D\mathcal{F}(x_0) = \begin{bmatrix} F & 0 \\ 0 & 0 \end{bmatrix} \quad \text{and} \quad D\mathcal{V}(x_0) = \begin{bmatrix} V & 0 \\ J_3 & J_4 \end{bmatrix},$$

where F and V are the $m \times m$ matrices defined by

$$F = \left[\frac{\partial \mathcal{F}_i}{\partial x_j}(x_0) \right] \quad \text{and} \quad V = \left[\frac{\partial \mathcal{V}_i}{\partial x_j}(x_0) \right] \quad \text{with } 1 \leq i, j \leq m.$$

Further, F is non-negative, V is a non-singular *M-matrix* and J_3, J_4 are matrices associated with the transition terms of the model, and all eigenvalues of J_4 have positive real part.

The following theorem states that \mathcal{R}_0 is a threshold quantity that govern the persistence or effective control (elimination of the disease).

Theorem 2.2.1 (*van den Driessche and Watmough [107]*) Consider the disease transmission model given by (2.2.1) with $f(x)$ satisfying conditions (A1)-(A5). If x_0 is a DFE of the model, then x_0 is locally asymptotically stable if $\mathcal{R}_0 < 1$, but unstable if $\mathcal{R}_0 > 1$, where \mathcal{R}_0 is defined by $\mathcal{R}_0 = \rho(FV^{-1})$.

2.3 Bifurcations

A dynamical system typically involves a number of parameter values, in addition to the state variables. Bifurcation is a point in parameter space where equilibria appear, disappear, or change stability [17]. Typically, in epidemic modeling, bifurcation occurs when the associated reproduction number equals unity. There are different types of bifurcations, such as saddle-node, transcritical, pitchfork, backward and Hopf bifurcations (the last two are relevant to this thesis) [84, 116].

2.3.1 Backward bifurcation

Analyses of some compartmental epidemic models have shown that a stable disease-free equilibrium coexists with a stable endemic equilibrium even when the basic reproductive number (\mathcal{R}_0) is less than unity [21, 106, 111]. This phenomenon is called *backward bifurcation*. In other words, under some conditions in parameter space, an outbreak can occur, or a stable endemic equilibrium can exist, even when the threshold quantity (\mathcal{R}_0) of the model being studied is less than unity. In such situations, the reduction of the associated reproduction number (\mathcal{R}_0) below unity is insufficient for disease eradication in the community. Figure 2.1 displayed a schematic diagram for backward bifurcation with force of infection λ^* , evaluated at equilibrium and basic reproduction number \mathcal{R}_0 . The center manifold theory described in [21, 33, 42, 50, 97, 106] is often used to establish the presence of *backward bifurcation* in a disease transmission model. The theorem shows that the direction of bifurcation at $\mathcal{R}_0 = 1$ is backward (with the first solution branch, a saddle, separating the basin of attraction of the associated DFE and that of a stable end branch). The center manifold theorem (in particular, Theorem 4.1 in [21] reproduced below for convenience) is used to establish the presence of backward bifurcation phenomenon in Chapter 4 of this thesis.

Theorem 2.3.1 (*Castillo-Chavez and Song [21]*) Consider a general system of ordinary differential equations with a parameter ϕ :

$$\frac{dx}{dt} = f(x, \phi), \quad f : \mathbb{R}^p \times \mathbb{R} \rightarrow \mathbb{R}^p \text{ and } f \in C^2(\mathbb{R}^p \times \mathbb{R}). \quad (2.3.1)$$

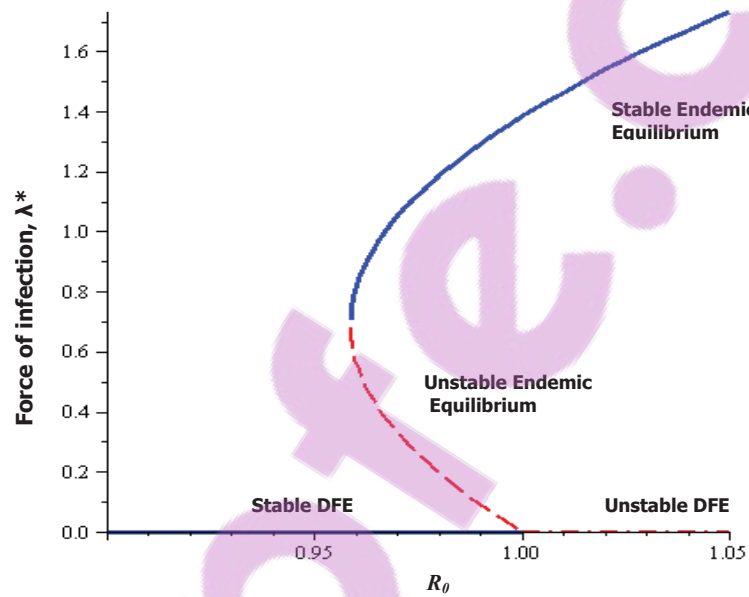


Figure 2.1: Backward bifurcation diagram.

Without loss of generality, it is assumed that 0 is an equilibrium for system (2.3.1) for all values of the parameter ϕ , that is

$$f(0, \phi) \equiv 0 \text{ for all } \phi, \quad (2.3.2)$$

and assume

A1: $A = D_x f(0, 0) = \left(\frac{\partial f_i}{\partial x_j}(0, 0) \right)$ is the linearization matrix of System (2.3.1) around the equilibrium 0 with ϕ evaluated at 0. zero is a simple eigenvalue of A and all other eigenvalues of A have negative real parts;

A2: Matrix A has a nonnegative right eigenvector w and a left eigenvector v corresponding to the zero eigenvalue. Let f_k be the k th component of

f and

$$a = \sum_{k,i,j=1}^n v_k w_i w_j \frac{\partial^2 f_k}{\partial x_i \partial x_j}(0,0), \quad (2.3.3)$$

$$b = \sum_{k,i,j=1}^n v_k w_i \frac{\partial^2 f_k}{\partial x_i \partial \phi}(0,0). \quad (2.3.4)$$

The local dynamics of (2.3.1) around 0 are totally determined by a and b .

- (i). $a > 0, b > 0$. When $\phi < 0$ with $|\phi| \ll 1$, 0 is locally asymptotically stable and there exists a positive unstable equilibrium; when $0 < \phi \ll 1$, 0 is unstable and there exists a negative and locally asymptotically stable equilibrium;
- (ii). $a < 0, b < 0$. When $\phi < 0$ with $|\phi| \ll 1$, 0 is unstable; when $0 < \phi \ll 1$, 0 is locally asymptotically stable, and there exists a positive unstable equilibrium;
- (iii). $a > 0, b < 0$. When $\phi < 0$ with $|\phi| \ll 1$, 0 is unstable, and there exists a locally asymptotically stable negative equilibrium; when $0 < \phi \ll 1$, 0 is stable, and a positive unstable equilibrium appears;
- (iv). $a < 0, b > 0$. When ϕ changes from negative to positive, 0 changes its stability from stable to unstable. Correspondingly a negative unstable equilibrium becomes positive and locally asymptotically stable.

In particular, a backward bifurcation occurs at $\phi = 0$ when Condition (i) holds.

2.3.2 Hopf bifurcation

Hopf bifurcation occurs when a certain parameter μ is not only a point of change in stability, but also a point near which periodic solutions are born.

Definition 2.3.1 Let $f(\bar{x}, \mu) = 0$ for all $\mu \in \mathbb{R}$. A point μ_0 is said to be a Hopf bifurcation point from an equilibrium point \bar{x} of (2.1.1) if there exists a

sequence of parameter values $\mu_n \rightarrow \mu_0$ as $n \rightarrow \infty$ such that, for $\mu = \mu_n$ the system (2.1.1) has a periodic solution $\mu_n(t)$ with period T_n and

$$\max_{0 \leq t \leq T_n} \|x_n(t) - \bar{x}\| \rightarrow 0 \text{ as } n \rightarrow \infty.$$

Theorem 2.3.2 (Hopf Bifurcation Theorem) Consider the system (2.1.1) with $p = 2$ Assume that

- (i) $f \in C^r(\mathbb{R}^p \times \mathbb{R}, \mathbb{R}^p)$ for some $r \geq 2$ and that $f(\bar{x}, \mu) = 0$ for all $\mu \in \mathbb{R}$;
- (ii) $df(\bar{x}, \mu)$ has a pair of complex eigenvalues $\lambda_{\pm}(\mu)$ which satisfy $\lambda_{\pm}(\mu_0) = \pm ia$ for some $a \in \mathbb{R} \setminus \{0\}$;
- (iii) $\frac{d}{d\mu}(Re(\lambda(\mu))) \neq 0$ for $\mu = \mu_0$.

Then μ_0 is a Hopf bifurcation point from \bar{x} .

Definition 2.3.2 (Conservation Law [82]) Consider a system modeled by a system of n -first-order differential equations

$$\frac{dX}{dt} = F(X), \quad (2.3.5)$$

where

$$X(t)^T = (x_1(t), \dots, x_n(t)), \quad F(X)^T = (f_1(X), \dots, f_n(X)). \quad (2.3.6)$$

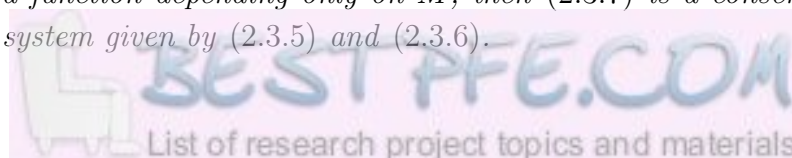
Let

$$M(t) = \sum_{i=1}^n x_i(t).$$

If $M(t)$ satisfies a scalar differential equation of the form

$$\frac{dM}{dt} = f(M), \quad (2.3.7)$$

where f is a function depending only on M , then (2.3.7) is a conservation law for the system given by (2.3.5) and (2.3.6).



2.4 Discrete-time dynamical systems

In this section, we focus on the properties of discrete dynamical systems associated with the numerical discretization of some continuous dynamical systems. For discrete time dynamical systems, the nonnegative time interval $[0, \infty)$ is replaced by a set of nonnegative integers, $[0, 1, 2, \dots, n, \dots)$.

Let $F : \mathbb{R}^p \rightarrow \mathbb{R}^p$. Consider a sequence $\{x_n\}_{n=0}^{\infty}$ be defined recursively from $x_0 \in \mathbb{R}^p$ by

$$x_{n+1} = F(x_n). \quad (2.4.1)$$

Definition 2.4.1 Equation (2.4.1) defines a discrete dynamical system on $\Omega \subset \mathbb{R}^p$ if, for every $x_0 \in \Omega$, the sequence $\{x_n\}_{n=0}^{\infty}$ remains in Ω .

Definition 2.4.2 A vector $\bar{x} \in \Omega \subset \mathbb{R}^p$ is said to be a fixed point of a discrete dynamical system on Ω defined by Equation (2.4.1) if $f(\bar{x}) = \bar{x}$ for all $n \geq 0$.

Definition 2.4.3 Let $\bar{x} \in \Omega \subset \mathbb{R}^p$ be a fixed point of a discrete dynamical system (2.4.1) on Ω . Then \bar{x} is said to be

(1.) stable if, for any $\epsilon > 0$, there exists $\delta = \delta(\epsilon) > 0$ such that $x_0 \in \Omega$,

$$||x_0 - \bar{x}|| < \delta$$

implies $||x_n - \bar{x}|| < \epsilon$ for all $n \geq 0$.

(2.) (locally) asymptotically stable if (1) holds and in addition there exists a constant $b > 0$ such that, $x_0 \in \Omega$, $||x_0 - \bar{x}|| < b$ implies

$$\lim_{n \rightarrow \infty} ||x_n - \bar{x}|| = 0$$

(3.) globally asymptotically stable on (Ω) if (1.) above holds and

$$\lim_{x \rightarrow \infty} ||x_n - \bar{x}|| = 0$$

for any $x_0 \in \Omega$.

(4.) *unstable if it is not stable (i.e., 1. above fails).*

Assume that the map F is of class C^1 . Let $J = DF(\bar{x})$, the Jacobian matrix of F at \bar{x} . Then,

$$y_{n+1} = Jy_n, \quad n = 0, 1, 2, \dots, \quad (2.4.2)$$

is the linearization of (2.4.1) around \bar{x} where $y_n = x_n - \bar{x}$. The stability properties of the linear system is determined by the eigenvalues of the Jacobian matrix J .

Definition 2.4.4 *A fixed point \bar{x} of the discrete dynamical system given by Equation (2.4.1) is said to be hyperbolic if the Jacobian matrix J has no eigenvalue of unit modulus. Otherwise the fixed point is called non-hyperbolic.*

The map F in (2.4.1) is said to be hyperbolic if all fixed points are hyperbolic.

Theorem 2.4.1 *(Hartman-Grobman Theorem) Let $F : \mathbb{R}^p \rightarrow \mathbb{R}^p$ be of class C^1 have a hyperbolic fixed point \bar{x} . Then there exist $\delta > 0$, a neighborhood $N \subset \mathbb{R}^p$ of the origin and a homeomorphism $h : \mathcal{B}(\bar{x}, \delta) \rightarrow N$ such that*

$$h(F(x_0)) = Jh(x_0)$$

for all $x_0 \in \mathcal{B}(\bar{x}, \delta)$.

In practice, Theorem 2.4.1 is implemented as shown below:

Theorem 2.4.2 *Consider f in (2.1.1) with a hyperbolic fixed point \bar{x} . Then \bar{x} is asymptotically stable if and only if for $x_n = J^n x_0$, solution of $x_{n+1} = Jx_n$ with $\|x_0\| := \|y_0 - \bar{y}\|$ small enough, we have*

$$\lim_{n \rightarrow \infty} x_n = 0$$

or equivalently $|\lambda| < 1$ for all $\lambda \in \sigma(J)$. The fixed point is unstable if and only if there exists at least one $\lambda \in \sigma(J)$ such that $|\lambda| > 1$ or

$$\lim_{n \rightarrow \infty} x_n = \infty.$$

2.4.1 Jury stability criterion

The Jury stability criterion is a method applied to test the stability of fixed points for discrete dynamical systems. It gives the step-by-step process of determining whether the roots of a discrete polynomial of degree n all have magnitude lying within the unit disk.

Definition 2.4.5 ([65]) *A necessary and sufficient condition for the following polynomial*

$$F(z) = a_0 + a_1z + a_2z^2 + \cdots + a_{n-1}z^{n-1} + a_nz^n, \quad a_n > 0 \quad (2.4.3)$$

to have all its roots inside the unit circle is given by:

- (1) $F(1) > 0$
- (2) $F(-1) \begin{cases} > 0 & \text{for } n \text{ even} \\ < 0 & \text{for } n \text{ odd} \end{cases}$
- (3) (a) $|a_0| < a_n$,
 (b) $|b_0| > |b_{n-1}|$,
 (c) $|c_0| > |c_{n-2}|$,
 (d) $|d_0| > |d_{n-3}|$,
 \vdots
 (e) $|r_0| > |r_2|$,

where the coefficients b_0 to r_2 are obtained from the table

The elements of row three through $(2n - 3)$ are given by the following determinants:

$$b_k = \begin{vmatrix} a_0 & a_{n-k} \\ a_n & a_k \end{vmatrix}, \quad k = 0, 1, 2, \dots, n-1; \quad c_k = \begin{vmatrix} b_0 & b_{n-1-k} \\ b_{n-1} & b_k \end{vmatrix}, \quad k = 0, 1, 2, \dots, n-2$$

$$d_k = \begin{vmatrix} c_0 & c_{n-2-k} \\ c_{n-2} & c_k \end{vmatrix}, \quad k = 0, 1, 2, \dots, n-3; \quad e_k = \begin{vmatrix} d_0 & d_{n-3-k} \\ d_{n-3} & d_k \end{vmatrix}, \quad k = 0, 1, 2, \dots, n-4$$

Row	z^0	z^1	z^2	z^3	.	.	.	z^{n-2}	z^{n-1}	z^n
1	a_0	a_1	a_2	a_3	.	.	.	a_{n-2}	a_{n-1}	a_n
2	a_n	a_{n-1}	a_{n-2}	a_{n-3}	.	.	.	a_2	a_1	a_0
3	b_0	b_1	b_2	b_3	.	.	.	b_{n-2}	b_{n-1}	
4	b_{n-1}	b_{n-2}	b_{n-3}	b_{n-4}	.	.	.	b_1	b_0	
5	c_0	c_1	c_2	c_3	.	.	.	c_{n-2}		
6	c_{n-2}	c_{n-3}	c_{n-4}	c_0		
.	
.	
.	
$2n - 3$	r_0	r_1	r_2							

Definition 2.4.6 ([80]) *The Systems (2.1.1) and (2.4.1) are said to have the same general solution if and only if*

$$x_k = x(t_k)$$

.

Definition 2.4.7 (Exact scheme ([80])) *An exact finite difference scheme is one for which the solution to the difference equation (2.4.1) has the same general solution as the associated differential equation (2.1.1).*

Definition 2.4.8 *Consider the differential equation in (2.1.1). Let a finite difference scheme for (2.1.1) be*

$$x_{k+1} = f(x_k, t_k, h). \quad (2.4.4)$$

Let the differential equation and/or its solutions have property P . The discrete model, (2.4.4), is dynamically consistent with respect to property P if it and/or its solutions also has property P .

2.5 Nonstandard finite difference method

The Nonstandard finite difference (NSFD) scheme, a numerical discretization method invented by Mickens [80, 81, 82], is especially designed to capture the

essential qualitative features of the corresponding continuous-time dynamical system being discretized. Usually, these continuous dynamical systems are formulated using systems of non-linear differential equations, whose exact solution, if at all exists, is very difficult to determine. This compels the use of numerical methods, preferably, those that best approximate and replicate the basic properties of the continuous systems. The NSFD schemes do not, in general, suffer from the instabilities and/or convergence to spurious zeros of standard finite-difference methods (such as the explicit forward-Euler and Runge-Kutta methods), as observed in [43, 49, 81, 90]. Further details of the mathematical framework are given in [5, 7].

A finite difference method is NSFD if it satisfies the following rules [7, 80]:

- Rule 1** The orders of the discrete derivatives should be equal to the orders of the corresponding derivatives of the differential equations.
- Rule 2** The traditional denominator, h is replaced by a non-negative function, $\phi(h)$ such that $\phi(h) = h + O(h^2)$ as $h \rightarrow 0$.
- Rule 3** Nonlinear terms are approximated in a nonlocal way, i.e. by a suitable function of several points of the mesh.
- Rule 4** Special conditions that hold for either the differential equation and/or its solutions should also hold for the difference equation model and/or its solutions.

CHAPTER 3

SIS MODEL

3.1 Introduction

The aim of this chapter is to construct and analyze a reliable numerical method for solving an SIS model (where infection with the disease does not confer permanent immunity against re-infection so that those who survived the infection revert to the class of wholly-susceptible individuals [55]) with discrete time delay. Although the SIS model with time delay has been studied in the literature (see, for instance [25, 59, 60, 91, 104] and some of the references therein), some of the pertinent aspects of the analyses are unreported. As discussed in Chapter 1, disease transmission models are usually designed by splitting the total population of interest at time t , denoted by $N(t)$, into mutually-exclusive epidemiological compartments based on the infection status of the members of the population. The simplest of such models take the form of an SIS model where $N(t)$ is split into compartments of susceptible individuals ($S(t)$) and infected individuals ($I(t)$), so that $N(t) = S(t) + I(t)$. Diseases, such as Meningitis, Gonorrhea, Influenza, Chagas, Rocky mountain, Malaria and Sleeping sickness, can be modeled using an SIS framework [54, 58]. Numerous classical SIS models, using different assumptions on demographic and incidence parameters, are widely studied in the literature in

[58, 108, 119] and the references therein.

Infection occurs following effective contact between an infectious individual and a susceptible individual. There is often a time lag (delay) before the newly-infected individual become infectious (typically at the end of the incubation period, when the infected individual displays clinical symptoms of the disease). In other words, time delay is used to represent a latent period (incubation period), maturation time or wearing time of immunity [25, 59, 104]. Compartmental models with time delay are known to generally exhibit complex dynamic of behaviour (including sustained oscillations associated with the (Hopf) bifurcation of an EE into a limit cycle [47, 57, 69, 113]). Moreover, the explicit solutions of such models are formulated using systems of non-linear differential equations, whose exact solution, if at all exists, are very difficult (or impossible) to compute in close form. This necessitate the use of numerical methods, preferably, those that best approximate and replicate the basic properties of the governing continuous-time systems. Time delays have also been used in other biological and non biological studies, such as respiratory system [109] tumor growth [110], chemostat models [118] and neural networks [19].

The main objective of this chapter is two-fold. The first is to qualitatively analyze the SIS delay differential equation system ((3.3.1)-(3.3.2)). The second is to construct a robust numerical method for approximating its solution. For the later objective, a reliable numerical method (NSFD scheme) for a linear delay differential equation is designed for solving some classes of epidemiological models (including an SIS delay model). It is shown, theoretically and computationally, that the NSFD scheme is dynamically consistent with respect to the asymptotic stability of the trivial equilibrium solution of the continuous time model. The NSFD scheme has been extended to a logistic epidemic model and finally to SIS delay model in a reliable manner.

Before studying the DDE system (3.3.1)-(3.3.2), it is instructive to study the non-delayed model (3.2.1), for comparison purposes. This is done in Section 3.2. Afterwards, in Section 3.3, we consider the complete qualitative and quantitative analysis of the SIS model with discrete delay. Section 3.4 is based on the construction of dynamically consistent NSFD scheme for

SIS model with delay (starting, first, with setting down the foundation by analyzing a linear delay differential equation, followed by nonlinear logistic epidemiological delay logistic model). Numerical simulations are provided for each of these cases to illustrate the theoretical results derived.

3.2 SIS model without time delay

As stated earlier, the focus of this chapter is to study the dynamics of an SIS model with discrete time delay. However, to make the presentation self-contained, it is outlined, in this section, some of the key facts and notations that will later be used in future (regarding the SIS model without delay). The non-delayed SIS model is given by the following deterministic system of nonlinear differential equations [18, 55]:

$$\begin{aligned}\frac{dS(t)}{dt} &= \Pi + \gamma I(t) - \beta S(t) \frac{I(t)}{N(t)} - \mu S(t), \\ \frac{dI(t)}{dt} &= \beta S(t) \frac{I(t)}{N(t)} - (\gamma + \mu + \delta) I(t),\end{aligned}\tag{3.2.1}$$

where

- ▶ Π is the constant recruitment rate of individuals by birth and immigration;
- ▶ β is the effective contact rate;
- ▶ μ is the natural death rate;
- ▶ δ is the disease-induced death rate;
- ▶ γ is the transition rate from the infected class to susceptible class. It can also stand for assumed rate of loss of infection-acquired immunity.

The term $\beta SI/N$ is the incidence rate. It measures the average number of susceptible individuals infected by infectious person per contact per unit

of time. The system (3.2.1) is to be solved subject to the following initial conditions:

$$S(0) = S_0 \geq 0, I(0) = I_0 \geq 0. \quad (3.2.2)$$

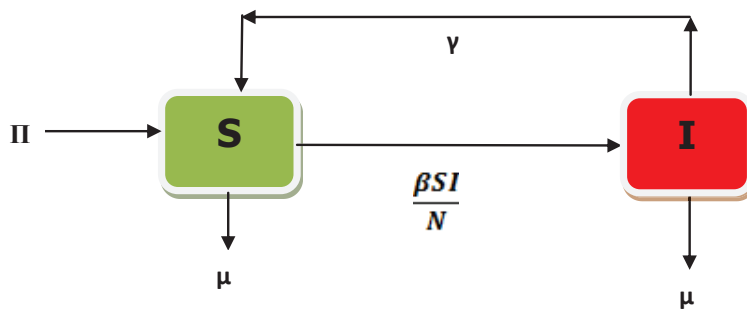


Figure 3.1: Schematic diagram of an SIS model.

The flow chart of the non-delayed SIS model (3.2.1) is given in Figure 3.1. Adding the equations in (3.2.1), gives

$$\frac{dN(t)}{dt} = \Pi - \mu N(t) - \delta I(t). \quad (3.2.3)$$

Qualitative analysis

The following standard results hold for the model (3.2.1) [18, 55, 108, 119]:

Theorem 3.2.1 (i) *The model (3.2.1) is a dynamical system in the biological feasible region*

$$\Gamma = \left\{ (S, I) \in \mathbb{R}_+^2 : S + I \leq \frac{\Pi}{\mu} \right\}. \quad (3.2.4)$$

(ii) *The basic reproductive number of the model is given by*

$$\mathcal{R}_0 = \frac{\beta}{\delta + \gamma + \mu}. \quad (3.2.5)$$

(iii) If $\mathcal{R}_0 \leq 1$, then the DFE, given by

$$E_0 = (S^*, I^*) = (\Pi/\mu, 0), \quad (3.2.6)$$

is GAS in Γ . When $\mathcal{R}_0 > 1$, the DFE is unstable and there exists a unique EE, given by

$$E_1 = (S^{**}, I^{**}) = \left(\frac{\Pi}{\mu + (\delta + \mu)(\mathcal{R}_0 - 1)}, \frac{\Pi(\mathcal{R}_0 - 1)}{\mu + (\delta + \mu)(\mathcal{R}_0 - 1)} \right), \quad (3.2.7)$$

which is GAS in Γ .

Theorem 3.2.1 shows that the model (3.2.1) undergoes a transcritical bifurcation at $\mathcal{R}_0 = 1$. Furthermore, the unique EE (E_1) collapses into the DFE (E_0) at $\mathcal{R}_0 = 1$ (the bifurcation point).

Nonstandard finite difference method

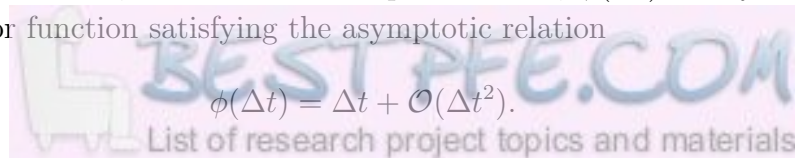
Although the SIS model is simple, it cannot be solved explicitly (in terms of elementary functions of $S(t)$ and $I(t)$) owing to its nonlinearity. Thus, its solution has to be obtained numerically. In this section, we present an NSFD scheme which captures the essential qualitative properties of the SIS model (3.2.1). The equations of the model (3.2.1) are discretized in the following way (see [73]):

$$\frac{S_{n+1} - S_n}{\phi(\Delta t)} = \Pi + \gamma I_n - \frac{\beta I_n S_{n+1}}{S_{n+1} + I_n} - \mu S_{n+1}, \quad (3.2.8)$$

$$\frac{I_{n+1} - I_n}{\phi(\Delta t)} = \frac{\beta I_n S_{n+1}}{S_{n+1} + I_n} - \gamma I_n - (\delta + \mu) I_{n+1},$$

where $S_n \approx S(t_n)$ and $I_n \approx I(t_n)$ are the approximations of number of susceptible and infective individuals, respectively, at time $t_n = n\Delta t$, respectively. Furthermore, $\Delta t > 0$ is the step size. Also, $\phi(\Delta t)$ is any complex denominator function satisfying the asymptotic relation

$$\phi(\Delta t) = \Delta t + \mathcal{O}(\Delta t^2). \quad (3.2.9)$$



In practice, we will use [81]

$$\phi = \phi(\Delta t) \equiv \phi(h) = \frac{1 - e^{-\mu h}}{\mu}, \quad (3.2.10)$$

or,

$$\phi(h) = \frac{1 - e^{-(\mu+\gamma+\delta)h}}{\mu + \gamma + \delta}. \quad (3.2.11)$$

It should be mentioned that the complex denominator functions in (3.2.10) and (3.2.11) are obtained from the conservation law (3.2.3) as follows:

$$\begin{aligned} \frac{dN(t)}{dt} &= \Pi - \mu N(t) - \delta I(t), \\ &\geq \Pi - (\mu + \delta + \gamma)N(t). \end{aligned} \quad (3.2.12)$$

Adding the equations in (3.2.8) shows that the NSFD replicates the conservation law (3.2.3) in the form

$$\frac{N_{n+1} - N_n}{\phi(h)} = \Pi - \mu N_{n+1} - \delta I_{n+1}. \quad (3.2.13)$$

More generally, the discrete analog of Theorem 3.2.1 is summarized below [73, 103]:

Theorem 3.2.2 *The NSFD scheme (3.2.8) is dynamically consistent with respect to the qualitative properties of the SIS model (3.2.1), stated in Theorem 3.2.1, in the following specific ways:*

- (i) *The NSFD scheme (3.2.8) is a dynamical system in the biological feasible region Γ .*
- (ii) *The fixed points of the NSFD scheme (3.2.8) are precisely the equilibria of the continuous model (3.2.1).*
- (iii) *The disease-free fixed point,*

$$E_0 = (S^*, I^*) = (\Pi/\mu, 0), \quad (3.2.14)$$

is GAS in Ω if $\mathcal{R}_0 \leq 1$.

(iv) If $\mathcal{R}_0 > 1$, the disease-free fixed point is unstable and there is a unique endemic fixed point

$$E_1 = (S^{**}, I^{**}) = \left(\frac{\Pi}{\mu + (\delta + \mu)(\mathcal{R}_0 - 1)}, \frac{\Pi(\mathcal{R}_0 - 1)}{\mu + (\delta + \mu)(\mathcal{R}_0 - 1)} \right), \quad (3.2.15)$$

which is LAS.

Consider now, the model (3.2.1) with $\delta = 0$. Adding the equations in (3.2.1), with $\delta = 0$, we have

$$\frac{dN(t)}{dt} = \Pi - \mu N(t),$$

so that $N(t) = \frac{\Pi}{\mu}$ as $t \rightarrow \infty$. Thus, it can be remarked that the SIS model (3.2.1), with $\delta = 0$, is equivalent to the logistic equation given by

$$\frac{dI(t)}{dt} = \beta \left(1 - \frac{1}{\mathcal{R}_0} \right) \left(1 - \frac{I(t)}{N(1 - \frac{1}{\mathcal{R}_0})} \right) I(t). \quad (3.2.16)$$

The exact solution of the logistic model (3.2.16) is given by [54], with $N(t) = \frac{\Pi}{\mu}$,

$$I(t) = \frac{\frac{\Pi}{\mu}(1 - \frac{1}{\mathcal{R}_0})I_0}{I_0 + \left[\frac{\Pi}{\mu}(1 - \frac{1}{\mathcal{R}_0}) - I_0 \right] e^{-\beta(1 - \frac{1}{\mathcal{R}_0})t}}. \quad (3.2.17)$$

Similarly, the exact numerical scheme for (3.2.16) is given by [73]

$$\frac{I_{n+1} - I_n}{\phi} = \beta \left(1 - \frac{1}{\mathcal{R}_0} \right) \left(1 - \frac{I_{n+1}}{\frac{\Pi}{\mu}(1 - \frac{1}{\mathcal{R}_0})} \right) I_n, \quad (3.2.18)$$

where the denominator function,

$$\phi \equiv \phi(h) = \frac{1 - \exp[-|\beta(1 - \frac{1}{\mathcal{R}_0})|h]}{|\beta(1 - \frac{1}{\mathcal{R}_0})|},$$

satisfies the asymptotic relation (3.2.9).

3.3 SIS model with discrete time delay

To account for effect of latency in disease transmission, the non-delayed SIS model (3.2.1) is extended to include time delay, denoted by $\tau > 0$, resulting in the following delay differential equation (DDE) system [59, 91, 119]:

$$\begin{aligned}\frac{dS(t)}{dt} &= \Pi + \gamma I(t) - \frac{\beta I(t-\tau)S(t)e^{-\mu\tau}}{N(t)} - \mu S(t), \\ \frac{dI(t)}{dt} &= \frac{\beta I(t-\tau)S(t)e^{-\mu\tau}}{N(t)} - (\gamma + \delta + \mu)I(t).\end{aligned}\tag{3.3.1}$$

The parameters (noting the addition of $\tau > 0$, the discrete time delay) and variables of the delayed SIS model (3.3.1) have the same meaning as those for the non-delayed SIS model (3.2.1). However, it is worthwhile noting henceforth that:

- $I(t-\tau)$ is the population of individuals who were infected at time $(t-\tau)$ and become infectious after τ units of time have elapsed;
- $e^{-\mu\tau}$ is the probability that a newly-infected individual survives natural death (μ) during the time τ period, and become infectious.

Moreover, the initial conditions (3.2.2) must be replaced by

$$S(t) = \psi_1(t), I(t) = \psi_2(t), t \in [-\tau, 0].\tag{3.3.2}$$

3.3.1 Basic properties of continuous-time delayed system

As a consequence to the way the analysis of delay differential equations system are scattered, and in view of our future quest of constructing a dynamically consistent discrete delay scheme, it is of paramount importance to study the qualitative properties of the continuous model in full detail. We start by proving the well-posedness of the model (3.3.1)-(3.3.2), as below.

Theorem 3.3.1 *Assume that the initial function $\psi = (\psi_1, \psi_2) \geq 0$ is of class $C^0([-\tau, 0], \mathbb{R}^2)$ and satisfies $0 \leq \psi_1 + \psi_2 \leq \frac{\Pi}{\mu}$. Then, there exists a*

unique solution $\mathbf{X} \equiv (S, I) \geq 0$ of class $\mathcal{C}^0([-\tau, +\infty), \mathbb{R}^2) \cap \mathcal{C}^1((0, +\infty), \mathbb{R}^2)$ of (3.3.1)-(3.3.2) such that $0 \leq S + I \leq \frac{\Pi}{\mu}$.

Proof. By the fundamental theorem of calculus, the DDE system (3.3.1)-(3.3.2) is equivalent to the following system of integral equations [51]:

$$S(t) = \begin{cases} \psi_1(t), & \text{for } t \in [-\tau, 0], \\ \psi_1(0) + \int_0^t f_1[S(u), I(u - \tau), I(u)] du, & \text{for } t > 0, \end{cases} \quad (3.3.3)$$

$$I(t) = \begin{cases} \psi_2(t), & \text{for } t \in [-\tau, 0], \\ \psi_2(0) + \int_0^t f_2[S(u), I(u - \tau), I(u)] du, & \text{for } t > 0, \end{cases} \quad (3.3.4)$$

where

$$\begin{aligned} f_1[S(u), I(u - \tau), I(u)] &= \Pi - \frac{\beta I(u - \tau) S(u) e^{-\mu\tau}}{N(u)} - \mu S(u) + \gamma I(u), \\ f_2[S(u), I(u - \tau), I(u)] &= \frac{\beta I(u - \tau) S(u) e^{-\mu\tau}}{N(u)} - (\gamma + \delta + \mu) I(u). \end{aligned} \quad (3.3.5)$$

Let $\mathcal{T} = (\mathcal{T}_1, \mathcal{T}_2)$ be an operator that transforms the function $\mathbf{X} = (S, I)$ into $\mathbf{Y} = \mathcal{T}\mathbf{X} = (\mathcal{T}_1\mathbf{X}, \mathcal{T}_2\mathbf{X})$ defined for every $t \in (0, +\infty)$ through (3.3.2) and (3.3.1) as follows:

$$\begin{aligned} (\mathcal{T}_1\mathbf{X})(t) &= \psi_1(0) + \int_0^t f_1[S(u), I(u - \tau), I(u)] du, \\ (\mathcal{T}_2\mathbf{X})(t) &= \psi_2(0) + \int_0^t f_2[S(u), I(u - \tau), I(u)] du. \end{aligned} \quad (3.3.6)$$

It follows that solving the DDE system (3.3.1)-(3.3.2) is equivalent to finding the fixed points of the operator \mathcal{T} :

$$\mathbf{X} = \mathcal{T}\mathbf{X}. \quad (3.3.7)$$

The fixed points of the system (3.3.7) are obtained via the following stages:

Stage 1: In this stage, (which follows Theorem 2.3 in [51]), the existence of a local solution is proved. We employ the Banach contraction principle [117],

following the structure in [66].

Given $r > 0$, let $\bar{\mathcal{B}} = \bar{\mathcal{B}}(\psi(\mathbf{0}), r) \subset \mathbb{R}^2$ be the closed ball with center $\psi(\mathbf{0})$ and radius r . Furthermore, for $T > 0$ and $q > 0$, let $\mathcal{C}_q([-\tau, T], \bar{\mathcal{B}})$ be the set of continuous functions from $[-\tau, T]$ into $\bar{\mathcal{B}}$, which is a complete metric space under the metric defined, for any $\mathbf{y}, \mathbf{w} \in \mathcal{C}_q([-\tau, T], \bar{\mathcal{B}})$, by

$$d_q(\mathbf{y}, \mathbf{w}) := \sup_{-\tau \leq t \leq T} e^{-qt} \|\mathbf{y}(t) - \mathbf{w}(t)\|.$$

We show below that there exist T and q such that the operator \mathcal{T} is a contraction from $\mathcal{C}_q([-\tau, T], \bar{\mathcal{B}})$ into $\mathcal{C}_q([-\tau, T], \bar{\mathcal{B}})$. For any $\mathbf{y} \in \mathcal{C}_q([-\tau, T], \bar{\mathcal{B}})$, we have by (3.3.6)

$$\begin{aligned} \|\mathcal{T}(\mathbf{y})(t) - \psi(\mathbf{0})\| &\leq \int_0^t \|f(y_1(u), y_2(u - \tau), y_2(u))\| du, \\ &\leq T \sup_{x \in \bar{\mathcal{B}}} \|f(y_1(x), y_2(x - \tau), y_2(x))\|, \end{aligned}$$

where T is chosen to be

$$T := \frac{r}{\sup_{x \in \bar{\mathcal{B}}} \|f(y_1(x), y_2(x - \tau), y_2(x))\|}.$$

This shows that \mathcal{T} operates from $\mathcal{C}_q([-\tau, T], \bar{\mathcal{B}})$ into $\mathcal{C}_q([-\tau, T], \bar{\mathcal{B}})$.

Fix $\mathbf{y}, \mathbf{w} \in \mathcal{C}_q([-\tau, T], \bar{\mathcal{B}})$. Since the function f in (3.3.5) is Lipschitz on \mathcal{B} (with Lipschitz constant $L_{\mathcal{B}}$), it follows that:

$$\begin{aligned} \|\mathcal{T}(\mathbf{y})(t) - \mathcal{T}(\mathbf{w})(t)\| &\leq \int_0^t \|f(\mathbf{y}(s)) - f(\mathbf{w}(s))\| ds, \\ &\leq L_{\mathcal{B}} \int_0^t \|\mathbf{y}(s) - \mathbf{w}(s)\| ds, \\ &= L_{\mathcal{B}} \int_0^t e^{qs} e^{-qs} \|\mathbf{y}(s) - \mathbf{w}(s)\| ds, \\ &\leq L_{\mathcal{B}} \|\mathbf{y} - \mathbf{w}\|_{\mathcal{C}_q([-\tau, T], \bar{\mathcal{B}})} \int_0^t e^{qs} ds, \\ &= L_{\mathcal{B}} \left(\frac{e^{qt} - 1}{q} \right) \|\mathbf{y} - \mathbf{w}\|_{\mathcal{C}_q([-\tau, T], \bar{\mathcal{B}})}. \end{aligned}$$

Thus,

$$e^{-qt} \|\mathcal{T}(\mathbf{y})(t) - \mathcal{T}(\mathbf{w})(t)\| \leq \frac{L_{\mathcal{B}}}{q} \|\mathbf{y} - \mathbf{w}\|,$$

and taking the supremum of both sides gives

$$d_q(\mathcal{T}(\mathbf{y}), \mathcal{T}(\mathbf{w})) \leq \frac{L_{\mathcal{B}}}{q} d_q(\mathbf{y}, \mathbf{w}).$$

For the choice of $q > L_{\mathcal{B}}$, the operator \mathcal{T} is a contraction. Hence, by Banach contraction principle, there exists a unique fixed point of \mathcal{T} (and, thus, a unique local solution of the DDE system (3.3.1)).

Stage 2: The second stage of the proof is based on using Theorem 3.1 in [51]. We show that whenever the solution exists at some time t , it satisfies some apriori estimate, namely $0 \leq S(t), 0 \leq I(t)$ and $S(t) + I(t) \leq \frac{\Pi}{\mu}$. This is specifically done in Theorem 3.3.2 and Theorem 3.3.3 below.

Stage 3: The final (third) stage is to establish the global existence result and is covered by Theorem 3.3.4 below. ■

The following result, which is needed in the proof of Theorem 3.3.1, reflects a qualitative property of the solution.

Theorem 3.3.2 *Whenever it exists, the solution $S(t), I(t)$ of the DDE system (3.3.1) corresponding to the non-negative initial data (3.3.2), remains non negative for all $t > 0$.*

Proof. Assume that $S(t) > 0$ and $I(t) > 0$, for all $t \in [-\tau, 0]$. Let $t^0 = \sup\{t > 0 : S(t) > 0\}$ and $\underline{t}^0 = \sup\{t > 0 : I(t) > 0\}$.

We claim that $t^0 = +\infty$ and $\underline{t}^0 = +\infty$. Assume, by contradiction, that $t^0 < +\infty$ and $\underline{t}^0 < +\infty$ or $t^0 < +\infty$ and $\underline{t}^0 = +\infty$ or $t^0 = +\infty$ and $\underline{t}^0 < +\infty$. We deal with the case when $t^0 < +\infty$ and $\underline{t}^0 < +\infty$, other cases being relatively easy. By continuity $S(t)$ changes sign at least once in the interval $[t^0, +\infty)$ and $I(t)$ also changes sign at least once in the interval $[\underline{t}^0, +\infty)$. Let $t^1 \in [t^0, +\infty)$ be the first real number such that $S(t^1) = 0$ and $\underline{t}^1 \in [\underline{t}^0, +\infty)$

be the first real number such that $I(\underline{t}^1) = 0$. Without loss of generality, we assume that $t^1 \leq \underline{t}^1$. Hence,

$$S(t) \geq 0, \quad \forall 0 < t < t^1, \quad S(t^1) = 0 \text{ and } S'(t^1) \leq 0.$$

It follows from the first equation in (3.3.1) that

$$S'(t^1) = \Pi + \gamma I(t^1) > 0.$$

But t^1 is extremum of S so that $S'(t^1) = 0$, which is a contradiction. Therefore, $t^0 = +\infty$ and $\underline{t}^0 = +\infty$. ■

The result below is a qualitative property of the model (3.3.1), namely the a priori estimate needed in the proof of Theorem 3.3.1.

Theorem 3.3.3 *Whenever it exists, the solution $S(t)$, $I(t) \geq 0$ of (3.3.1) corresponding to non negative initial data (3.3.2) such that $\psi_1 + \psi_2 \leq \frac{\Pi}{\mu}$ belong to the compact set Γ .*

Proof. Assume that (3.3.1) has a non negative solution $\mathbf{X} = (S, I)$. From the conservation law (3.2.3), we have

$$\frac{dN}{dt} \leq \Pi - \mu N.$$

It follows from the Gronwall lemma [48] that

$$N(t) \leq N(0)e^{-\mu t} - \frac{\Pi}{\mu} (e^{-\mu t} - 1) = \left(N(0) - \frac{\Pi}{\mu} \right) e^{-\mu t} + \frac{\Pi}{\mu}.$$

Hence,

$$0 \leq N(t) = S(t) + I(t) \leq \frac{\Pi}{\mu}, \quad \text{if } 0 \leq N(0) \leq \frac{\Pi}{\mu}.$$

■

Theorem 3.3.4 *Let the initial function ψ be as in Theorem 3.3.1. Consider the sequence of times $(T_m)_{m \geq 0}$ defined by*

$$T_m = \frac{m \frac{\Pi}{\mu}}{\sup_{x \in \Gamma} \|f(y_1(x), y_2(x - \tau), y_2(x))\|}.$$

Then there exists a sequence of functions

$$Y^m : [T_m - \tau, T_{m+1}] \rightarrow \Gamma,$$

such that each Y^m is the unique solution of the model (3.3.1) on the interval $[T_m, T_{m+1}]$ and satisfies the compatibility conditions

$$Y^0(t) = \psi(t), \text{ for } t \in [-\tau, 0]$$

$$Y^m(t) = Y^{m-1}(t), \text{ for } t \in [T_m - \tau, T_{m+1}] \text{ } m = 1, 2, 3, \dots$$

Consequently, the function

$$Y := \bigcup_{m \geq 0} Y^m : [-\tau, +\infty) \rightarrow \Gamma,$$

is the global solution of the model (3.3.1)-(3.3.2).

Proof. The construction of the sequence $(Y^m)_{m \geq 0}$ is done by mathematical induction. The function Y^0 is obtained, as in the proof of the second step of Theorem 3.3.1, by applying Banach contraction principle to the operator \mathcal{T} in (3.3.6) defined on $\mathcal{C}_q([-\tau, T_1], \Gamma)$.

Assume that the function $Y^m \in \mathcal{C}_q([T_m - \tau, T_{m+1}], \Gamma)$ satisfying the compatibility condition is constructed. Then the function $Y^{m+1} \in \mathcal{C}_q([T_{m+1} - \tau, T_{m+2}], \Gamma)$ is constructed as follows:

We modify the operator \mathcal{T} in (3.3.6) into

$$(\mathcal{T}X)(t) = Y^m(T_{m+1}) + \int_{T_{m+1}}^t f[X_1(u), X_2(u - \tau), X_2(u)] du,$$

for $X \in \mathcal{C}_q([T_{m+1} - \tau, T_{m+2}], \Gamma)$.

Following the procedure in the proof of the second step of Theorem 3.3.1, it is easy to show that for a suitable choice of q , the operator \mathcal{T} is a contraction on $\mathcal{C}_q([T_{m+1} - \tau, T_{m+2}], \Gamma)$. This proves the existence and uniqueness of Y^{m+1} . ■

Remark 3.3.1 *Theorem 3.3.1 is the analog of Part (i) of Theorem 3.2.1 for the DDE system (3.3.1).*

The rest of this subsection is devoted to the qualitative analysis of the system (3.3.1). Let us first find its equilibrium points. To this end, we set the right hand side of (3.3.1) to be zero; we want to find (S^{**}, I^{**}) in Γ defined in (3.2.4) such that

$$\begin{aligned} \Pi + \gamma I^{**} - \frac{\beta I^{**} S^{**} e^{-\mu\tau}}{S^{**} + I^{**}} - \mu S^{**} &= 0, \\ \frac{\beta I^{**} S^{**} e^{-\mu\tau}}{S^{**} + I^{**}} - (\gamma + \delta + \mu) I^{**} &= 0. \end{aligned} \quad (3.3.8)$$

Note that at equilibrium $I(t - \tau) = I(t) = I^{**}$. At DFE ($I^{**} = 0$), we have

$$E^0 = (S^*, I^*) = (\Pi/\mu, 0). \quad (3.3.9)$$

However, in the presence of disease, i.e. $I^{**} \neq 0$, solving (3.3.8) for the EE, $[E_1 = (S^{**}, I^{**})]$, from the second equation we have:

$$\left[\frac{\beta S^{**} e^{-\mu\tau}}{S^{**} + I^{**}} - (\gamma + \delta + \mu) \right] I^{**} = 0.$$

Therefore, $\frac{\beta S^{**} e^{-\mu\tau}}{(S^{**} + I^{**})(\gamma + \delta + \mu)} - 1 = 0$.

Hence,

$$I^{**} = S^{**} \left[\frac{\beta e^{-\mu\tau}}{(\gamma + \delta + \mu)} - 1 \right]. \quad (3.3.10)$$

Substituting (3.3.10) into the first equation of (3.3.8), and simplifying for S^{**} , gives:

$$\begin{aligned} S^{**} &= \frac{\Pi}{\left(\frac{\beta e^{-\mu\tau}}{(\gamma + \delta + \mu)} - 1 \right)(\gamma + \delta + \mu) - \gamma \left(\frac{\beta e^{-\mu\tau}}{(\gamma + \delta + \mu)} - 1 \right) + \mu}, \\ &= \frac{\Pi}{\left(\frac{\beta e^{-\mu\tau}}{(\gamma + \delta + \mu)} - 1 \right)(\delta + \mu) + \mu}. \end{aligned} \quad (3.3.11)$$

Substituting (3.3.11) into (3.3.10) gives

$$I^{**} = \frac{\Pi(\frac{\beta e^{-\mu\tau}}{(\gamma+\delta+\mu)} - 1)}{(\frac{\beta e^{-\mu\tau}}{(\gamma+\delta+\mu)} - 1)(\delta + \mu) + \mu}. \quad (3.3.12)$$

Therefore, the EE is given by

$$E^* = (S^{**}, I^{**}) = \left(\frac{\Pi}{(\mathcal{R}_0(\tau) - 1)(\delta + \mu) + \mu}, \frac{\Pi(\mathcal{R}_0(\tau) - 1)}{(\mathcal{R}_0(\tau) - 1)(\delta + \mu) + \mu} \right). \quad (3.3.13)$$

Hence, the unique EE exists only whenever $\frac{\beta e^{-\mu\tau}}{\delta + \gamma + \mu} > 1$ and no equilibrium otherwise.

From (3.3.11) - (3.3.12), we single out the expression

$$\mathcal{R}_0(\tau) = \frac{\beta e^{-\mu\tau}}{\delta + \gamma + \mu}, \quad (3.3.14)$$

which, apart from helping to determine the existence or nonexistence of an EE, is the threshold quantity for the stability as seen in Theorem 3.3.5 below.

Here, the quantity $\mathcal{R}_0(\tau)$, *basic reproduction number*, is the product of the infection rate $\beta e^{-\mu\tau}$ and the average duration of infectiousness $(\frac{1}{\delta + \gamma + \mu})$.

To determine the local asymptotic stability of an arbitrary equilibrium of the DDE system (3.3.1), we linearize the system about this equilibrium point [24, 102]. More precisely, Taylor expansion of the right hand side with respect to dependent variables $S(t)$, $I(t)$, $I(t - \tau)$ yields:

$$\begin{bmatrix} \frac{d\hat{S}(t)}{dt} \\ \frac{d\hat{I}(t)}{dt} \end{bmatrix} = \mathbf{A} \begin{bmatrix} \hat{S}(t) \\ \hat{I}(t) \\ \hat{I}(t - \tau) \end{bmatrix}, \quad (3.3.15)$$

where $\hat{S}(t) = S(t) - S^*$, $\hat{I}(t) = I(t) - I^*$ and

$$\mathbf{A} = \begin{bmatrix} -\frac{\beta e^{-\mu\tau} I^{*2}}{(S^* + I^*)^2} - \mu & \frac{\beta e^{-\mu\tau} S^* I^*}{(S^* + I^*)^2} + \gamma & -\frac{\beta e^{-\mu\tau} S^*}{(S^* + I^*)} \\ \frac{\beta e^{-\mu\tau} I^{*2}}{(S^* + I^*)^2} & -\frac{\beta e^{-\mu\tau} S^* I^*}{(S^* + I^*)^2} - (\gamma + \delta + \mu) & \frac{\beta e^{-\mu\tau} S^*}{(S^* + I^*)} \end{bmatrix}.$$

Thus, assuming solutions of the form $\underline{S}(t) = c_1 e^{\lambda t}$ and $\underline{I}(t) = c_2 e^{\lambda t}$, where c_1, c_2 are constants and λ is a complex number, Equation (3.3.15) gives:

$$\begin{bmatrix} c_1 \lambda e^{\lambda t} \\ c_2 \lambda e^{\lambda t} \end{bmatrix} = \mathbf{A} \begin{bmatrix} c_1 e^{\lambda t} \\ c_2 e^{\lambda t} \\ c_2 e^{\lambda t} e^{-\lambda \tau} \end{bmatrix}. \quad (3.3.16)$$

$$\text{Let } J_1 = \begin{bmatrix} -\frac{\beta e^{-\mu \tau} I^{*2}}{(S^* + I^*)^2} - \mu & \frac{\beta e^{-\mu \tau} S^* I^*}{(S^* + I^*)^2} + \gamma \\ \frac{\beta e^{-\mu \tau} I^{*2}}{(S^* + I^*)^2} & -\frac{\beta e^{-\mu \tau} S^* I^*}{(S^* + I^*)^2} - (\gamma + \delta + \mu) \end{bmatrix} \text{ and}$$

$$J_2 = \begin{bmatrix} 0 & -\frac{\beta e^{-\mu \tau} S^*}{(S^* + I^*)} \\ 0 & \frac{\beta e^{-\mu \tau} S^*}{(S^* + I^*)} \end{bmatrix},$$

then (3.3.16) can be further simplified to give

$$[\lambda \mathbf{I} - J_1 - e^{-\lambda \tau} J_2] \hat{J} = \mathbf{0},$$

where \mathbf{I} is the identity matrix of order 2, $\hat{J} = [c_1 e^{\lambda t} \ c_2 e^{\lambda t}]^T$ and $\mathbf{0}$ is 2×1 zero matrix. Hence for nontrivial solution (i.e. $\hat{J} \neq \mathbf{0}$), the following transcendental/characteristic equation in λ , must be solved:

$$\det(\lambda \mathbf{I} - J_1 - e^{-\lambda \tau} J_2) = 0. \quad (3.3.17)$$

It should be noted that the local asymptotic stability of equilibrium is determined by showing that all the roots of (3.3.17) have negative real parts. We claim the following result which is in line with the one in [11, 59, 60].

Theorem 3.3.5 *Consider, the DDE system (3.3.1)-(3.3.2).*

(a) *The DFE,*

$$E_0 = (S^*, I^*) = (\Pi/\mu, 0), \quad (3.3.18)$$

is LAS if $\mathcal{R}_0(\tau) < 1$ and unstable if $\mathcal{R}_0(\tau) > 1$ for all $\tau \geq 0$.

(b) *For $\mathcal{R}_0(\tau) > 1$, we have two possibilities depending on the disease induced death rate δ :*

- (i) If $\delta = 0$, then the unique EE (3.3.13), is LAS for all $\tau \geq 0$.
- (ii) If $\delta > 0$, there exists a critical value τ^* of the delay such that the EE is LAS for $\tau \in (0, \tau^*)$, while there will be periodic solutions (stability switches) around the point EE, as $\tau > \tau^*$ increases.

The proof of Theorem 3.3.5 is based on the following results in [11, 24]:

Lemma 3.3.1 Consider the transcendental equation in (3.3.17) expressed as

$$G(\lambda) = P(\lambda) + Q(\lambda)e^{-\lambda\tau} = 0, \quad (3.3.19)$$

where $P(\lambda)$ and $Q(\lambda)$ are polynomials in λ . Assume that for $\tau = 0$ each root λ of $G(\lambda) = 0$ is such that $\text{Re}\lambda < 0$. Assume further that for $\tau > 0$ there is no purely imaginary root, $\lambda = \pm iy$, $y > 0$, of the polynomial (3.3.19). Then any root λ of (3.3.19) satisfies the relation $\text{Re}\lambda < 0$ for all $\tau \geq 0$. However, if there is any purely imaginary root then any root λ of (3.3.19) satisfies the relation $\text{Re}\lambda < 0$ for $\tau \in (0, \tau^*)$.

Before we prove this result, it is worth noting that the second and third assumptions in Lemma 3.3.1 are needed to guarantee the finite “exit”, if there is any, for roots to cross from the left half plane to the right and vice versa for any given τ .

Proof. (a) At the DFE, $E^0 = (S^0, I^0) = (\frac{\Pi}{\mu}, 0)$, the transcendental equation (3.3.19) gives

$$\begin{aligned} P(\lambda) &= \lambda^2 + \lambda K_1 + K_2, \\ Q(\lambda) &= -(\lambda + \mu)K_3\mathcal{R}_0(\tau), \end{aligned}$$

with $K_1 = K_3 + \mu$, $K_2 = \mu K_3$, $K_3 = \gamma + \delta + \mu$.

If $\tau = 0$, then the polynomial in (3.3.19) becomes

$$\lambda^2 + \lambda[\mu + K_3(1 - \mathcal{R}_0(\tau))] + K_2(1 - \mathcal{R}_0(\tau)) = 0.$$

It follows from Descartes Rule of Signs that all the roots of (3.3.19) have negative real parts whenever $\mathcal{R}_0(\tau) < 1$ for all $\tau \geq 0$. Furthermore, without

loss of generality, assume $\lambda = iy$, $y > 0$ is a root of the polynomial (3.3.19), we have

$$-y^2 + iyK_1 + K_2 = (iy + \mu)K_3\mathcal{R}_0(\tau)e^{-iy\tau}. \quad (3.3.20)$$

Separating the real and imaginary parts, (3.3.20) gives

$$\begin{aligned} -y^2 + K_2 &= yK_3\mathcal{R}_0 \sin y\tau + \mu K_3\mathcal{R}_0 \cos y\tau, \\ yK_1 &= yK_3\mathcal{R}_0 \cos y\tau - \mu K_3\mathcal{R}_0 \sin y\tau. \end{aligned} \quad (3.3.21)$$

Simplifying further by squaring and adding the equations in (3.3.21), we have

$$y^4 + y^2[\mu^2 + K_3^2(1 - \mathcal{R}_0(\tau)^2)] + \mu^2 K_3^2(1 - \mathcal{R}_0(\tau)^2) = 0, \quad (3.3.22)$$

Therefore, according to Descartes Rule of Signs, equation (3.3.22) has no positive real root y . Consequently, the transcendental equation (3.3.19) has no purely imaginary roots. Hence, any root λ of (3.3.19) satisfies the relation $\text{Re}\lambda < 0$ for all $\tau \geq 0$ when $\mathcal{R}_0(\tau) < 1$.

(b)(i) At the EE, with $\delta = 0$, the point is given by

$E_1 = (S^{**}, I^{**}) = \left(\frac{\Pi}{[(\mathcal{R}_0(\tau)-1)+1]\mu}, S^*(\mathcal{R}_0(\tau) - 1) \right)$ while $\mathcal{R}_0(\tau) = \frac{\beta e^{-\mu\tau}}{\gamma + \mu}$. The polynomials in Equation (3.3.19) are given as

$$\begin{aligned} P(\lambda) &= \lambda^2 + (2\mu + \gamma + K_5\mathcal{R}_0(\tau))\lambda + \mu\gamma + \mu^2 + \mu K_5\mathcal{R}_0(\tau), \\ Q(\lambda) &= -(\lambda + \mu)K_4, \end{aligned}$$

and $K_4 = \frac{\beta e^{-\mu\tau}}{\mathcal{R}_0(\tau)}$, $K_5 = \frac{K_4(\mathcal{R}_0(\tau)-1)}{\mathcal{R}_0(\tau)}$. Suppose $\tau = 0$. Then (3.3.19) can be simplified to

$$G(\lambda) = \lambda^2 + [\mu + K_4(\mathcal{R}_0(\tau) - 1)]\lambda + \mu K_4(\mathcal{R}_0(\tau) - 1). \quad (3.3.23)$$

Again it follows from Descartes Rule of Signs that (3.3.19) has roots with negative real parts whenever $\mathcal{R}_0(\tau) > 1$. Also, as in (a) above, substituting $\lambda = iy$ in the polynomial (3.3.19), and simplifying, gives

$$\begin{aligned} &-y^2 + (2\mu + \gamma + K_5\mathcal{R}_0(\tau))iy + \mu\gamma + \mu^2 + \mu K_5\mathcal{R}_0(\tau) \\ &= (iy + \mu)K_4\mathcal{R}_0(\tau)(\cos y\tau - i \sin y\tau). \end{aligned} \quad (3.3.24)$$

Separating the real and imaginary parts of Equation (3.3.24) gives

$$\begin{aligned} -y^2 + \mu\gamma + \mu^2 + \mu K_5 \mathcal{R}_0(\tau) &= y K_4 \mathcal{R}_0 \sin y\tau + \mu K_4 \mathcal{R}_0 \cos y\tau, \\ (2\mu + \gamma + K_5 \mathcal{R}_0(\tau))y &= y K_4 \mathcal{R}_0 \cos y\tau - \mu K_4 \mathcal{R}_0 \sin y\tau. \end{aligned} \quad (3.3.25)$$

Further simplifications and squaring, and adding the equations in (3.3.25), gives

$$y^4 + [\mu^2 + K_4^2(\mathcal{R}_0(\tau)^2 - 1)]y^2 + \mu^2 K_4^2(\mathcal{R}_0(\tau)^2 - 1) = 0, \quad (3.3.26)$$

Once again, Descartes Rule of Signs imply that (3.3.26) has no positive real roots whenever $\mathcal{R}_0(\tau) > 1$. As a result, the transcendental equation (3.3.19) has no purely imaginary roots, hence any root λ of (3.3.19) satisfies the relation $\text{Re}\lambda < 0$ for all $\tau \geq 0$ when $\mathcal{R}_0(\tau) > 1$.

(ii) To prove the stability of EE when $\delta > 0$, the polynomials in Equation (3.3.19) are, again, given as

$$\begin{aligned} P(\lambda) &= \lambda^2 + (2\mu + \gamma + \delta + K_5 \mathcal{R}_0(\tau))\lambda + \mu\gamma + \mu^2 + \mu\delta + (\mu + \delta)K_5 \mathcal{R}_0(\tau), \\ Q(\lambda) &= -(\lambda + \mu)K_4. \end{aligned} \quad (3.3.27)$$

Therefore, when $\tau = 0$, the transcendental equation (3.3.19) becomes

$$G(\lambda) = \lambda^2 + [\mu + K_4(\mathcal{R}_0(\tau) - 1)]\lambda + (\mu + \delta)K_4(\mathcal{R}_0(\tau) - 1). \quad (3.3.28)$$

It also follows from Descartes Rule of Signs that all the roots of (3.3.19) have negative real parts whenever $\mathcal{R}_0(\tau) > 1$. Using similar approach as in b(i) above, assuming $\lambda = iy$ is a root of the polynomial (3.3.19), then it implies that

$$\begin{aligned} -y^2 + (2\mu + \gamma + \delta + K_5 \mathcal{R}_0(\tau))iy + \mu(\gamma + \delta) + \mu^2 + (\mu + \delta)K_5 \mathcal{R}_0(\tau) \\ = (iy + \mu)K_4 \mathcal{R}_0(\tau)(\cos y\tau - i \sin y\tau). \end{aligned} \quad (3.3.29)$$

Separating the real and imaginary parts, Equation (3.3.29) can be re-written as

$$\begin{aligned} -y^2 + \mu(\gamma + \delta) + \mu^2 + (\mu + \delta)K_5 \mathcal{R}_0(\tau) &= y K_4 \mathcal{R}_0 \sin y\tau + \mu K_4 \mathcal{R}_0 \cos y\tau, \\ (2\mu + \gamma + \delta + K_5 \mathcal{R}_0(\tau))y &= y K_4 \mathcal{R}_0 \cos y\tau - \mu K_4 \mathcal{R}_0 \sin y\tau, \end{aligned} \quad (3.3.30)$$

which can be simplified as:

$$y^4 + [\mu^2 + K_4(\mathcal{R}_0(\tau) - 1)[K_4(\mathcal{R}_0(\tau) - 1) - 2\delta]]y^2 + (\mu + \delta)K_4^2(\mathcal{R}_0(\tau) - 1)[2\mu + (\mathcal{R}_0(\tau) - 1)(\mu + \delta)] = 0. \quad (3.3.31)$$

With $\mathcal{R}_0(\tau) > 1$, there are two possibilities with regard to the sign of the coefficient of y^2 in the polynomial (3.3.31):

- (iia) If $\mu^2 + K_4(\mathcal{R}_0(\tau) - 1)[K_4(\mathcal{R}_0(\tau) - 1) - 2\delta] > 0$, then (3.3.31) has no positive real roots, therefore the equation (3.3.19) has no imaginary roots. Hence the real parts of all the roots in (3.3.19) are negative for all $\tau \geq 0$.
- (iib) The more interesting case is when $\mu^2 + K_4(\mathcal{R}_0(\tau) - 1)[K_4(\mathcal{R}_0(\tau) - 1) - 2\delta] < 0$, since according to Descartes Rule of Signs there are at most two or zero positive real roots in (3.3.19). Therefore, there exists a critical delay value τ^* such that the EE is LAS for $\tau \in (0, \tau^*)$, while there will be periodic solutions around the point EE, as $\tau > \tau^*$ increases.

The critical delay, τ^* , can be obtained by first simplifying Equation (3.3.30) to have:

$$\begin{aligned} \sin y\tau &= \frac{-P_R Q_I + P_I Q_R}{|Q|^2}, \\ \cos y\tau &= -\frac{P_R Q_R + P_I Q_I}{|Q|^2}, \end{aligned} \quad (3.3.32)$$

where, $P_R = \mu(\gamma + \delta) + \mu^2 + (\mu + \delta)K_5\mathcal{R}_0(\tau) - y^2$, $P_I = (2\mu + \gamma + \delta + K_5\mathcal{R}_0(\tau))y$, $Q_R = -\mu K_4$, $Q_I = -K_4 y$ and $|Q|^2 = Q_R^2 + Q_I^2$.

Therefore, we seek for a unique $\theta = y\tau$, with $\theta \in [0, 2\pi]$, that will satisfy (3.3.32). Dividing the second equation of (3.3.32) by the first gives

$$\theta = \cot^{-1} \left(-\frac{P_R Q_R + P_I Q_I}{-P_R Q_I + P_I Q_R} \right). \quad (3.3.33)$$

Hence the critical delay is given by

$$\tau^* = \frac{\theta}{y}, \quad (3.3.34)$$

where y is any positive root of the polynomial in (3.3.31).

In general, we obtain a sequence of positive values of τ_n , corresponding to any positive root y , given by:

$$\tau_n = \frac{(\theta + 2n\pi)}{y}, \quad \text{for } n = 0, 1, 2, \dots \quad (3.3.35)$$

Thus, for fixed parameter values, and each positive root of (3.3.31), there exists an integer k , such that $\tau^* = \tau_0 < \tau_1 < \tau_2 < \dots < \tau_{k-1} < \tau_k$, as τ varies from 0 to τ_k , we have alternately, switching from stability, when $0 \leq \tau < \tau_0$, $\tau_1 < \tau < \tau_2$, \dots , to instability when $\tau_0 < \tau < \tau_1$, $\tau_2 < \tau < \tau_3$ \dots , and back to stability k times, and eventually, unstable for all $\tau > \tau_k$.

■

3.4 Towards the construction of NSFD scheme for delayed SIS model

3.4.1 Main setting

As stated in Section 3.2, even though the SIS model without delay is simple, it cannot be solved explicitly. The situation is even more challenging for the case of the SIS model with time delay. The results stated in Section 3.3 are strongly related, and come from the linearization of the *SIS* delay model (3.3.1) about the equilibrium as shown in Equation (3.3.15). Using the relation $\hat{S} = \hat{N} - \hat{I}$, the system (3.3.15) can be transformed to

$$\begin{aligned} \frac{d\hat{I}}{dt} = & \left[-\frac{\beta e^{-\mu\tau} S^* I^*}{(S^* + I^*)^2} - \frac{\beta e^{-\mu\tau} I^{*2}}{(S^* + I^*)^2} (\hat{N} - \hat{I})(t) - (\gamma + \mu) \right] \hat{I}(t) \\ & + \frac{\beta e^{-\mu\tau} S^*}{(S^* + I^*)} \hat{I}(t - \tau), \end{aligned} \quad (3.4.1)$$

$$\frac{d\hat{N}}{dt} = \Pi - \mu N + \delta I(t).$$

To motivate what follows, in (3.4.1), when $\delta = 0$ and assuming the total population $N(t)$ is constant. The model (3.3.1) is reduced to

$$\frac{dI}{dt} = \beta e^{-\mu\tau} I(t - \tau) \left[1 - \frac{I(t)}{N} \right] - (\gamma + \mu) I(t), \quad (3.4.2)$$

and the linearized form of (3.4.2) is reduced to the scalar equation

$$\frac{d\hat{I}}{dt} = \beta e^{-\mu\tau} \left[1 - \frac{I^*}{N} \right] \hat{I}(t - \tau) - \left[\frac{\beta e^{-\mu\tau} I^*}{N} + (\gamma + \mu) \right] (\hat{I})(t). \quad (3.4.3)$$

In view of equation (3.4.3), the general setting of this constructive part is therefore a linear delay differential equation (LDDE),

$$\begin{aligned} x'(t) &= Ax(t) + Bx(t - \tau) + f(t) \quad t > 0, \\ x(t) &= \phi(t) \quad t \in [-\tau, 0], \end{aligned} \quad (3.4.4)$$

where A and B are constants, while $f : [0, +\infty) \rightarrow \mathbb{R}$ and $\phi : [-\tau, 0] \rightarrow \mathbb{R}$ are continuous functions, with ϕ being the initial function.

The NSFD scheme consists of two time splits as follows:

- (a) It is an exact scheme at the early time evolution $-\tau \leq t \leq \tau$, where τ is the discrete value of the delay.
- (b) Thereafter, it is a nonstandard finite difference (NSFD) scheme obtained by suitable discretizations at the backtrack points.

The existence and uniqueness Theorem 3.3.4 applies to the linear delay differential equation. However, given the specific nature of this equation, we provide a well-posedness result of the LDDE (3.4.4), which is best fitted to our numerical purpose.

Theorem 3.4.1 *Let A, B be constants and f, ϕ are continuous functions, with ϕ being the initial function, there exists a unique continuously differentiable function $x : [-\tau, +\infty) \rightarrow \mathbb{R}$ which solves LDDE (3.4.4). The solution is represented by the Volterra integral equation*

$$\begin{aligned} x(t) &= \phi(t), \quad t \in [-\tau, 0], \\ x(t) &= e^{At} \phi(0) + \int_0^t e^{A(t-s)} [Bx(s - \tau) + f(s)] ds, \quad t \geq 0. \end{aligned} \quad (3.4.5)$$

Proof. We follow [51] and the integrating factor approach for the proof of this Theorem as follows:

Assume, that f is a continuous function and ϕ is the initial function. Multiplying the first equation in (3.4.4) by e^{-At} , gives

$$e^{-At}[x'(t) - Ax(t)] = e^{-At}[Bx(t - \tau) + f(t)].$$

Integrating both sides over the interval $[0, t]$, gives

$$\begin{aligned} \int_0^t \frac{d}{ds} (e^{-As}x(s)) ds &= \int_0^t e^{-As}[Bx(s - \tau) + f(t)]ds, \\ e^{-At}[x(t) - x(0)] &= \int_0^t e^{-As}[Bx(s - \tau) + f(t)]ds, \\ x(t) &= e^{At}x(0) + e^{At} \int_0^t e^{-As}[Bx(s - \tau) + f(t)]ds, \\ \text{but } x(0) &= \phi(0), \\ \text{hence,} \\ x(t) &= e^{At}\phi(0) + \int_0^t e^{A(t-s)}[Bx(s - \tau) + f(t)]ds. \end{aligned}$$

To prove the uniqueness of solution, we use the principle of mathematical induction as follows:

Assume first of all, that $x(t)$ and $y(t)$ are solutions of (3.4.4) such that $x(t) \neq y(t)$ and the initial function is such that $x(t) = y(t) = \phi(t)$ for $t \in [-\tau, 0]$.

Furthermore, consider the interval $[(k - 1)\tau, k\tau]$, for any $k = 0, 1, 2, \dots$. For $k = 0$, the interval is given by $[-\tau, 0]$, the solution from the initial function is $x(t) = y(t) = \phi(t)$. Assuming the solution is unique for any k so that $x(t) = y(t)$, for $t \in [(k - 1)\tau, k\tau]$.

Therefore, for any integer $k + 1$, the interval is $[k\tau, (k + 1)\tau]$, and the solution (3.4.5), is given by

$$x(t) - y(t) = \int_{\tau}^t e^{A(t-s)}B[x(s - \tau) - y(s - \tau)]ds. \quad (3.4.6)$$

But for any $s \in [k\tau, (k+1)\tau]$ we have $s - \tau \in [(k-1)\tau, k\tau]$. Hence, it follows from the assumption above, that $x(s - \tau) = y(s - \tau)$. Substituting $x(s - \tau) = y(s - \tau)$ into (3.4.6) gives

$$x(t) - y(t) = \int_{\tau}^t e^{A(t-s)} B[x(s - \tau) - x(s - \tau)] ds.$$

Hence,

$$x(t) = y(t), \quad t \in [k\tau, (k+1)\tau].$$

Therefore, the solution is unique ($x(t) = y(t)$) at any interval $[(k-1)\tau, k\tau]$, for any $k = 0, 1, 2, \dots$. This proves the uniqueness of the solution. ■

Regarding the qualitative feature of (3.4.4), we consider the homogeneous equation

$$x'(t) = Ax(t) + Bx(t - \tau), \quad (3.4.7)$$

in which we assume, without loss of generality, that $A + B \neq 0$. Hence, $x = 0$ is the only equilibrium point of (3.4.7). The associated characteristic equation of (3.4.7) is given by

$$\lambda - A - Be^{-\lambda\tau} = 0. \quad (3.4.8)$$

The general Theorem 3.3.5 for stability applies to the LDDE. However, we have, once again, a specific result due to Hayes (Theorem 13.8 in [10]), given below.

Theorem 3.4.2 *The equilibrium $x = 0$ is asymptotically stable, or equivalently, all roots of (3.4.8) have their real parts strictly less than zero if, and only if, the following two conditions hold:*

- (a) $A < 1/\tau$;
- (b) $A < -B < \sqrt{(a_1/\tau)^2 + A^2}$ where a_1 is the root of the equation $a = A \tan a$ with $0 < a_1 < \pi$, $a \in \mathbb{R}$, on the understanding that $a_1 = \pi/2$ if $A = 0$.

In the absence of delay ($\tau = 0$) and if $f \equiv 0$, the LDDE (3.4.4) reduces to

$$x'(t) = (A + B)x(t). \quad (3.4.9)$$

Equation (3.4.9) is the well-known exponential equation [80], which is of paramount importance from both the theoretical and numerical analysis point of view in the study of dynamical systems, without delay, of the form

$$x'(t) = g(x), \quad g(0) = 0. \quad (3.4.10)$$

3.4.2 Combined exact and theta-NSFD schemes

The relevance of (3.4.9) from the constructive point of view hinges on the explicit and implicit knowledge of its exact scheme, which is [80],

$$\frac{x_{n+1} - x_n}{(\exp[(A + B)\Delta t] - 1)/(A + B)} = (A + B)x_n, \quad (3.4.11)$$

or

$$\frac{x_{n+1} - x_n}{[1 - \exp(-(A + B)\Delta t)]/(A + B)} = (A + B)x_{n+1}, \quad (3.4.12)$$

where x_n denotes here and after an approximation of the solution $x(t)$ at the discrete time $t_n = n\Delta t$, $n = 0, 1, 2, \dots$, Δt being the time step size. Most reliable nonstandard finite difference (NSFD) schemes for Equation (3.4.10) are designed on the basis of the exact scheme (3.4.11) or (3.4.12), assuming that (3.4.9) is the linearized equation of (3.4.10) about the trivial equilibrium. We follow similar methodology, for a nonlinear delay differential equation. For the time being, let us focus on the construction of NSFD scheme for the linear delay differential equation (3.4.4).

The ideal situation is to produce its exact scheme. According to Theorem 1.1 in [80], an exact scheme is readily determined once the solution of the continuous differential model is known. However, this theorem does not apply here because the second formula in Theorem 3.4.1 is an integral equation, which therefore does not give the solution explicitly. A further complication with the numerical approximation of the delay differential equation (3.4.4), already observed in the literature [9], is that the backtrack points $(t_n - \tau)$,

$n \geq 0$, do not in general coincide with the grid points. To overcome these difficulties, we proceed as in our paper [44] in which the underlying idea is to use the following time splitting strategy:

- (a) We design an exact scheme of (3.4.4) for early times $t \in [-\tau, \tau]$;
- (b) When $t > \tau$, we switch to the construction of a NSFD scheme.

This leads to the combined exact and θ -NSFD schemes below in which \tilde{x}_n is a suitable approximation of the solution at the backtrack points and $\psi(\Delta t)$ is a complex denominator function to be specified shortly:

$$\frac{x_{n+1} - x_n}{\psi(\Delta t)} = \begin{cases} Ax_n + \frac{1}{\psi(\Delta t)} \int_{t_n}^{t_{n+1}} e^{A(t_{n+1}-s)} (B\phi(s-\tau) + f(s)) ds, & \text{if } t_{n+1} \leq \tau, \\ Ax_n + B\phi(t_n - \tau) + f(t_n), & \text{if } t_n \leq \tau < t_{n+1}, \\ A[(1-\theta)x_n + \theta x_{n+1}] + B[(1-\theta)\tilde{x}_n + \theta \tilde{x}_{n+1}] + f(t_n), & \text{if } t_n > \tau. \end{cases} \quad (3.4.13)$$

To the best of our knowledge, exact schemes have never been constructed for delay differential equations, while the design and implementation of NSFD schemes for such problems are not well developed. We now explain step by step of how the numerical scheme is constructed.

Let $x(t)$ be the unique solution of equation (3.4.4) given in Theorem 3.4.1. Considering the second equation at the discrete times $t_{n+1} = (n+1)\Delta t$ and $t_n = n\Delta t$, we have

$$\begin{aligned} x(t_{n+1}) - x(t_n) &= e^{At_n} (e^{A\Delta t} - 1) \phi(0) \\ &+ \int_0^{t_n} (e^{A\Delta t} - 1) e^{A(t_n-s)} [Bx(s-\tau) + f(s)] ds \\ &+ \int_{t_n}^{t_{n+1}} e^{A(t_n-s)} e^{A\Delta t} [Bx(s-\tau) + f(s)] ds. \end{aligned} \quad (3.4.14)$$

Hence,

$$\begin{aligned} \frac{x(t_{n+1}) - x(t_n)}{\frac{(e^{A\Delta t} - 1)}{A}} &= A \left[e^{At_n} \phi(0) + \int_0^{t_n} e^{A(t_n-s)} (Bx(s-\tau) + f(s)) ds \right] \\ &+ \frac{Ae^{A\Delta t}}{(e^{A\Delta t} - 1)} \int_{t_n}^{t_{n+1}} e^{A(t_n-s)} (Bx(s-\tau) + f(s)) ds. \end{aligned} \quad (3.4.15)$$

By using again the second equation in Theorem 3.4.1, Equation (3.4.15) becomes

$$\frac{x(t_{n+1}) - x(t_n)}{\psi_1(\Delta t)} = Ax(t_n) + \frac{1}{\psi_1(\Delta t)} \int_{t_n}^{t_{n+1}} e^{A(t_{n+1}-s)} (Bx(s-\tau) + f(s)) ds, \quad (3.4.16)$$

where,

$$\psi_1(\Delta t) = \frac{e^{A\Delta t} - 1}{A} = \Delta t + \mathcal{O}(\Delta t^2). \quad (3.4.17)$$

It follows, by applying the mean-value theorem to the integral in (3.4.16), that there exists $s_n \in [t_n, t_{n+1}]$ such that

$$\begin{aligned} & \frac{1}{\psi_1(\Delta t)} \int_{t_n}^{t_{n+1}} e^{A(t_{n+1}-s)} (Bx(s-\tau) + f(s)) ds, \\ &= [Bx(s_n - \tau) + f(s_n)] \frac{1}{\psi_1(\Delta t)} \int_{t_n}^{t_{n+1}} e^{A(t_{n+1}-s)} ds, \\ &= Bx(s_n - r) + f(s_n). \end{aligned} \quad (3.4.18)$$

We consider three different cases regarding the time intervals.

Case 1: Suppose that $t_{n+1} \leq \tau$. Then $s - \tau \leq t_{n+1} - \tau \leq 0$ for $s \in [t_n, t_{n+1}]$. It follows from the first equation in Theorem 3.4.1 that Equation (3.4.16) reduces to the exact scheme:

$$\frac{x(t_{n+1}) - x(t_n)}{\psi_1(\Delta t)} = Ax(t_n) + \frac{1}{\psi_1(\Delta t)} \int_{t_n}^{t_{n+1}} e^{A(t_{n+1}-s)} (B\phi(s-\tau) + f(s)) ds. \quad (3.4.19)$$

Case 2: Suppose that $t_{n+1} > \tau \geq t_n$. In this case, the initial condition (given by the first equation of Theorem 3.4.1) can be used to show that $x(t_n - \tau) = \phi(t_n - \tau)$.

Case 3: Suppose that $t_n > \tau$. In this case, the backtrack point $t_n - \tau$ does not necessarily coincide with a discrete time. Let n^* be the positive integer such that $t_{n^*} \leq t_n - \tau < t_{n^*+1}$. We consider

$$P(t) = x_{n^*+1} \left(\frac{t - t_{n^*}}{\Delta t} \right) - x_{n^*} \left(\frac{t - t_{n^*+1}}{\Delta t} \right), \quad (3.4.20)$$

the Lagrange interpolation polynomial of degree one at the points (t_n^*, x_n^*) and (t_{n^*+1}, x_{n^*+1}) . We approximate $x(t_n - \tau)$ as follows (see Figure 3.2):

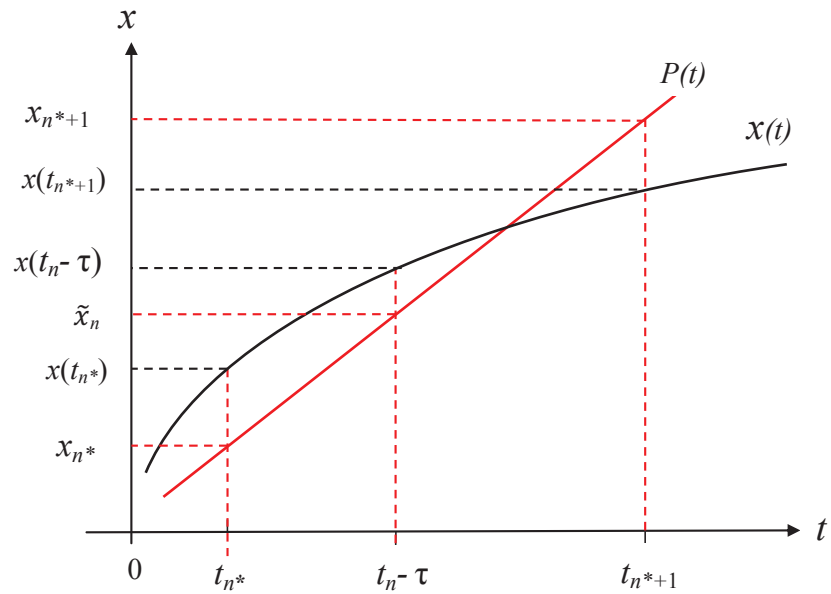


Figure 3.2: Approximation of the delay term $x(t_n - \tau)$.

$$x(t_n - \tau) \simeq \tilde{x}_n := P(t_n - \tau).$$

To make the approximation more explicit, we note that by construction, $n^* < n$ and n^* is the integer part $\left\lfloor \frac{t_n - \tau}{\Delta t} \right\rfloor$ of $\frac{t_n - \tau}{\Delta t}$. It should further be

noted that $n^* = \left\lfloor \frac{t_n - \tau}{\Delta t} \right\rfloor = n - m - 1$, where $m \equiv m_{\Delta t} = \left\lfloor \frac{\tau}{\Delta t} \right\rfloor$.

$$\begin{aligned}\tilde{x}_n &= x_{n^*+1} \left(\frac{t_n - \tau - t_{n^*}}{\Delta t} \right) - x_{n^*} \left(\frac{t_n - \tau - t_{n^*+1}}{\Delta t} \right), \\ &= x_{n^*+1} \left(\frac{(n - n^*)\Delta t - \tau}{\Delta t} \right) - x_{n^*} \left(\frac{(n - n^* - 1)\Delta t - \tau}{\Delta t} \right), \\ &= x_{n-m} \left(\frac{(m+1)\Delta t - \tau}{\Delta t} \right) - x_{n-m-1} \left(\frac{m\Delta t - \tau}{\Delta t} \right),\end{aligned}$$

Setting $u = \frac{(m+1)\Delta t - \tau}{\Delta t} \in [0, 1]$, gives

$$\tilde{x}_n = ux_{n-m} + (1-u)x_{n-m-1}. \quad (3.4.21)$$

In addition to (3.4.21), we consider the following approximation of $x(t_{n+1} - \tau)$:

$$\tilde{x}_{n+1} = ux_{n-m+1} + (1-u)x_{n-m}. \quad (3.4.22)$$

The approximation in (3.4.21) or (3.4.22) is implicit or explicit according as $m = 0$ or $m > 0$.

It follows from the above reasoning that the denominator function $\psi_1(\Delta t)$ appeared naturally. However, for our numerical scheme to capture the parameter values of the continuous model (3.4.4), we use the denominator function

$$\psi_2(\Delta t) = \frac{\Delta t}{1 + (Q\Delta t)^3} = \Delta t + O(\Delta t^3), \quad (3.4.23)$$

where $Q \geq |A| + |B|$. Indeed, the denominator function in (3.4.23) involves the underlying parameters A and B instead of the function $\psi_1(\Delta t)$ in (3.4.17) and (3.4.16). Hence, using the weighted average of (3.4.21) and (3.4.22) through a parameter value $\theta \in [0, 1]$, Equation (3.4.16) is approximated by

$$\begin{aligned}\frac{x_{n+1} - x_n}{\psi_2(\Delta t)} &= A[(1-\theta)x_n + \theta x_{n+1}] + B[(1-\theta)\tilde{x}_n + \theta\tilde{x}_{n+1}] \\ &\quad + [(1-\theta)f(t_n) + \theta f(t_{n+1})].\end{aligned} \quad (3.4.24)$$

It can be observed that when $\theta = 0$, $1/2$ and 1 , we have the nonstandard version of the forward Euler method, trapezoidal rule and backward Euler

method, respectively. To put the three cases together, we introduce the denominator function

$$\psi(\Delta t) = \begin{cases} \psi_1(\Delta t), & \text{in Cases 1 and 2} \\ \psi_2(\Delta t), & \text{in Case 3.} \end{cases} \quad (3.4.25)$$

Assume that the exact solution $x(t)$ is smooth enough and has bounded derivatives, leads to the following combined exact and NSFD results:

Theorem 3.4.3 *The combined Exact-NSFD scheme*

$$\frac{x_{n+1} - x_n}{\psi(\Delta t)} = \begin{cases} Ax_n + \frac{1}{\psi(\Delta t)} \int_{t_n}^{t_{n+1}} e^{A(t_{n+1}-s)} (B\phi(s-\tau) + f(s)) ds, & \text{if } t_{n+1} \leq \tau, \\ Ax_n + B\phi(t_n - \tau) + f(t_n), & \text{if } t_n \leq \tau < t_{n+1}, \\ A[(1-\theta)x_n + \theta x_{n+1}] + B[(1-\theta)\tilde{x}_n + \theta\tilde{x}_{n+1}] \\ + [(1-\theta)f(t_n) + \theta f(t_{n+1})], & \text{if } t_n > \tau, \end{cases}$$

approximates the LDDE (3.4.4) with global error being zero in the time interval $[-\tau, \tau]$.

It should be noted that the numerical method in Theorem 3.4.3 is a NSFD scheme in the sense of [7, 80]. Indeed, the rule on the complex denominator function of the discrete derivatives and the rule of the nonlocal approximation of right hand sides are reinforced.

Remark 3.4.1 *The NSFD theta-method was introduced in [5, 74] for reaction-diffusion equations and general dynamical systems. In these references, other examples of denominator functions satisfying the asymptotic relations in (3.4.17) and (3.4.23) that leads to second order convergence when $\theta = 1/2$ are given. When $t_n > \tau$, computations of the NSFD scheme are performed by observing that it is a linear equation in x_{n+1} which has the explicit solution*

$$x_{n+1} = \begin{cases} \frac{1}{1 - A\theta\psi_2(\Delta t)} \left\{ [1 + A(1-\theta)\psi_2(\Delta t)]x_n + B(1-\theta)\psi_2(\Delta t)\tilde{x}_n \right. \\ \left. + B\theta\psi_2(\Delta t)\tilde{x}_{n+1} + \psi_2(\Delta t)[(1-\theta)f(t_n) + \theta f(t_{n+1})] \right\}, & \text{if } m > 0, \\ \frac{1}{1 - A\theta\psi_2(\Delta t) - B\theta(1-u)\psi_2(\Delta t)} \left\{ [1 + A(1-\theta)\psi_2(\Delta t) + Bu\theta\psi_2(\Delta t)]x_n \right. \\ \left. + B(1-\theta)\psi_2(\Delta t)\tilde{x}_n + \psi_2(\Delta t)[(1-\theta)f(t_n) + \theta f(t_{n+1})] \right\}, & \text{if } m = 0. \end{cases} \quad (3.4.26)$$

The convergence order of convergence of the NSFD scheme are stated in the following result and rigorously proved:

Theorem 3.4.4 *The theta-NSFD scheme (3.4.24) has local truncation error, T_{n+1} , in the time interval $[\tau, \infty)$, given by $\mathcal{O}(\Delta t)$ if $\theta \neq \frac{1}{2}$ and $\mathcal{O}(\Delta t^2)$ if $\theta = \frac{1}{2}$.*

Proof. By definition ([92], pp335), the local truncation error T_{n+1} of the NSFD scheme (3.4.24) is the amount by which the solution of the continuous model fails to satisfy the numerical scheme. Thus replacing all the discrete solutions in (3.4.24) with their exact counterparts we have

$$\begin{aligned} \Delta t T_{n+1} = & x(t_{n+1}) - x(t_n) - \Delta t \{A[(1 - \theta)x(t_n) + \theta x(t_{n+1})] \\ & + B[(1 - \theta)\tilde{P}(t_n - \tau) + \mathcal{O}(\Delta t^2) + \theta\tilde{P}(t_{n+1} - \tau) + \mathcal{O}(\Delta t^2)]\} \\ & + [(1 - \theta)f(t_n) + \theta f(t_{n+1})] \}, \end{aligned} \quad (3.4.27)$$

where $E_n = x(t_n - \tau) - \tilde{P}(t_n - \tau) = \mathcal{O}(\Delta t^2)$.

Next, we Taylor-expand all the involved variables about $x(t_n)$, $f(t_n)$ and $x(t_n - \tau)$ as the case may be in (3.4.27) as follows.

$$\begin{aligned} \Delta t T_{n+1} = & \Delta t x'(t_n) + \frac{\Delta t^2 x''(t_n)}{2!} + \frac{\Delta t^3 x'''(t_n)}{3!} + \dots \\ & - \Delta t \left\{ A \left[(1 - \theta)x(t_n) + \theta x(t_n) + \theta \Delta t x'(t_n) + \frac{\theta \Delta t^2 x''(t_n)}{2!} \right. \right. \\ & \left. \left. + \frac{\theta \Delta t^3 x'''(t_n)}{3!} + \dots \right] + B \left[(1 - \theta)x(t_n - \tau) + \mathcal{O}(\Delta t^2) + \theta x(t_n - \tau) \right. \right. \\ & \left. \left. + \mathcal{O}(\Delta t^2) + \theta \Delta t x'(t_n - \tau) + \frac{\theta \Delta t^2 x''(t_n - \tau)}{2!} + \frac{\theta \Delta t^3 x'''(t_n - \tau)}{3!} + \dots \right] \right. \\ & \left. \left[(1 - \theta)f(t_n) + \theta f(t_n) + \theta \Delta t f'(t_n) + \frac{\theta \Delta t^2 f''(t_n)}{2!} + \dots \right] \right\}. \end{aligned} \quad (3.4.28)$$

Evaluating (3.4.28) when $\theta = \frac{1}{2}$, gives

$$\begin{aligned}
\Delta t T_{n+1} &= \Delta t x'(t_n) + \frac{\Delta t^2 x''(t_n)}{2} + \frac{\Delta t^3 x'''(t_n)}{6} + \dots \\
&\quad - \Delta t \left\{ A \left[x(t_n) + \frac{\Delta t x'(t_n)}{2} + \frac{\Delta t^2 x''(t_n)}{4} + \frac{\Delta t^3 x'''(t_n)}{12} + \dots \right] \right. \\
&\quad \left. + B \left[x(t_n - \tau) + \frac{\Delta t x'(t_n - \tau)}{2} + \frac{\Delta t^2 x''(t_n - \tau)}{4} + \frac{\Delta t^3 x'''(t_n - \tau)}{12} + \dots \right] \right. \\
&\quad \left. + \left[f(t_n) + \frac{\Delta t f'(t_n)}{2} + \frac{\Delta t^2 f''(t_n)}{4} + \dots \right] \right\}. \tag{3.4.29} \\
&= \Delta t x'(t_n) - \Delta t [Ax(t_n) + Bx(t_n - \tau) + f(t_n)] \\
&\quad + \frac{\Delta t^2 x''(t_n)}{2} - \Delta t \left[\frac{A \Delta t x'(t_n)}{2} + \frac{B \Delta t x'(t_n - \tau)}{2} + \frac{\Delta t f'(t_n)}{2} \right] \\
&\quad + \frac{\Delta t^3 x'''(t_n)}{6} - \Delta t \left[\frac{A \Delta t^2 x''(t_n)}{4} + \frac{B \Delta t^2 x''(t_n - \tau)}{4} + \frac{\Delta t^2 f''(t_n)}{4} \right] + \dots.
\end{aligned}$$

With $x'(t_n) = Ax(t_n) + Bx(t_n - \tau) + f(t_n)$ and $x''(t_n) = Ax'(t_n) + Bx'(t_n - \tau) + f'(t_n)$, Equation (3.4.29), becomes

$$\Delta t T_{n+1} = \frac{\Delta t^3 x'''(t_n)}{6} - \Delta t^3 \left[\frac{Ax''(t_n)}{4} + \frac{Bx''(t_n - \tau)}{4} + \frac{f''(t_n)}{4} \right] + \dots,$$

so that,

$$T_{n+1} = \mathcal{O}(\Delta t^2).$$

If $\theta \neq \frac{1}{2}$, it follows from (3.4.28), that

$$\begin{aligned}
 \Delta t T_{n+1} &= \Delta t x'(t_n) + \frac{\Delta t^2 x''(t_n)}{2} + \frac{\Delta t^3 x'''(t_n)}{6} + \dots \\
 &\quad - \Delta t \left\{ A \left[x(t_n) + \theta \Delta t x'(t_n) + \frac{\theta \Delta t^2 x''(t_n)}{2} + \dots \right] \right. \\
 &\quad \left. + B \left[x(t_n - \tau) + \theta \Delta t x'(t_n - \tau) + \frac{\theta \Delta t^2 x''(t_n - \tau)}{2} + \dots \right] \right. \\
 &\quad \left. + \left[f(t_n) + \theta \Delta t f'(t_n) + \frac{\theta \Delta t^2 f''(t_n)}{2} + \dots \right] \right\} . \\
 &= \Delta t x'(t_n) - \Delta t [Ax(t_n) + Bx(t_n - \tau) + f(t_n)] \\
 &\quad + \frac{\Delta t^2 x''(t_n)}{2} - \Delta t^2 [\theta Ax'(t_n) + \theta Bx'(t_n - \tau) + \theta \Delta t f'(t_n)] + \dots , \\
 &= \frac{\Delta t^2 x''(t_n)}{2} - \Delta t^2 [\theta Ax'(t_n) + \theta Bx'(t_n - \tau) + \theta \Delta t f'(t_n)] + \dots , \\
 &= \mathcal{O}(\Delta t^2).
 \end{aligned}$$

Therefore, $T_{n+1} = \mathcal{O}(\Delta t)$.

It follows, by combining these values of T_{n+1} , that:

$$T_{n+1} = \begin{cases} \mathcal{O}(\Delta t), & \text{if } \theta \neq 1/2 \\ \mathcal{O}(\Delta t^2), & \text{if } \theta = 1/2 \end{cases} \quad (3.4.30)$$

■

3.4.3 Dynamic consistency of the NSFD scheme

In this section, we show that the NSFD scheme preserves the stability property of the LDDE (3.4.7), as stated in Theorem 3.4.2. The conditions in this theorem regarding the parameters A, B and τ are supposed to be satisfied in what follows. The NSFD scheme under consideration for (3.4.7) is given by (3.4.26) with $f(t_n) = 0$, i.e.

$$x_{n+1} = \begin{cases} \frac{[1 + A(1 - \theta)\psi_2(\Delta t)]x_n + B(1 - \theta)\psi_2(\Delta t)\tilde{x}_n + B\theta\psi_2(\Delta t)\tilde{x}_{n+1}}{1 - A\theta\psi_2(\Delta t)}, & \text{if } m > 0, \\ \frac{[1 + A(1 - \theta)\psi_2(\Delta t) + Bu\theta\psi_2(\Delta t)]x_n + B(1 - \theta)\psi_2(\Delta t)\tilde{x}_n}{1 - A\theta\psi_2(\Delta t) - B\theta(1 - u)\psi_2(\Delta t)}, & \text{if } m = 0. \end{cases} \quad (3.4.31)$$

It is clear that $x^* = 0$ is the only fixed-point of the NSFD scheme. Thus, it preserves the unique equilibrium point $x^* = 0$ of the LDDE. In view of (3.4.21) and (3.4.22), the characteristic equation of the difference equation (3.4.31) is

$$H(\lambda) \equiv H_{\tau, \Delta t}(\lambda) \equiv a_{m+2}\lambda^{m+2} + a_{m+1}\lambda^{m+1} + a_2\lambda^2 + a_1\lambda + a_0 = 0, \quad (3.4.32)$$

where,

$$a_{m+2} = 1 - A\theta\psi_2, \quad a_{m+1} = -(1 + A(1 - \theta)\psi_2), \quad a_m = \cdots, \quad a_3 = 0,$$

$$a_2 = -B\theta\psi_2u, \quad a_1 = -[B(1 - \theta)\psi_2u + B\theta\psi_2(1 - u)], \quad a_0 = -B(1 - \theta)\psi_2(1 - u),$$

if $m > 0$,

$$\text{and } a_2 = 1 - A\theta\psi_2 - B\theta(1 - u)\psi_2, \quad a_1 = -(1 + A(1 - \theta)\psi_2 + B\psi_2u),$$

$$a_0 = -B(1 - \theta)\psi_2(1 - u), \quad \text{if } m = 0.$$

The stability of the fixed-point using the linear delay difference equation (3.4.31) is given in the following theorem and rigorously achieved in subsequent theorems (see Theorem 3.4.6, Jury conditions and Theorem 3.4.7).

Theorem 3.4.5 *The fixed-point $x^* = 0$ is LAS for equation (3.4.31) if and only if all the roots λ , of (3.4.32) lie within the unit circle: $|\lambda| < 1$*

The task ahead is to check the condition $|\lambda| < 1$ for every m . This is normally done by using the Jury conditions [65]. However, this is a challenge because for fixed τ , the degree m of the polynomial in (3.4.32) increases to ∞ as Δt decreases to zero. Nevertheless, we start by proving the following partial result.

Theorem 3.4.6 *For $A + B < 0$, the roots λ of (3.4.32) satisfy the condition $|\lambda| < 1$ for any m whenever $B > 0$ or $B < 0$ with $A < B$.*

Proof. Equation (3.4.32) is a special case of Volterra difference equations of convolution type investigated in [18]. It follows from Theorem 6.18 of [18] that the condition $|\lambda| < 1$ is satisfied if

$$\begin{aligned} & \frac{1}{|1 - A\theta\psi_2|} [|1 + \psi_2A(1 - \theta)| + |\psi_2B(1 - \theta) + \psi_2B\theta|] \\ & = \frac{1}{|1 - A\theta\psi_2|} [|1 + \psi_2A(1 - \theta)| + |\psi_2B|] < 1. \end{aligned} \quad (3.4.33)$$

Assume that $B > 0$ (so that $A < 0$). Then,

$$\begin{aligned} \frac{1}{|1 - A\theta\psi_2|} [|1 + \psi_2 A(1 - \theta)| + |\psi_2 B|] &= \frac{1}{|1 - A\theta\psi_2|} [|1 - \psi_2 |A|(1 - \theta)| + \psi_2 B], \\ &= \frac{1}{(1 - A\theta\psi_2)} [1 - \psi_2 A\theta + \psi_2(A + B)], \\ &< \frac{(1 - A\theta\psi_2)}{(1 - A\theta\psi_2)}, \text{ since } A + B < 0, \\ &< 1. \end{aligned}$$

Next, we assume that $B < 0$ and $A < B$. Then,

$$\begin{aligned} \frac{1}{|1 - A\theta\psi_2|} [|1 + \psi_2 A(1 - \theta)| + |\psi_2 B|] &= \frac{1}{(1 - A\theta\psi_2)} [|1 - \psi_2 |A|(1 - \theta)| - \psi_2 B], \\ &= \frac{1}{(1 - A\theta\psi_2)} [1 - \psi_2 |A|(1 - \theta) - \psi_2 B], \\ &= \frac{1}{(1 - A\theta\psi_2)} [1 + \psi_2 A - \psi_2 A\theta - \psi_2 A], \\ &\text{since } -B < -A, \\ &< \frac{(1 - A\theta\psi_2)}{(1 - A\theta\psi_2)}, \\ &< 1. \end{aligned}$$

■

Noting Theorem 3.4.6, the challenge raised before this result occurs actually when A and B satisfying the conditions in Theorem 3.4.2 are such that $B < 0$ and $A > B$. Since the Theorem 6.18 of [18], used in the proof of Theorem 3.4.6, is not a necessary condition for $|\lambda| < 1$ to hold, we will for the case under consideration check Theorem 3.4.5 fully for $m = 0, 1$, and partially for $m = 2$.

The case $m = 0$, i.e. $0 \leq \tau < \Delta t$

The Jury conditions for the polynomial in (3.4.32) read:

- (1) $H(1) > 0$, $H(-1) > 0$.
- (2) $a_0 - a_2 < 0$, $a_0 + a_2 > 0$.



By definition,

$$\begin{aligned} H(1) &= 1 - \theta\psi_2(A + B) + B\psi_2\theta u - B\psi_2\theta u - 1 - \psi_2(A + B) + \theta\psi_2(A + B), \\ &= -\psi_2(A + B) > 0, \text{ since } A + B < 0. \end{aligned}$$

Similarly,

$$\begin{aligned} H(-1) &= 2 + \psi_2A - 2\psi_2\theta A + 2\psi_2Bu - \psi_2B, \\ &= 2 + (A - B)\psi_2 - 2\psi_2\theta A + 2\psi_2Bu, \\ &> 2 - 2\psi_2\theta A + 2\psi_2Bu, \text{ as } (A - B) > 0, \\ &> 1 + 2B\psi_2\theta, \text{ } (-A > B), \\ &> 1 + 2B\psi_2\theta \\ &> 0, \end{aligned}$$

since $\psi_2 < \frac{1}{-B}$ in view of the definition of ψ_2 in (3.4.23) which implies that

$$\psi_2 < \frac{1}{|A| + |B|}. \quad (3.4.34)$$

From condition (2) above, we have

$$\begin{aligned} a_0 - a_2 &= -B\psi_2 + B\psi_2u + B\psi_2\theta - B\psi_2u\theta - 1 + A\theta\psi_2 + B\psi_2\theta - B\psi_2\theta u, \\ &< -1 + B - B\psi_2(u - 1) + B\psi_2\theta - B\psi_2\theta + A\theta\psi_2 + B\psi_2\theta - B\psi_2\theta, \\ &< -1 + A\theta\psi_2, \\ &< -1 + B\theta\psi_2, \\ &< 0, \text{ since } B < 0. \end{aligned}$$

Similarly,

$$\begin{aligned} a_0 + a_2 &= -B\psi_2 + B\psi_2u + B\psi_2\theta - B\psi_2u\theta + 1 - A\theta\psi_2 - B\psi_2\theta + B\psi_2\theta u, \\ &= B\psi_2(u - 1) + 1 - A\theta\psi_2, \\ &> B\psi_2(u - 1) + 1 + B\theta\psi_2, \\ &> 1 + B\psi_2, \\ &> 0 \text{ by (3.4.34)}. \end{aligned}$$

Therefore, by the Jury stability conditions, when $m = 0$, all the roots of $H(\lambda)$ lie within the unit circle. Hence, $x^* = 0$ is LAS.

The case $m = 1$, i.e. $\Delta t \leq \tau < 2\Delta t$

The Jury conditions for the polynomial in (3.4.32) read:

$$\begin{aligned} H(1) &> 0, \\ H(-1) &< 0, \\ b_0 - b_2 &< 0, \\ b_0 + b_2 &< 0, \end{aligned} \tag{3.4.35}$$

where,

$$\begin{aligned} b_0 &= (B\psi_2 - B\psi_2u - B\psi_2\theta + B\psi_2\theta u)^2 - (1 - A\theta\psi_2)^2, \\ b_2 &= (B\psi_2 - B\psi_2u - B\psi_2\theta + B\psi_2\theta u)(1 + A\psi_2 - A\theta\psi_2 + B\psi_2\theta u) \\ &\quad + (B\psi_2u - B\psi_2\theta u + B\psi_2\theta - B\psi_2\theta u)(1 - A\theta\psi_2). \end{aligned}$$

The first condition in Equation (3.4.35) is straightforward because $H(1) = -\psi_2(A + B) > 0$ as $A + B < 0$.

Likewise, from the second condition in Equation (3.4.35), we have,

$$\begin{aligned} H(-1) &= -2 + 2\psi_2\theta A - \psi_2(A + B) - 4B\theta\psi_2u + 2B\psi_2\theta + 2B\psi_2u, \\ &< -2 + 2A\psi_2\theta - \psi_2(A + B) - 2B\psi_2u + 2B\psi_2u - 2B\psi_2\theta + 2B\psi_2\theta, \\ &< -2 + 2B\psi_2\theta - \psi_2(-B + B), \quad (B < A, -B > A) \\ &< -2 + B\psi_2\theta \\ &< 0, \quad (B < 0). \end{aligned}$$

From the expression,

$$\begin{aligned}
 b_0 - b_2 &= (B\psi_2 - B\psi_2u - B\psi_2\theta + B\psi_2\theta u)^2 \\
 &\quad - (B\psi_2 - B\psi_2u - B\psi_2\theta + B\psi_2\theta u)(1 + A\psi_2 - A\theta\psi_2 + B\psi_2\theta u) \\
 &\quad - (B\psi_2u - B\psi_2\theta u + B\psi_2\theta - B\psi_2\theta u)(1 - A\theta\psi_2), \\
 &< [B\psi_2\theta(u-1)]^2 - [B\psi_2\theta(u-1)(1 + A\psi_2 - A\theta\psi_2 + B\psi_2\theta u)], \\
 &< B\psi_2\theta(u-1) - 1 - A\psi_2 + A\theta\psi_2 - B\psi_2\theta u, \\
 &< B\psi_2\theta(u-1-u) - 1 - A\psi_2 + A\theta\psi_2, \\
 &< -B\psi_2\theta - 1 - A\psi_2(1-\theta), \text{ if } A > 0, \\
 &< -B\psi_2 - 1, \\
 &< 0, \text{ by (3.4.34)}.
 \end{aligned}$$

If $A < 0$, then

$$\begin{aligned}
 b_0 - b_2 &< -B\psi_2\theta - 1 - A\psi_2(1-\theta), \\
 &< -B\psi_2 - 1 - A\psi_2, \\
 &< 0, \text{ since } \psi_2 < \frac{1}{-(A+B)} \text{ by (3.4.34)}.
 \end{aligned}$$

Similarly, from the fourth condition in Equation (3.4.35),

$$\begin{aligned}
 b_0 + b_2 &= (B\psi_2 - B\psi_2u - B\psi_2\theta + B\psi_2\theta u)^2 \\
 &\quad + (B\psi_2 - B\psi_2u - B\psi_2\theta + B\psi_2\theta u)(1 + A\psi_2 - A\theta\psi_2 + B\psi_2\theta u) \\
 &\quad - (B\psi_2u - B\psi_2\theta u + B\psi_2\theta - B\psi_2\theta u)(1 - A\theta\psi_2), \\
 &< [B\psi_2\theta(u-1)]^2 + [B\psi_2\theta(u-1)(1 + A\psi_2 - A\theta\psi_2 + B\psi_2\theta u)], \\
 &< B\psi_2\theta(u-1) + 1 + A\psi_2 - A\theta\psi_2 + B\psi_2\theta u, \\
 &= B\psi_2\theta(2u-1) + 1 + A\psi_2 - A\theta\psi_2, \\
 &< B\psi_2\theta + 1 + A\psi_2 - B\theta\psi_2, \\
 &< 0, \text{ since } \psi_2 < \frac{1}{|A|} \text{ by (3.4.34)}.
 \end{aligned}$$

From (3.4.35), the Jury stability conditions are satisfied, with $m = 1$, hence all the roots of $H(\lambda)$ lie within the unit circle. Therefore the fixed point

$x^* = 0$ is LAS.

The case $m = 2$, i.e. $2\Delta t \leq \tau < 3\Delta t$

The Jury conditions for the polynomial in (3.4.32) read:

$$\begin{aligned} H(1) &> 0, \\ H(-1) &> 0, \\ a_0 - a_4 &< 0, \\ a_0 + a_4 &> 0, \\ c_0 - c_2 &> 0, \\ c_0 + c_2 &> 0, \end{aligned} \tag{3.4.36}$$

where,

$$\begin{aligned} c_0 &= b_0^2 - b_3^2, \\ &= [(B\psi_2 - B\psi_2u - B\psi_2\theta + B\psi_2\theta u)^2 - (1 - A\theta\psi_2)^2]^2 \\ &\quad - [(B\psi_2 - B\psi_2u - B\psi_2\theta + B\psi_2\theta u)(1 + A\psi_2 - A\theta\psi_2) \\ &\quad + (B\psi_2u - B\psi_2\theta u + B\psi_2\theta - B\psi_2\theta u)(1 - A\theta\psi_2)]^2 \end{aligned}$$

$$\begin{aligned} c_2 &= b_0b_2 - b_1b_3, \\ &= [(B\psi_2 - B\psi_2u - B\psi_2\theta + B\psi_2\theta u)^2 - (1 - A\theta\psi_2)^2] \\ &\quad [((B\psi_2 - B\psi_2u - B\psi_2\theta + B\psi_2\theta u) + (1 - A\theta\psi_2))B\psi_2\theta u] \\ &\quad - [(B\psi_2 - B\psi_2u - B\psi_2\theta + B\psi_2\theta u)(B\psi_2u - B\psi_2\theta u + B\psi_2\theta - B\psi_2\theta u) \\ &\quad + (1 - A\theta\psi_2)(1 + A\psi_2 - A\theta\psi_2)] [(B\psi_2 - B\psi_2u - B\psi_2\theta + B\psi_2\theta u) \\ &\quad (1 + A\psi_2 - A\theta\psi_2) + (B\psi_2u - B\psi_2\theta u + B\psi_2\theta - B\psi_2\theta u)(1 - A\theta\psi_2)] \end{aligned}$$

The the first condition in Equation (3.4.36) is obtained as follows

$$\begin{aligned} H(1) &= -\psi_2(A + B) \\ &> 0, \text{ as } A + B < 0. \end{aligned}$$

To check the second condition in (3.4.36), we have,

$$\begin{aligned} H(-1) &= 2 - 2A\psi_2\theta + A\psi_2 - 4B\theta\psi_2u + 2Bu\psi_2 + 2B\theta\psi_2u + 2B\theta\psi_2 - B\psi_2, \\ &> 2 + \psi_2A(2\theta - 1) - 2\psi_2Bu(2\theta - 1) + B\psi_2(2\theta - 1), \\ &= 2 + \psi_2(2\theta - 1)(A + B) - 2\psi_2Bu(2\theta - 1). \end{aligned}$$

we distinguish two cases :

When $\theta \in [0, 1/2]$, i.e. $(2\theta - 1) \leq 0$, we have

$$\begin{aligned} H(-1) &> 2 - 2\psi_2Bu(2\theta - 1), \\ &> 1 - 1\psi_2B(2\theta - 1), \\ &> 0, \text{ since } \psi_2 < \frac{1}{B(2\theta - 1)}, \text{ by (3.4.34).} \end{aligned}$$

When $\theta \in (1/2, 1]$, i.e. $(2\theta - 1) \geq 0$, we have

$$\begin{aligned} H(-1) &> 2 + \psi_2(2\theta - 1)(A + B) - 2\psi_2Bu(2\theta - 1), \\ &> 1 + \psi_2(2\theta - 1)(A + B), \\ &> 0, \text{ as } \psi_2 < \frac{1}{-(A + B)(2\theta - 1)} \text{ by (3.4.34).} \end{aligned}$$

The third and fourth conditions in Equation (3.4.36) are obtained from (3.4.34) as follows:

$$\begin{aligned} a_0 - a_4 &= -B\psi_2 + B\psi_2u + B\psi_2\theta - B\psi_2u\theta - 1 + A\theta\psi_2, \\ &< -B\psi_2 + B\psi_2\theta u - B\psi_2\theta u - 1 + (A + B)\theta\psi_2, \\ &< -1 - B\psi_2, \\ &< 0, \end{aligned}$$

and,

$$\begin{aligned} a_0 + a_4 &= -B\psi_2 + B\psi_2u + B\psi_2\theta - B\psi_2u\theta + 1 - A\theta\psi_2, \\ &> 1 + (B - A)\psi_2\theta, \\ &> 1 + (B - A)\psi_2, \\ &> 0. \end{aligned}$$

After some computations, the quantities involved in the fifth and sixth conditions in Equation (3.4.36) are given by

$$\begin{aligned}
 c_0 - c_2 = & \left[(B\psi_2(1-\theta)(1-u))^2 - (1 - A\theta\psi_2)^2 \right]^2 \\
 & - \left[(B\psi_2(1-u)(1-\theta))(1 + A\psi_2 - A\theta\psi_2) \right. \\
 & \left. + B\psi_2u(1-\theta) + B\psi_2\theta(1-u)(1 - A\theta\psi_2) \right]^2 \\
 & - \left[(B\psi_2(1-\theta)(1-u))^2 - (1 - A\theta\psi_2)^2 \right] \left[(B\psi_2(1-\theta)(1-u))B\psi_2\theta u \right. \\
 & \left. + (1 - A\theta\psi_2)B\psi_2\theta u \right] + \left[(B\psi_2(1-\theta)(1-u))(B\psi_2u(1-\theta)) \right. \\
 & \left. + (1 - A\theta\psi_2)(1 + A\psi_2 - A\theta\psi_2) \right] \left[(B\psi_2(1-\theta)(1-u))(1 + A\psi_2 - A\theta\psi_2) \right. \\
 & \left. + (B\psi_2u(1-\theta) + B\psi_2\theta(1-u))(1 - A\theta\psi_2) \right],
 \end{aligned} \tag{3.4.37}$$

and,

$$\begin{aligned}
 c_0 + c_2 = & \left[(B\psi_2(1-\theta)(1-u))^2 - (1 - A\theta\psi_2)^2 \right]^2 \\
 & - \left[(B\psi_2(1-u)(1-\theta))(1 + A\psi_2 - A\theta\psi_2) \right. \\
 & \left. + B\psi_2u(1-\theta) + B\psi_2\theta(1-u)(1 - A\theta\psi_2) \right]^2 \\
 & + \left[(B\psi_2(1-\theta)(1-u))^2 - (1 - A\theta\psi_2)^2 \right] \left[(B\psi_2(1-\theta)(1-u))B\psi_2\theta u \right. \\
 & \left. + (1 - A\theta\psi_2)B\psi_2\theta u \right] - \left[(B\psi_2(1-\theta)(1-u))(B\psi_2u(1-\theta)) \right. \\
 & \left. + (1 - A\theta\psi_2)(1 + A\psi_2 - A\theta\psi_2) \right] \left[(B\psi_2(1-\theta)(1-u))(1 + A\psi_2 - A\theta\psi_2) \right. \\
 & \left. + (B\psi_2u(1-\theta) + B\psi_2\theta(1-u))(1 - A\theta\psi_2) \right],
 \end{aligned} \tag{3.4.38}$$

respectively.

Due to the complex expressions (3.4.37) and (3.4.38), the fifth and sixth conditions in (3.4.36) are checked partially (namely for $\theta = 0$ and 1).

When $\theta = 0$, Equation (3.4.37) gives

$$\begin{aligned}
 c_0 - c_2 &= [\psi_2^2 B^2 (1 - u)^2 - 1]^2 - [(1 + \psi_2 A)(\psi_2 B - \psi_2 B u) + \psi_2 B u]^2 \\
 &\quad + [\psi_2^2 B^2 u (1 - u) + (1 + \psi_2 A)] [\psi_2 B (1 + \psi_2 A)(1 - u) + \psi_2 B u], \\
 &\geq -\psi_2^2 B^2 u^2 + [\psi_2^2 B^2 u (1 - u) + (1 + \psi_2 A)] \psi_2 B u, \\
 &= -\psi_2^2 B^2 u^2 + [\psi_2^2 B^2 u - \psi_2^2 B^2 u^2 + 1 + \psi_2 A] \psi_2 B u, \\
 &= -\psi_2 B [\psi_2 B - (\psi_2^2 B^2 - \psi_2^2 B^2 u) - 1 - \psi_2 A], \\
 &> \psi_2 B - 1 - \psi_2 A, \\
 &> 0, \text{ by using } \psi_2 < \frac{1}{(B - A)}, \text{ from (3.4.34)}.
 \end{aligned}$$

Also when $\theta = 1$, Equation (3.4.37) becomes

$$\begin{aligned}
 c_0 - c_2 &= (1 - A\psi_2)^4 - [(B\psi_2(1 - u)(1 - \theta))]^2 - [-(1 - A\psi_2)^2][(1 - A\psi_2)B\psi_2 u] \\
 &\quad + (1 - A\psi_2)B\psi_2(1 - u)(1 - A\psi_2), \\
 &= (1 - A\psi_2)^4 - (B\psi_2(1 - u))^2(1 - \theta)^2 + (1 - A\psi_2)^3 B\psi_2 u \\
 &\quad + (1 - A\psi_2)^2 B\psi_2(1 - u), \\
 &> (1 - A\psi_2)^2 - (B\psi_2(1 - u))^2 + (1 - A\psi_2)B\psi_2 u + B\psi_2(1 - u), \\
 &> (1 - A\psi_2)(1 - \psi_2(A - B)) + (-B\psi_2 u + B\psi_2 u)(B\psi_2 - B\psi_2 u + 1), \\
 &> (1 - A\psi_2)(1 - \psi_2(A - B)), \\
 &> 0, \text{ by (3.4.34)}.
 \end{aligned}$$

If $\theta = 0$, Equation (3.4.38) reduces to

$$\begin{aligned}
 c_0 + c_2 &= [\psi_2^2 B^2 (1 - u)^2 - 1]^2 - [(1 + \psi_2 A)(\psi_2 B - \psi_2 B u) + \psi_2 B u]^2 \\
 &\quad - [\psi_2^2 B^2 u (1 - u) + (1 + \psi_2 A)] [\psi_2 B (1 + \psi_2 A)(1 - u) + \psi_2 B u], \\
 &> -\psi_2^2 B^2 - [\psi_2^2 B^2 u (1 - u) + (1 + \psi_2 A)] \psi_2 B, \\
 &> -\psi_2 B [\psi_2 B + (\psi_2^2 B^2 - \psi_2^2 B^2 u^2) + (1 + \psi_2 A)], \\
 &> \psi_2 B + 1 + \psi_2 A, \\
 &> 0, \text{ by (3.4.34)}.
 \end{aligned}$$

For $\theta = 1$, we have from Equation (3.4.38),

$$\begin{aligned}
 c_0 + c_2 &= (1 - A\psi_2)^4 - [(B\psi_2(1 - u)(1 - \theta))]^2 + [-(1 - A\psi_2)^2] [(1 - A\psi_2)B\psi_2u] \\
 &\quad - (1 - A\psi_2)B\psi_2(1 - u)(1 - A\psi_2), \\
 &= (1 - A\psi_2)^4 - (B\psi_2(1 - u))^2(1 - \theta)^2 \\
 &\quad - (1 - A\psi_2)^3B\psi_2u - (1 - A\psi_2)^2B\psi_2(1 - u), \\
 &> (1 - A\psi_2)^2 - (B\psi_2(1 - u))^2 - (1 - A\psi_2)B\psi_2u - B\psi_2(1 - u), \\
 &> (1 - A\psi_2)(1 - \psi_2(A + B)) - B\psi_2(1 - u)[B\psi_2(1 - u) + 1], \\
 &> 0 \text{ by (3.4.34)}.
 \end{aligned}$$

Since all the conditions in (3.4.36) are satisfied, all the roots, λ of (3.4.32) lie within the unit circle for the case under consideration. Therefore the equilibrium point $x^* = 0$ is asymptotically stable.

Apart from Theorem 3.4.6, the case when $B > 0$ guarantees the dynamic consistency of our NSFD scheme with respect to positivity as stated in the following result:

Theorem 3.4.7 *If $B > 0$, then the NSFD scheme (3.4.31) preserves positivity at all time t whenever the initial conditions are positive.*

Proof. Assume that $B > 0$ and $x_0, x_1, \dots, x_n \geq 0$. From (3.4.21) and (3.4.31) we have, for $m > 0$,

$$\begin{aligned}
 x_{n+1} &= \frac{[1 + A\psi_2(\Delta t) - A\theta\psi_2(\Delta t)]x_n + B(1 - \theta)\psi_2(\Delta t)\tilde{x}_n + B\theta\psi_2(\Delta t)\tilde{x}_{n+1}}{1 - A\theta\psi_2(\Delta t)}, \\
 &> \frac{[1 + A\psi_2(\Delta t) + B\theta\psi_2(\Delta t)]x_n}{1 - A\theta\psi_2(\Delta t)}, \text{ with } B < -A, \\
 &> \frac{[1 - (-A - B\theta)\psi_2(\Delta t)]x_n}{1 - A\theta\psi_2(\Delta t)}, \\
 &> \frac{1 - (-A - B)\psi_2(\Delta t)}{1 - A\theta\psi_2(\Delta t)}, \\
 &> 0, \text{ since } \psi_2 < \frac{1}{-(A + B)} \text{ and } \frac{1}{|A|} \text{ by (3.4.34)}.
 \end{aligned}$$

Similarly, if $m = 0$, we have

$$\begin{aligned}
 x_{n+1} &= \frac{[1 + A\psi_2(\Delta t) - A\theta\psi_2(\Delta t) + Bu\theta\psi_2(\Delta t)]x_n + B(1 - \theta)\psi_2(\Delta t)\tilde{x}_n}{1 - A\theta\psi_2(\Delta t) - B\theta\psi_2(\Delta t) + Bu\psi_2(\Delta t)}, \\
 &> \frac{[1 + A\psi_2(\Delta t) + B\theta\psi_2(\Delta t) + Bu\theta\psi_2(\Delta t)]x_n}{1 - A\theta\psi_2(\Delta t) - B\theta\psi_2(\Delta t) + Bu\psi_2(\Delta t)}, \text{ with } B < -A, \\
 &> \frac{1 - (-A - B\theta)\psi_2(\Delta t)}{1 - (A + B)\theta\psi_2(\Delta t) + B\theta u\psi_2(\Delta t)}, \\
 &> 0, \text{ since } \psi_2 < \frac{1}{-(A + B)}, \text{ by (3.4.34).}
 \end{aligned}$$

■

Remark 3.4.2 *The analyses above reveal the following: For fixed τ , the case when $m = 0$ (i.e. $\Delta t > \tau$) is highly relevant from the nonstandard approach perspective as it allows us to consider arbitrary values of Δt (a situation which is not permissible in the standard numerical analysis setting). In other words, the impact of the delay on the long term dynamics of the model could be to reduce, or to increase, the step size Δt .*

In view of the rigorous analysis done above for $m = 0, 1, 2$, Theorems 3.4.6, 3.4.7 and of the numerical simulation results displayed in Figures 3.6, 3.7 and 3.8, we conjecture that Theorem 3.4.6 is valid in the case when $B < 0$ and $A > B$ meet the requirements in Theorem 3.4.3. Equally, the positivity of the scheme (Theorem 3.4.7) when $B < 0$ is an issue of interest.

3.4.4 Numerical simulations

In this section, we present numerical simulations that support the theoretical results obtained in the previous sections. As mentioned above, and also pointed out in [75], the problem of analysing the location of the zeros of a general polynomial, such as Equation (3.4.32), is a nontrivial one. This is evident when the delay parameter τ , or m , is large. Moreover, at each value there are different conditions to be satisfied by Δt . Hence, the numerical approach is essential. Here, we show the convergence of solution to the fixed point $x^* = 0$ or the asymptotic stability of this fixed point using different

values of the time step size, Δt (different m values), for fixed value of the delay, τ , $\theta = 0, 1/2$ and different values of A and B . In Figures 3.3 (a) and (b), it has been shown that, starting with initial values close to the fixed point, delay $\tau = 2$, $A = -0.7$ and $B = -1.3$, the solutions of (3.4.31) converge to the fixed point $x^* = 0$. Furthermore, the robustness of the NSFD is evident against the Euler scheme and Trapezoidal rule for the same fixed value of the delay. Figures 3.3 (a) and (b) are the results generated by the NSFD, in which the solutions converge irrespective of Δt sizes, in contrast to the Euler scheme and Trapezoidal rule Figures 3.4 (a) and (b) respectively, which diverges even with much smaller values of Δt as indicated. The effect of time delay is also apparent in the two schemes: NSFD, Figure 3.3 (c) and Euler, Figure 3.3 (d) without delay, respectively. It should be noticed that models with delay cause the solutions to oscillate before converging to the fixed point, while such phenomenon is absent from models without delay. Moreover, the Euler scheme without delay causes the trajectories to diverge from the fixed point only with slightly higher values of Δt , compared with the scheme with delay. These facts and simulations regarding models without delay are in agreement with existing results in the literature (see for instance [7]). However, the NSFD scheme still converges even with higher values of Δt .

In Figure 3.5(a), the combined Exact and NSFD schemes are shown with $\theta = 0$. The exact scheme is defined when t is in $[-\tau, \tau]$. When $t > \tau$, the solution of the linear delay differential equation (3.4.7), is shown to be approximated by the NSFD scheme. Figure 3.5 (b), is the Euler scheme in which the exact nature of our scheme is lost and the poor performance of Euler is observed even with much smaller step size. Figure 3.5 (c) depicts Theorem 3.4.7, in which the solution is positive at all times when $B > 0$ for any positive initial condition.

From Theorems 3.4.5 and 3.4.6, the point $x^* = 0$ is LAS fixed point, for Equation (3.4.31) if and only if all the roots of (3.4.32) are within a unit circle. This has been shown analytically for some values of m and in Theorem 3.4.6 for any value of m . For higher values of m , this result can be shown numerically. In Figures 3.6, 3.7 and 3.8 with $\theta = 0, 1/2$ and 1,

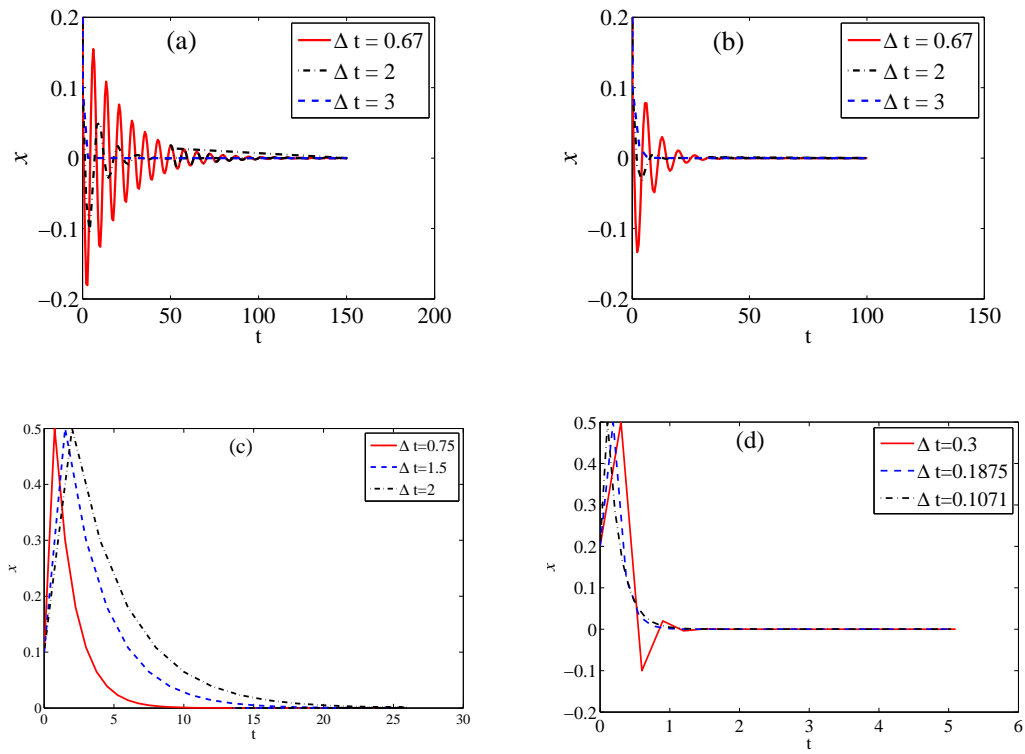


Figure 3.3: Simulations of the NSFD scheme (3.4.26) for $A = -0.7$, $B = -1.3$, $\tau = 2$, in (a) $\theta = 0$ and (b) $\theta = 1/2$, while in (c) NSFD (3.4.26) and (d) Euler schemes, without delay.

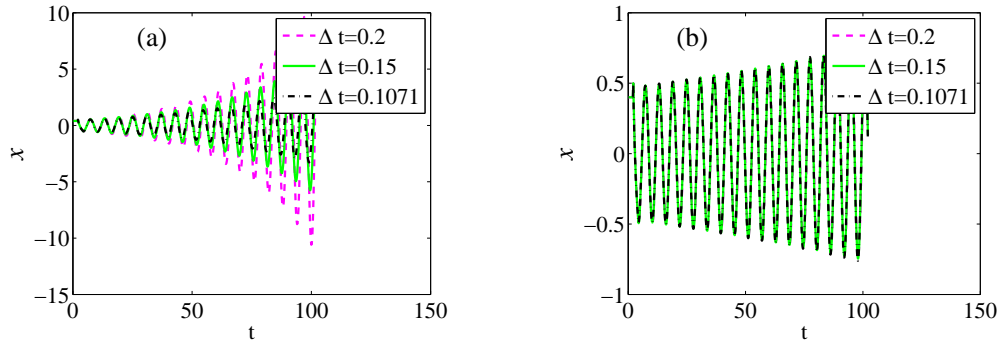


Figure 3.4: Simulations with values of $A = -0.7$, $B = -1.3$ and $\tau = 2$: (a) Euler scheme and (b) Trapezoidal rule.

respectively, it can be seen that all the roots of (3.4.32) are located within the unit circles for values of $m = 0, 1, 2, \dots, 1000$ (different values of time step sizes, Δt) with fixed delay $\tau = 2$ for $B < A < 0$.

3.4.5 NSFD scheme for SIS delay model

The Exact-NSFD scheme presented in the previous section is primarily designed to handle nonlinear epidemiological delay models in a reliable manner. In anticipation to this goal, we first consider the delay logistic equation:

$$\begin{aligned} x'(t) &= Bx(t)[1 - x(t - \tau)], \quad t > 0, \quad B > 0, \\ x(t) &= \phi(t) > 0, \quad -\tau \leq t \leq 0, \end{aligned} \quad (3.4.39)$$

which models the transmission dynamics of a wide range of viral diseases such as gonorrhea [17]. For this model, we consider the NSFD scheme

$$\frac{x_{n+1} - x_n}{\psi(\Delta t)} = \begin{cases} -\frac{B}{\psi(\Delta t)} \int_{t_n}^{t_{n+1}} \phi(s - \tau) ds + \frac{\Delta t}{\psi(\Delta t)} B - B(x_n - 1)[\phi(t_n - \tau) - 1], & \text{if } t_{n+1} \leq \tau, \\ B\phi(t_n - \tau) + B - B(x_n - 1)[\phi(t_n - \tau) - 1], & \text{if } t_n \leq \tau < t_{n+1}, \\ \begin{aligned} & -B(1 - \theta)\tilde{x}_n - B\theta\tilde{x}_{n+1} + B \\ & -B[(1 - \theta)x_n + \theta x_{n+1} - 1][(1 - \theta)\tilde{x}_n + \theta\tilde{x}_{n+1} - 1], \end{aligned} & \text{if } t_n > \tau. \end{cases} \quad (3.4.40)$$

It is clear that the NSFD scheme (3.4.40) reduces to the combined Exact-NSFD scheme for the linearized delay logistic equation about the asymp-

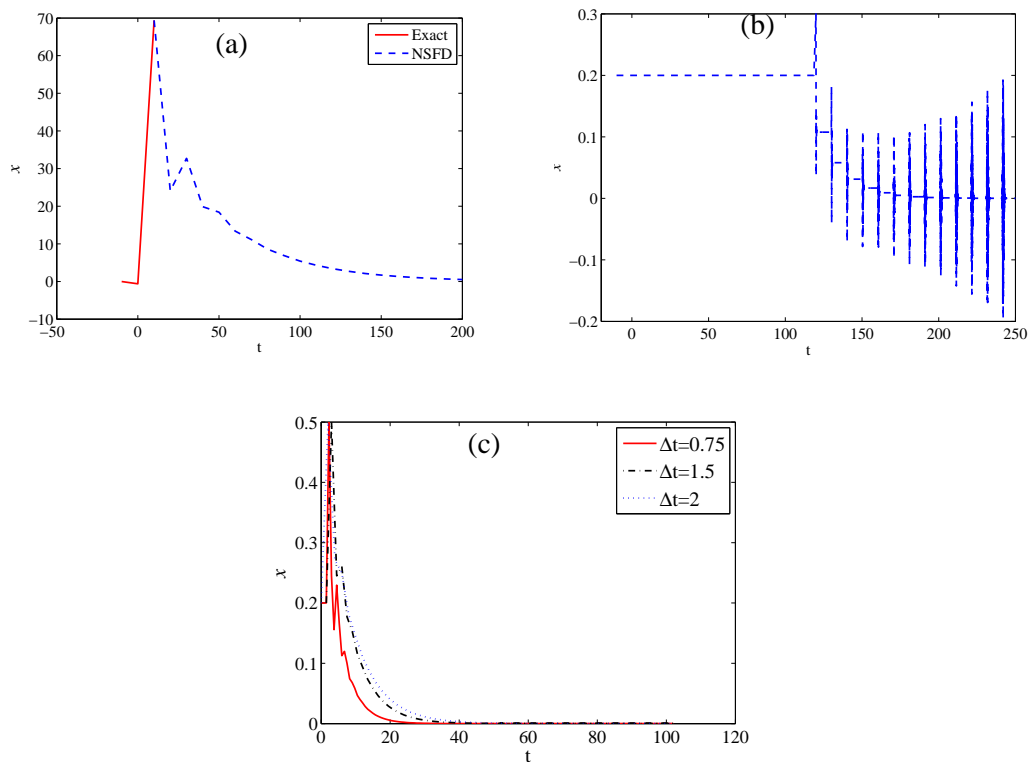


Figure 3.5: Simulations with $A = -13, B = 7, \tau = 10$; of (a) Combined exact-NSFD scheme (3.4.26), with $\Delta t = 10, \theta = 0$ (b) Euler scheme, $\Delta t = 0.11$ (c) the NSFD scheme (3.4.26), illustrating positivity of solution (Theorem 3.4.7).

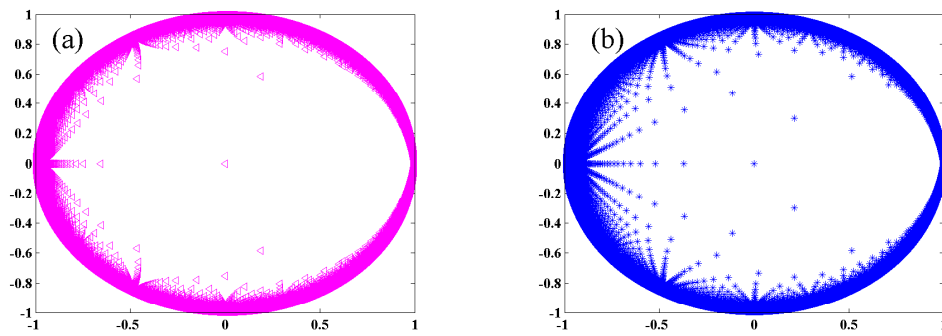


Figure 3.6: Simulations showing the roots of the characteristic polynomial for (3.4.32) within unit circles corresponding to values of $m = 0, 1, 2, \dots, 1000$ (different values of Δt), $\tau = 2$, $A = -1.3$, $B = -1.7$ in (a) $\theta = 0$, (b) $\theta = 1/2$.

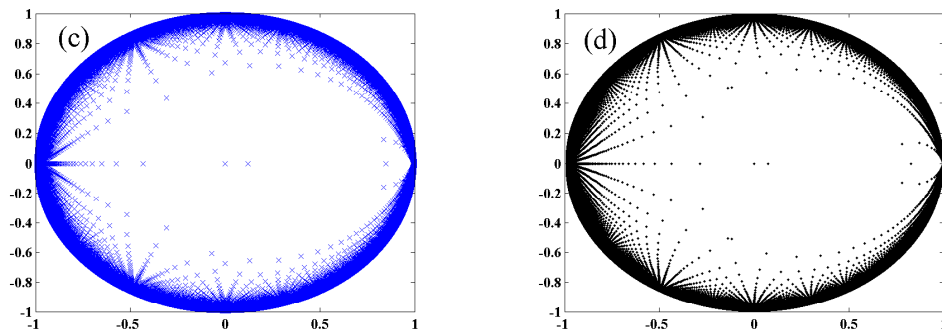


Figure 3.7: Simulations showing the roots of the characteristic polynomial for (3.4.32) within unit circles corresponding to values of $m = 0, 1, 2, \dots, 1000$ (different values of Δt), $\tau = 0.54$, $A = 1.3$, $B = -1.7$ in (c) $\theta = 0$, (d) $\theta = 1/2$.

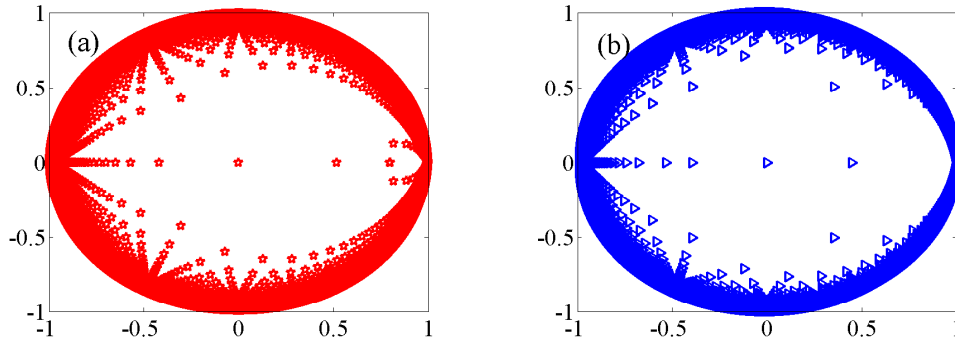


Figure 3.8: Simulations showing the roots of the characteristic polynomial for (3.4.32) within unit circles corresponding to values of $m = 0, 1, 2, \dots, 1000$ (different values of Δt), $\theta = 1$, in (a) $\tau = 0.54$, $A = 1.3$, $B = -1.7$ in (b) $\tau = 2$, $A = -1.3$, $B = -1.7$.

totically stable fixed point $x^* = 1$ when we ignore the nonlinear term, $B[(1 - \theta)x_n + \theta x_{n+1} - 1][(1 - \theta)\tilde{x}_n + \theta\tilde{x}_{n+1} - 1]$.

For computation, we use the following explicit expression instead of (3.4.40):

$$x_{n+1} = x_n + \begin{cases} -B \int_{t_n}^{t_{n+1}} \phi(s - \tau) ds + \Delta t B - B\psi(x_n - 1)[\phi(t_n - \tau) - 1], & \text{if } t_{n+1} \leq \tau, \\ B\psi\phi(t_n - \tau) + B\psi - B\psi(x_n - 1)[\phi(t_n - \tau) - 1], & \text{if } t_n \leq \tau < t_{n+1}, \\ -B\psi(1 - \theta)\tilde{x}_n - B\psi\theta\tilde{x}_{n+1} + B\psi, & \text{if } t_n > \tau. \end{cases} \quad (3.4.41)$$

The illustration of the NSFD scheme (3.4.40) or (3.4.41) is carried out for $\psi_2 = \frac{\Delta t}{1 + (|B|\Delta t)^2}$, $\phi(t) = 1 + e^t$, the set of values $\tau = 5.1$, $B = 0.31$ and $A = 0$ i.e. $a_1 = \pi/2$. In accordance with the dynamics of the delay logistic equations in [18]. Figure 3.9 shows the NSFD scheme in which the fixed point $x^* = 1$ is asymptotically stable for $0 < B < \pi/2\tau$, irrespective of the step sizes used. The profiles of the discrete solutions confirm that the trapezoidal NSFD scheme ($\theta = 1/2$) is more accurate than the Euler NSFD scheme ($\theta = 0$). On the contrary, Figure 3.10 displays the poor performance of both classical Euler and trapezoidal schemes.

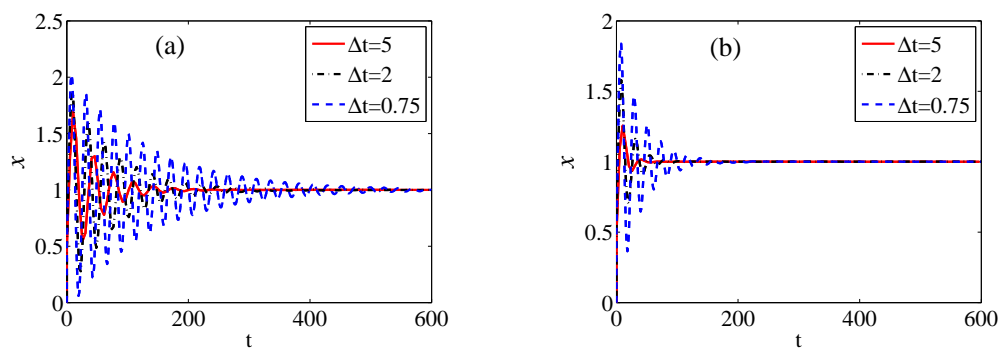


Figure 3.9: Simulations for NSFD scheme (3.4.41) using $\tau = 5.1$, $B = 0.31$; in (a) $\theta = 0$ (b) $\theta = 1/2$.

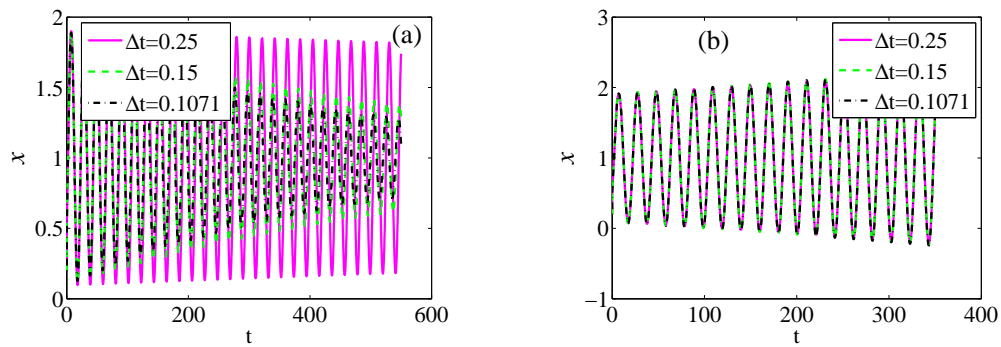


Figure 3.10: Numerical simulations For $\tau = 5.1$ and $B = 0.31$: using (a) the Euler scheme (b) Trapezoidal rule.

Next, we consider the SIS delay model (3.3.1)-(3.3.2), which is the central point of this chapter. For mathematical convenience, we assume that there is no disease induced death rate (i.e. $\delta = 0$). The SIS delay model (3.3.1), with $\delta = 0$, takes then the equivalent form

$$\begin{aligned}\frac{dI}{dt} &= \frac{\beta e^{-\mu\tau} I(t-\tau)(N-I)(t)}{N(t)} - (\gamma + \mu)I(t), \\ \frac{dN}{dt} &= \Pi - \mu N(t).\end{aligned}\tag{3.4.42}$$

The exact solution of the second equation in (3.4.42) with initial condition $0 \leq N(0) \leq \frac{\Pi}{\mu}$ is given by

$$N(t) = e^{-\mu t} \left[N(0) - \frac{\Pi}{\mu} \right] + \frac{\Pi}{\mu}.\tag{3.4.43}$$

To motivate our construction of the NSFD scheme for (3.4.42), we assume that the total population $N(t) \equiv N$ is constant, the system (3.4.42) is then reduce to the scalar equation

$$\frac{dI}{dt} = \beta e^{-\mu\tau} \left[1 - \frac{I(t)}{N} \right] I(t-\tau) - (\gamma + \mu)I(t).\tag{3.4.44}$$

Inspired by the construction done above for the logistic delay equation, we have the following forward Euler ($\theta = 0$) NSFD scheme for (3.4.44):

$$\frac{I_{n+1} - I_n}{\phi(h)} = -\beta e^{-\mu\tau} \left(1 - \frac{I_n}{N} \right) \tilde{I}_n - (\gamma + \mu)I_{n+1},\tag{3.4.45}$$

where we recall that $\tilde{I}_n = uI_{n-m} + (1-u)I_{n-m-1}$, with u and m as defined in Section 3.4.2.

Let us now consider the case when N is not constant in (3.4.42). In this case, the exact scheme of (3.4.42)₂ is well-known and is given by

$$\frac{N_{n+1} - N_n}{h} = \Pi - \mu N_{n+1}.\tag{3.4.46}$$

In view of this fact and of (3.4.45), it is natural to consider the following forward Euler NSFD scheme for the nonlinear delay model (3.4.44):

$$\frac{I_{n+1} - I_n}{\phi(h)} = -\beta e^{-\mu\tau} I_n \frac{\tilde{I}_n}{N_n} + \beta e^{-\mu\tau} \tilde{I}_n - (\gamma + \mu)I_{n+1}.\tag{3.4.47}$$

We have restricted ourselves to forward Euler NSFD scheme, though other cases ($\theta \neq 0$) can also be formulated.

In explicit form, equation (3.4.47) can be express as

$$I_{n+1} = \frac{\phi(h)\beta e^{-\mu\tau} \tilde{I}_n \left(1 - \frac{I_n}{N_n}\right) + I_n}{1 + \phi(h)(\gamma + \mu)}. \quad (3.4.48)$$

The equivalent representation (3.4.48) of the NSFD scheme (3.4.47) suggests that the scheme preserves the essential features of the continuous model (3.3.1) such as positivity of solution and equilibria. The rigorous qualitative analysis of this NSFD scheme is outside the scope of this thesis. Here, we are simply interested in providing numerical simulations that legitimate the suggestion made above.

In what follows, we give numerical simulations for the NSFD scheme (3.4.48). The parameter values used are: $\Pi = 50$, $\mu = 0.026$, $\gamma = 0.012$, with varying values, of β and τ to differentiate between the DFE, EE and the effect of delay on the infectivity of the disease respectively. The numerical

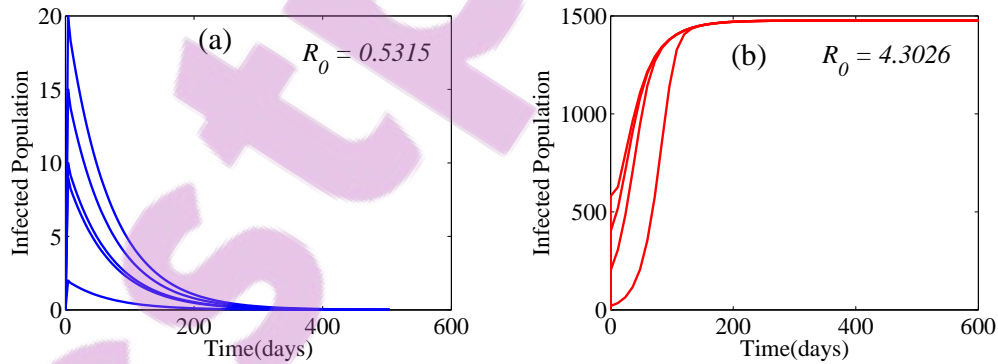


Figure 3.11: Simulations for NSFD scheme (3.4.48) in (a) $h = 4$, $\beta = 0.021$ (b) $h = 12$, $\beta = 0.17$ for Endemic fixed point.

simulation of NSFD scheme (3.4.48) in Figure 3.11, illustrating the convergence of the infected individuals in (a) to disease free fixed point, where $\mathcal{R}_0 = 0.5315 < 1$, and in (b) to endemic fixed point, where $\mathcal{R}_0 = 4.3026 > 1$, using different values of initial conditions.

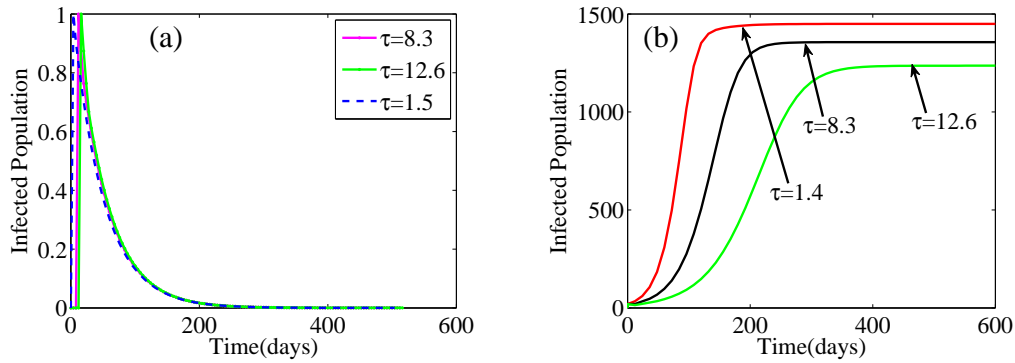


Figure 3.12: Simulations of NSFD scheme (3.4.48) for (a) $h = 4$, $\beta = 0.014$, (b) $h = 12$, $\beta = 0.16$.

Figure 3.12 (a), depicts the numerical simulations of the NSFD scheme (3.4.48) with $\tau = 1.5, 8.3$ and 12.6 so that $\mathcal{R}_0 = 0.3543, 0.2969$ and 0.2655 , respectively, where the population of infected individuals converges to the disease free fixed point. This agree with the result of the continuous model in Theorem 3.3.5 (a). The numerical simulation in Figure 3.12 illustrate, in (b), with $\tau = 1.4, 8.3$ and 12.6 so that $\mathcal{R}_0 = 4.060, 3.4021$ and 2.7994 , respectively. This results, on the other hand, illustrate the endemic fixed point and the effect of delay value on the number of infected individuals. This also coincide with the result of the continuous model in Theorem 3.3.5 (b), when disease induced death rate $\delta = 0$.

CHAPTER 4

MODELING TRANSMISSION DYNAMICS OF BTB-MTB IN HUMAN-BUFFALO POPULATION

4.1 Introduction

This chapter focuses on the second main objective of the thesis, which is to model the transmission dynamics of *Bovine* and *Mycobacterium* (BTB-MTB) tuberculosis within a human-buffalo population. The aim is to gain qualitative insight into the transmission dynamics of the two diseases and, by so doing, contribute to the design of public health policy for effectively combatting their spread.

Mycobacterium tuberculosis and *Bovine* tuberculosis are chronic bacterial diseases classified amongst the closely-related species that form the *M. tuberculosis* complex (MTBC) [39]. The human MTB is caused by *tubercle bacillus* (*Mycobacterium tuberculosis*), while BTB is caused by *bovine bacillus* (*M. bovis*) [45]. Both MTB and BTB affect a wide range of hosts, including domestic livestock (such as cattle, goats, sheep, deer, bison, etc), wildlife (such as badgers, deer, bison, African buffalo, etc) which can either

List of research project topics and materials

be reservoir or spill-over, and humans [30].

Mycobacterium tuberculosis remains a major global health problem affecting millions of people each year [115]. It is ranked second to HIV as a leading cause of death worldwide [115]. For instance, in the year 2012, there were 8.6 million new MTB cases and 1.3 million MTB deaths globally [115]. Similarly, BTB remains a serious problem for animal and human health in many developing countries [41]. Its widespread distribution has drastic negative socio-economic development in terms of public health, international trade, tourism, animal mortality and milk production [40]. For example, in Argentina, the annual loss due to BTB is estimated to be US\$ 63 million [8]. A benefit/cost analyses of BTB eradication in the United States showed an actual cost of US\$ 538 million between 1917-1992 (current programs cost approximately US\$ 3.5-4.0 million *per year* [41]).

The African buffalo transmits BTB to humans, *via* aerosol or oral (as a result of consuming raw unpasteurized milk) [39]. Furthermore, BTB can be transmitted from human-to-human by direct contact [39]. As in cattle, the main source of BTB transmission in buffalo is by direct contact, aerosol, oral, through a bite or contamination of a skin wound [30] (other means of transmission, such as vertical and pseudo-vertical [31], also occur). Similarly, MTB can be transmitted from human-to-human, or from human to buffalo, *via* coughing or sneezing [39]. In humans, MTB is regarded to be airborne disease [36]. It typically affects the lungs (pulmonary TB), but can affect other parts of the body also (extrapulmonary TB) [30]. Common signs and symptoms of MTB include coughing, chest pain, fever, weakness and weight loss. The incubation period for MTB is approximately 2 to 12 weeks. African buffalos infected with BTB show clinical signs only when the disease has reached an advanced stage (the clinical signs of BTB in buffalo at such stage include: coughing, debilitation, poor body condition or emaciation and lagging when chased by helicopter [30, 31]). The incubation period for BTB is between 9 months to a year, and infections can remain dormant for years, and reactivate during periods of stress or in old age [40].

Bovine tuberculosis is typically controlled using isolation or quarantine of infected herds, test-and-slaughter policy, and pasteurization of milk [27]. In

South Africa's Kruger National Park, other control measures, such as culling, vaccination and their combination, are used [27] (a demographic map of KNP and sample of African Buffalos [89] is shown in Figure 4.1). Similarly, MTB in humans is controlled *via* standard six-month course of four antimicrobial drugs [1, 2, 13, 14]. The World Health Organization embarked on numerous global initiatives, such as "Stop TB Partnership", "International Standards of Tuberculosis care and patient's care" and the "Global Plan to Stop TB", with the hope of minimizing the burden of TB worldwide [1].

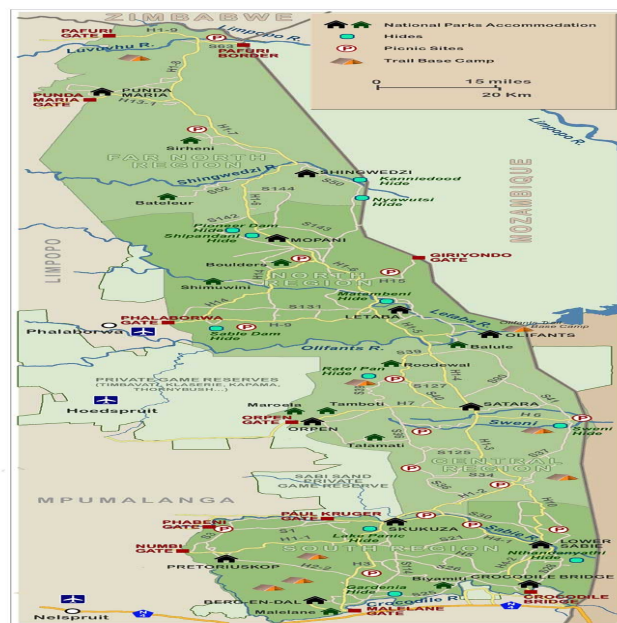
Several mathematical models have been used to gain insight into the transmission dynamics of BTB or MTB in populations (see, for instance, [1, 2, 6, 21, 27, 31, 67, 105] and some of the references therein). In these models, the underlying delay from initial infection to onset of symptoms (incubation period) is captured by using a compartment of exposed individuals. Furthermore, these studies do not incorporate humans in the transmission dynamics of BTB.

The main objective of this chapter is to gain insight into the qualitative dynamics of the two diseases in a human-buffalo population. To achieve this objective, a new deterministic model for the transmission dynamics of the two diseases will be design and rigorously analyse. A brief review of existing models for the two diseases individually is given below (the full BTB-MTB model will be designed based on gradual refinement of these models). Numerical simulations will be carried out to illustrate the theoretical results derived.

4.2 Basic SEIR model for TB

In this section, we consider the dynamics of a typical SEIR model for the transmission dynamics of bovine tuberculosis in a population of African buffalo. The population is divided into four mutually-exclusive epidemiological subpopulations consisting of susceptibles (S), exposed (E), infected but not yet infectious), infectious (I), and recovered (R), buffalos, so that the total buffalos population (N) is given by $N = S + E + I + R$. It is assumed that buffalos can be infected only through contact with infectious buffalos,

(a)



(b)



Figure 4.1: Demographic map of Kruger National Park and African buffalos [89].

and that recovery confers permanent (natural) immunity against re-infection. This model can be viewed as one strain *SEIT* model considered in ([20], page 370) when the treated class T is assumed to be recovered (through natural immunity or long term latency - no treatment) or the model in [105] when there is no relapse of BTB by the recovered class. It can also be considered as the general SEIR model for an infectious disease where the death rate depends on the number of individuals in the population as in [46]. The two diseases belongs to the same family as stated in the introduction, hence, the results of these models were adopted with this assumption on treated class. The model is given by the following system of differential equations The model can be formulated using the following system of ordinary differential equations:

$$\begin{aligned}\frac{dS}{dt} &= \Lambda - \beta c S \frac{I}{N} - \mu S, \\ \frac{dE}{dt} &= \beta c S \frac{I}{N} - (\mu + k)E, \\ \frac{dI}{dt} &= kE - (\mu + r + d)I, \\ \frac{dR}{dt} &= rI - \mu R, \\ N &= S + E + I + R,\end{aligned}\tag{4.2.1}$$

where Λ is the constant recruitment rate, β is the probability of a susceptible buffalos following contact with an infected buffalo, c is the *per-capita* contact rate, μ and d are the *per-capita* natural and disease-induced death rates, respectively. The parameter k is the progression rate from the exposed to infectious class and r is the recovery rate.

The basic reproductive number of the model (4.2.1) is given by

$$\mathcal{R}_0 = \left(\frac{\beta c}{\mu + r + d} \right) \left(\frac{k}{\mu + k} \right),$$

which represent the product of the infection rate of buffalos (βc), the fraction of buffalos that survived the exposed class and move to the infectious class ($\frac{k}{\mu + k}$) and the average duration in the infectious class ($\frac{1}{\mu + r + d}$). It is

convenient to define the biologically-feasible region

$$G = \left\{ (S, E, I, R) \in \mathbb{R}_+^4, S + E + I + R \leq \frac{\Lambda}{\mu} \right\}.$$

The following result is established:

Theorem 4.2.1 *The DFE $E^0 = \left(\frac{\Lambda}{\mu}, 0, 0, 0\right)$ of the model (4.2.1) is GAS in G whenever $\mathcal{R}_0 \leq 1$, and unstable if $\mathcal{R}_0 > 1$. The model has a unique, and GAS, EE whenever $\mathcal{R}_0 > 1$.*

4.3 A model for TB with exogenous reinfection

A major feature of TB disease is the phenomenon of exogenous reinfection (which is the potential reactivation of BTB (MTB) by continuous exposure of latently-infected (exposed) individuals to those who have active infections) [20, 22]. The model (4.2.1) is therefore extended to incorporated the effect of reinfection given by the system of differential equations [38] as follows, where the treated class is assumed to be recovered:

$$\begin{aligned} \frac{dS}{dt} &= \Lambda - \beta c S \frac{I}{N} - \mu S, \\ \frac{dE}{dt} &= \beta c S \frac{I}{N} - p \beta c E \frac{I}{N} - (\mu + k) E, \\ \frac{dI}{dt} &= p \beta c E \frac{I}{N} + k E - (\mu + r + d) I, \\ \frac{dR}{dt} &= r I - \mu R, \\ N &= S + E + I + R, \end{aligned} \tag{4.3.1}$$

where the parameters $\Lambda, \beta, c, \mu, k, r$ and d are as defined above. Reinfection of exposed buffalos is represented by the term $p \beta c E \frac{I}{N}$, where $p \in (0, 1)$ accounts for the assumption that reinfection occurs at a rate lower than primary infection.

The associated basic reproduction number for the model (4.3.1) is given by

$$\mathcal{R}_0 = \left(\frac{\beta c}{\mu + r + d} \right) \left(\frac{k}{\mu + k} \right).$$

The biologically-feasible region is given by

$$\Omega = \left\{ (S, E, I, R) | S, E, I, R \geq 0, N \leq \frac{\Lambda}{\mu} \right\}.$$

The model (4.3.1), has unique DFE $(\Lambda/\mu, 0, 0, 0)$ which is GAS when $\mathcal{R}_0 < 1$ and $p = 0$. However, when there is exogenous reinfection ($0 < p < 1$), system (4.3.1) exhibits a backward bifurcation (subcritical) at $\mathcal{R}_0 = 1$. Hence multiple endemic equilibria can occur for $\mathcal{R}_0 < 1$. The conditions for stability of equilibria are summarized in the following results [38]:

Let $p_0 = \frac{(1+Q)D_E}{1-D_E}$ be the critical value, where $D_E = \frac{k}{\mu+k}$, $Q = \frac{k}{\mu+r}$, and $\mathcal{R}_p = \frac{1}{p}[D_E(1+p-Q) + 2\sqrt{D_E Q(p-pD_E-D_E)}]$

Theorem 4.3.1 *Let $U_+^* = (S_+^*, E_+^*, I_+^*, T_+^*)$ and $U_-^* = (S_-^*, E_-^*, I_-^*, T_-^*)$ be the two endemic equilibria with $I_+^* > I_-^* > 0$. Then*

- (i) *If $\mathcal{R}_0 < 1$, then the disease free equilibrium is LAS.*
- (ii) *If $p > p_0$ and $\mathcal{R}_p < \mathcal{R}_0 < 1$, then U_+^* is LAS, and U_-^* is unstable.*
- (iii) *If $\mathcal{R}_0 > 1$, then the disease free equilibrium is unstable and the unique endemic equilibrium is LAS.*

4.4 A model for TB with exogenous reinfection and two stage exposed classes

Another important epidemiological feature of TB disease in African buffalo is the early and late-exposure to the disease [2, 20]. Below is a BTB transmission model that allows for early-and late-exposed classes [20], when the two TB strains are considered to be exposed classes without treatment and

the bovine tuberculosis model in [2] with no test-reactor classes:

$$\begin{aligned}
 \frac{dS}{dt} &= \Lambda - (\lambda + \mu)S, \\
 \frac{dE_1}{dt} &= \lambda S - (\theta_E \lambda + \kappa + \mu)E_1, \\
 \frac{dE_2}{dt} &= \kappa E_1 - (\theta_E \lambda + \sigma + \mu)E_2, \\
 \frac{dI}{dt} &= \sigma E_2 + (E_1 + E_2)\theta_E \lambda + \theta_R \lambda R - (\gamma + \mu + \delta)I, \\
 \frac{dR}{dt} &= \gamma I - (\theta_R \lambda + \mu)R, \\
 N &= S + E_1 + E_2 + I + R,
 \end{aligned} \tag{4.4.1}$$

Here, the force of infection, $\lambda = \frac{\beta I}{N}$. The result of the model (4.4.1) is stated below:

Theorem 4.4.1 *The biologically-feasible region of the model (4.4.1) is given by*

$$\Omega = \left\{ (S, E_1, E_2, I, R) \in \mathbb{R}_+^5 : S + E_1 + E_2 + I + R \leq \frac{\Lambda}{\mu} \right\}.$$

The basic reproduction number of the model is given by

$$\mathcal{R}_0 = \frac{\beta[\eta_1 C_2 C_3 + \kappa(\eta_2 C_3 + \gamma)]}{C_1 C_2 C_3}, \quad C_1 = \kappa + \mu, \quad C_2 = \sigma + \mu, \quad C_3 = \gamma + \mu + \delta.$$

- (i) *The DFE of the model, $E_0 = (\Lambda/\mu, 0, 0, 0, 0)$, is LAS if $\mathcal{R}_0 < 1$ and unstable if $\mathcal{R}_0 > 1$.*
- (ii) *The model undergo backward bifurcation when $\mathcal{R}_0 = 1$ under certain condition, i.e. there will be coexistence of DFE and EE for $\mathcal{R}_0 \leq 1$.*
- (iii) *In the absence of reinfection of exposed and recovered buffalos, there exists a unique EE, whenever $\mathcal{R}_0 > 1$ and no EE otherwise.*

4.5 The model of tuberculosis in human-African buffalo population

Based on the existing models described in the previous sections, we design and rigorously analyse a new model, used to gain the dynamical insight into the transmission dynamics of BTB and MTB in a given population consisting of both African buffalos and humans as follows:

4.5.1 Model formulation

The model to be designed is based on the transmission dynamics of MTB and BTB in a population consisting of humans and African buffalos. The total human population at time t , denoted by $N_H(t)$, is sub-divided into seven mutually-exclusive compartments of susceptible humans ($S_H(t)$), exposed humans (who have been infected with MTB but have not yet shown clinical symptoms of the disease) ($E_{H1}(t)$), exposed humans with BTB ($E_{H2}(t)$), infected humans with clinical symptoms of MTB ($I_{H1}(t)$), infected humans with clinical symptoms of BTB ($I_{H2}(t)$), humans who recovered from MTB ($R_{H1}(t)$) or BTB ($R_{H2}(t)$), so that

$$N_H(t) = S_H(t) + E_{H1}(t) + E_{H2}(t) + I_{H1}(t) + I_{H2}(t) + R_{H1}(t) + R_{H2}(t).$$

Similarly, the total buffalo population at time t , denoted by $N_B(t)$, is split into susceptible ($S_B(t)$), early-exposed with BTB ($E_{B1}(t)$), early-exposed with MTB ($E_{M1}(t)$), advanced-exposed with BTB ($E_{B2}(t)$), advanced-exposed with MTB ($E_{M2}(t)$), infected with clinical symptoms of BTB ($I_{BB}(t)$), infected with clinical symptoms of MTB ($I_{MB}(t)$), recovered from BTB ($R_{BB}(t)$) or MTB ($R_{MB}(t)$), so that

$$N_B(t) = S_B(t) + E_{B1}(t) + E_{M1}(t) + E_{B2}(t) + E_{M2}(t) + I_{BB}(t) + I_{MB}(t) + R_{BB}(t) + R_{MB}(t).$$

The susceptible human population ($S_H(t)$) is increased by the recruitment of people (either by birth or immigration) into the human-buffalo community

(at a rate Π_H). The population is decreased by infection with MTB (at a rate λ_H) or BTB (at a rate λ_B), where

$$\lambda_H = \frac{\beta_H}{N_H}(\eta_{H1}E_{H1} + I_{H1}) \text{ and } \lambda_B = \lambda_{HB} + \theta_{MM}\lambda_{BB}, \quad (4.5.1)$$

with,

$$\lambda_{HB} = \frac{\beta_H}{N_H}(\eta_{H2}E_{H2} + I_{H2}) \text{ and } \lambda_{BB} = \frac{\beta_B}{N_B}(\eta_{B1}E_{B1} + \eta_{B2}E_{B2} + I_{BB}) \quad (4.5.2)$$

In (4.5.1) and (4.5.2), β_H and β_B represent the effective contact rates (i.e., contacts capable of leading to MTB or BTB infection), respectively. Furthermore, $0 \leq \eta_{H1} < 1$ and $0 \leq \eta_{H2} < 1$ are modification parameters accounting for the assumed reduction in infectiousness of exposed humans, in comparison to infected humans with clinical symptoms of MTB or BTB, respectively. Similarly, $0 \leq \eta_{B1} < 1$ and $0 \leq \eta_{B2} < 1$ are modification parameters accounting for the assumed reduction in infectiousness of exposed buffalos, in comparison to infected buffalos with clinical symptoms of BTB. The modification parameter $0 \leq \theta_{MM} < 1$ accounts for the assumed reduced likelihood of susceptible humans acquiring BTB infection, in comparison to susceptible buffalos acquiring BTB infection. Natural death is assumed to occur in all human compartments at a rate μ_H . Thus, the rate of change of the susceptible human population is given by

$$\frac{dS_H}{dt} = \Pi_H - (\lambda_H + \lambda_B + \mu_H)S_H.$$

The population of exposed humans with MTB ($E_{H1}(t)$) is generated by the infection of susceptible humans with MTB (at the rate λ_H), and is decreased by the development of clinical symptoms of MTB (at a rate σ_1), exogenous re-infection (at a rate $\theta_{H1}\lambda_H$; where $0 \leq \theta_{H1} < 1$ accounts for the assumption that re-infection of exposed humans with MTB occurs at a rate lower than primary infection of susceptible humans with MTB) and natural death, so that

$$\frac{dE_{H1}}{dt} = \lambda_H S_H - (\sigma_1 + \theta_{H1}\lambda_H + \mu_H)E_{H1}.$$

Similarly, the population of exposed humans with BTB ($E_{H2}(t)$) is increased by the infection of susceptible humans with BTB (at the rate λ_B) and is reduced by the development of clinical symptoms of BTB (at a rate σ_2), exogenous re-infection (at a rate $\theta_{H2}\lambda_B$, with $0 \leq \theta_{H2} < 1$ similarly defined as θ_{H1}) and natural death. Thus,

$$\frac{dE_{H2}}{dt} = \lambda_B S_H - (\sigma_2 + \theta_{H2}\lambda_B + \mu_H)E_{H2}.$$

The population of humans with clinical symptoms of MTB ($I_{H1}(t)$) increases following the development of clinical symptoms of MTB by exposed humans (at the rate σ_1) and exogenous re-infection of exposed and recovered humans (at the rates $\theta_{H1}\lambda_H$ and $\theta_{RH}\lambda_H$, respectively; with $0 \leq \theta_{RH} < 1$). This population is decreased by recovery (at a rate γ_1), natural death and MTB-induced death (at a rate δ_{H1}), so that

$$\frac{dI_{H1}}{dt} = \sigma_1 E_{H1} + (\theta_{H1}E_{H1} + \theta_{RH}R_{H1})\lambda_H - (\gamma_1 + \mu_H + \delta_{H1})I_{H1}.$$

The population of infected humans with clinical symptoms of BTB ($I_{H2}(t)$) is generated by the development of clinical symptoms of BTB by exposed humans (at the rate σ_2) and re-infection of exposed and recovered humans (at the rates $\theta_{H2}\lambda_B$ and $\theta_{RB}\lambda_B$, respectively; with $0 \leq \theta_{RB} < 1$). This population is decreased by recovery (at a rate γ_2), natural death and BTB-induced death (at a rate δ_{H2}). This gives

$$\frac{dI_{H2}}{dt} = \sigma_2 E_{H2} + (\theta_{H2}E_{H2} + \theta_{RB}R_{H2})\lambda_B - (\gamma_2 + \mu_H + \delta_{H2})I_{H2}.$$

The population of humans who recovered from MTB ($R_{H1}(t)$) is generated by the recovery of humans with clinical symptoms of MTB (at the rate γ_1). It is decreased by exogenous re-infection (at the rate $\theta_{RH}\lambda_H$) and natural death. Hence,

$$\frac{dR_{H1}}{dt} = \gamma_1 I_{H1} - (\theta_{RH}\lambda_H + \mu_H)R_{H1}.$$

It should be mentioned that, since MTB-infected humans do not completely eliminate the bacteria from their body (usually the bacteria hide in the bone

marrow), “recovery” in this case implies (or represents) a long period of latency (which could ever last for a lifetime) [72, 105].

Similarly, the population of humans who recovered from BTB ($R_{H2}(t)$) is generated by the recovery of humans with clinical symptoms of BTB (at the rate γ_2), and is decreased by re-infection (at the rate $\theta_{RB}\lambda_B$) and natural death, so that

$$\frac{dR_{H2}}{dt} = \gamma_2 I_{H2} - (\theta_{RB}\lambda_B + \mu_H) R_{H2}.$$

The population of susceptible buffalos ($S_B(t)$) is generated by the recruitment of buffalos (either by birth or re-stocking from other herds) at a rate Π_B . It is assumed that all recruited buffalos are susceptible. The population of susceptible buffalos is decreased by acquisition of BTB infection (following effective contact with a human or buffalo infected with BTB), at the rate λ_B (where, $\lambda_B = \theta_{BB}\lambda_{HB} + \lambda_{BB}$; with the modification parameters $0 \leq \theta_{BB} < 1$ accounting for the expected reduced likelihood of humans transmitting of BTB to buffalo, in relation to BTB transmission from a human to another human), or MTB (following effective contact with a human infected with MTB), at a reduced rate $\theta_{HH}\lambda_H$ (where $0 \leq \theta_{HH} < 1$ is a modification parameter accounting for the assumed reduction in the transmissibility of MTB from humans to buffalos, in comparison to MTB transmission from humans to humans), and by natural death (at a rate μ_B ; buffalos in each epidemiological compartment suffer natural death at this rate). Thus,

$$\frac{dS_B}{dt} = \Pi_B - (\lambda_B + \theta_{HH}\lambda_H + \mu_B) S_B.$$

An important feature of BTB transmission within the buffalo population is that an infected buffalo could be in early or advanced stage of infection. This is owing to the fact that the clinical symptoms of BTB usually take months to manifest in buffalos [40]. Thus, BTB infections can remain dormant for years, and re-activate during periods of stress or in old age [40]. These (early- and advanced-exposed stage) features are incorporated in the model being develop. The population of buffalos early-exposed to BTB ($E_{B1}(t)$) is increased by the infection of susceptible buffalos with BTB (at the rate λ_B).

This population is decreased by exogenous re-infection with BTB (at a rate $\theta_{EB}\lambda_B$; with $0 \leq \theta_{EB} < 1$), progression to the advanced-exposed class (at a rate κ_1) and natural death. This gives

$$\frac{dE_{B1}}{dt} = \lambda_B S_B - (\theta_{EB}\lambda_B + \kappa_1 + \mu_B)E_{B1}.$$

The population of buffalos early-exposed to MTB is increased by the infection of susceptible buffalos with MTB (at the rate $\theta_{HH}\lambda_H$; where $0 \leq \theta_{HH} < 1$ is as defined above). The population is decreased by exogenous re-infection (at a rate $\theta_{EB}\lambda_H$), progression to the advanced-exposed MTB class (at a rate κ_2) and natural death. This gives

$$\frac{dE_{M1}}{dt} = \theta_{HH}\lambda_H S_B - (\theta_{EB}\lambda_H + \kappa_2 + \mu_B)E_{M1}.$$

The population of buffalos at advanced-exposed BTB class ($E_{B2}(t)$) is increased by the progression of buffalos in the early-exposed BTB class (at the rate κ_1). It is decreased by exogenous re-infection (at a rate $\theta_{EB}\lambda_B$), development of clinical symptoms of BTB (at a rate σ_{B2}) and natural death, so that

$$\frac{dE_{B2}}{dt} = \kappa_1 E_{B1} - (\theta_{EB}\lambda_B + \sigma_{B2} + \mu_B)E_{B2}.$$

Similarly, the population of buffalos at advanced-exposed MTB class ($E_{M2}(t)$) is generated by the progression of buffalos in the early-exposed MTB class (at the rate κ_2). It is decreased by exogenous re-infection (at a rate $\theta_{EB}\lambda_H$), development of clinical symptoms of MTB (at a rate σ_{M2}) and natural death. Hence,

$$\frac{dE_{M2}}{dt} = \kappa_2 E_{M1} - (\theta_{EB}\lambda_H + \sigma_{M2} + \mu_B)E_{M2}.$$

The population of buffalos with clinical symptoms of BTB ($I_{BB}(t)$) is increased by the development of clinical symptoms of exposed buffalos with BTB (at the rate σ_{B2}) and by the exogenous re-infection of exposed and recovered buffalos (at the rates $\theta_{EB}\lambda_B$ and $\theta_{RB}\lambda_B$, respectively). It is decreased

by recovery (at a rate γ_{B1}), natural death and by BTB-induced mortality (at a rate δ_B). Thus,

$$\frac{dI_{BB}}{dt} = \sigma_{B2}E_{B2} + (E_{B1} + E_{B2})\theta_{EB}\lambda_B + \theta_{RB}\lambda_B R_{BB} - (\gamma_{B1} + \mu_B + \delta_B)I_{BB}.$$

The population of buffalos with clinical symptoms of MTB ($I_{MB}(t)$) is increased by the development of clinical symptoms of exposed buffalos with MTB (at the rate σ_{M2}) and by the exogenous re-infection of exposed and recovered buffalos (at the rates $\theta_{EB}\lambda_H$ and $\theta_{RB}\lambda_H$, respectively). It is decreased by recovery (at a rate γ_{M1}), natural death and by MTB-induced mortality (at a rate δ_M). Thus,

$$\frac{dI_{MB}}{dt} = \sigma_{M2}E_{M2} + (E_{M1} + E_{M2})\theta_{EB}\lambda_H + \theta_{RB}\lambda_H R_{MB} - (\gamma_{M1} + \mu_B + \delta_M)I_{MB}.$$

The population of buffalos who recovered from BTB ($R_{BB}(t)$) is increased following the recovery of buffalos with clinical symptoms of BTB (at the rate γ_{B1}). It is decreased by re-infection (at the rate $\theta_{RB}\lambda_B$) and natural death, so that

$$\frac{dR_{BB}}{dt} = \gamma_{B1}I_{BB} - (\theta_{RB}\lambda_B + \mu_B)R_{BB}.$$

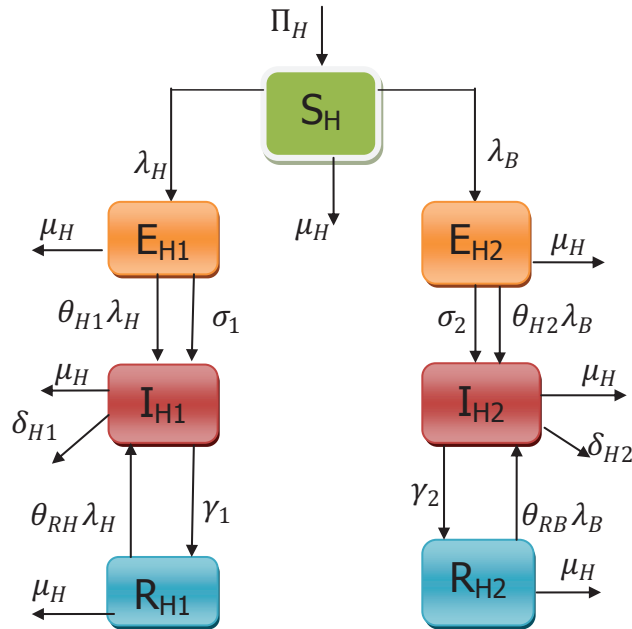
Finally, the population of buffalos who recovered from MTB ($R_{MB}(t)$) is generated by the recovery of buffalos with MTB (at the rate γ_{M1}), and is decreased following re-infection (at the rate $\theta_{RB}\lambda_H$) and natural death. This gives

$$\frac{dR_{MB}}{dt} = \gamma_{M1}I_{MB} - (\theta_{RB}\lambda_H + \mu_B)R_{MB}.$$

It is assumed that recovered buffalos and humans acquire permanent natural immunity against BTB or MTB infection so that recovered buffalos and humans do not return to their respective susceptible class (*albeit* buffalos and humans in recovered classes can acquire re-infection).

Thus, based on the above assumptions and formulations, the model for the BTB-MTB transmission dynamics in a human-buffalo population is given by the following deterministic system of non-linear differential equations (a flow

Humans



Buffalos

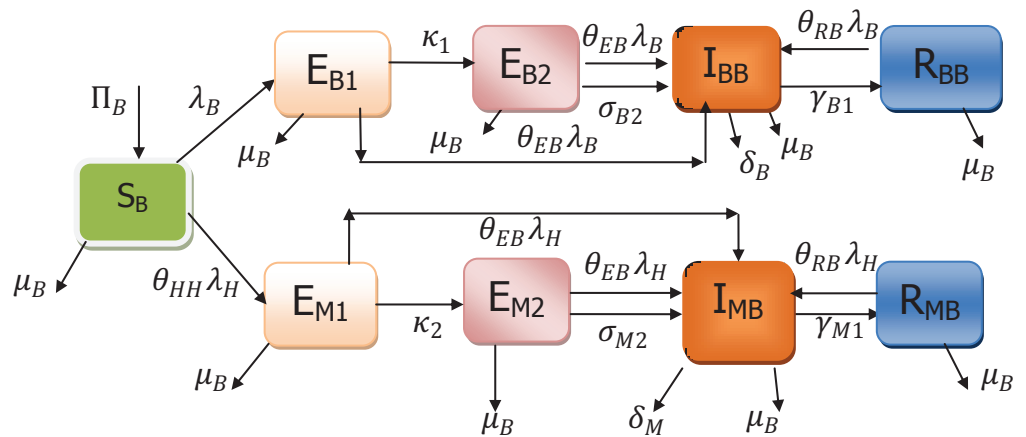


Figure 4.2: Schematic diagram of the BTB-MTB model (4.5.3).

Table 4.1: Description of the variables of the BTB-MTB model (4.5.3).

Variable	Interpretation
S_H	Population of susceptible humans
E_{H1}	Population of humans exposed to MTB
E_{H2}	Population of humans exposed to BTB
I_{H1}	Population of infected humans with clinical symptoms of MTB
I_{H2}	Population of infected humans with clinical symptoms of BTB
R_{H1}	Population of humans who recovered from MTB
R_{H2}	Population of humans who recovered from BTB
S_B	Population of susceptible buffalos
E_{B1}	Population of buffalos early-exposed to BTB
E_{M1}	Population of buffalos early-exposed to MTB
E_{B2}	Population of buffalos at advanced-exposed BTB stage
E_{M2}	Population of buffalos at advanced-exposed MTB stage
I_{BB}	Population of buffalos with clinical symptoms of BTB
I_{MB}	Population of buffalos with clinical symptoms of MTB
R_{BB}	Population of buffalos who recovered from BTB
R_{MB}	Population of buffalos who recovered from MTB

diagram of the model is depicted in Figure 4.2; and the associated variables and parameters are described in Tables 4.1 and 4.2, respectively):

$$\begin{aligned}
 &\text{Human Component} \left\{ \begin{aligned} \frac{dS_H}{dt} &= \Pi_H - (\lambda_H + \lambda_B + \mu_H)S_H, \\ \frac{dE_{H1}}{dt} &= \lambda_H S_H - (\theta_{H1}\lambda_H + \sigma_1 + \mu_H)E_{H1}, \\ \frac{dE_{H2}}{dt} &= \lambda_B S_H - (\theta_{H2}\lambda_B + \sigma_2 + \mu_H)E_{H2}, \\ \frac{dI_{H1}}{dt} &= \sigma_1 E_{H1} + (\theta_{H1}E_{H1} + \theta_{RH}R_{H1})\lambda_H - (\gamma_1 + \mu_H + \delta_{H1})I_{H1}, \\ \frac{dI_{H2}}{dt} &= \sigma_2 E_{H2} + (\theta_{H2}E_{H2} + \theta_{RB}R_{H2})\lambda_B - (\gamma_2 + \mu_H + \delta_{H2})I_{H2}, \\ \frac{dR_{H1}}{dt} &= \gamma_1 I_{H1} - (\theta_{RH}\lambda_H + \mu_H)R_{H1}, \\ \frac{dR_{H2}}{dt} &= \gamma_2 I_{H2} - (\theta_{RB}\lambda_B + \mu_H)R_{H2}. \end{aligned} \right. \\
 \\
 &\text{Buffalo Component} \left\{ \begin{aligned} \frac{dS_B}{dt} &= \Pi_B - (\theta_{HH}\lambda_H + \lambda_B + \mu_B)S_B, \\ \frac{dE_{B1}}{dt} &= \lambda_B S_B - (\theta_{EB}\lambda_B + \kappa_1 + \mu_B)E_{B1}, \\ \frac{dE_{M1}}{dt} &= \theta_{HH}\lambda_H S_B - (\theta_{EB}\lambda_H + \kappa_2 + \mu_B)E_{M1}, \\ \frac{dE_{B2}}{dt} &= \kappa_1 E_{B1} - (\theta_{EB}\lambda_B + \sigma_{B2} + \mu_B)E_{B2}, \\ \frac{dE_{M2}}{dt} &= \kappa_2 E_{M1} - (\theta_{EB}\lambda_H + \sigma_{M2} + \mu_B)E_{M2}, \\ \frac{dI_{BB}}{dt} &= \sigma_{B2} E_{B2} + (E_{B1} + E_{B2})\theta_{EB}\lambda_B + \theta_{RB}\lambda_B R_{BB} - (\gamma_{B1} + \mu_B + \delta_B)I_{BB}, \\ \frac{dI_{MB}}{dt} &= \sigma_{M2} E_{M2} + (E_{M1} + E_{M2})\theta_{EB}\lambda_H + \theta_{RB}\lambda_H R_{MB} - (\gamma_{M1} + \mu_B + \delta_M)I_{MB}, \\ \frac{dR_{BB}}{dt} &= \gamma_{B1} I_{BB} - (\theta_{RB}\lambda_B + \mu_B)R_{BB}, \\ \frac{dR_{MB}}{dt} &= \gamma_{M1} I_{MB} - (\theta_{RB}\lambda_H + \mu_B)R_{MB}. \end{aligned} \right. \tag{4.5.3}
 \end{aligned}$$

The model (4.5.3), to the authors' knowledge, is the first to incorporate humans and MTB dynamics in the transmission dynamics of BTB in a human-buffalo population. Furthermore, it extends numerous models for

BTB transmission in the literature, such as those in [1, 2, 6, 21, 31, 67, 105], by, *inter alia*,

- (i) Including the dynamics of early- and advanced- exposed buffalos. Exposed buffalo classes were not considered in [1, 6, 21, 31, 67].
- (ii) Allowing for BTB and MTB transmission by exposed buffalos and humans. This was not considered in [1, 6, 21, 31, 67, 105].
- (iii) Including the dynamics of humans. This was not considered in [2, 31, 67, 105].
- (iv) Allowing for the re-infection of exposed and recovered buffalos and humans (this was not considered in [1, 2, 6, 31, 67]).
- (v) Allowing for the transmission of both BTB and MTB in both the buffalo and human populations (this was not considered in [1, 2, 6, 21, 31, 67]).

The model (4.5.3) will now be rigorously analyzed to gain insight into its dynamical features. Before doing so, it is instructive, however, to consider the dynamics within the buffalo population only, as shown below.

4.5.2 Analysis of buffalo-only model

Consider the model (4.5.3) in the absence of humans (buffalo-only model), obtained by setting the human components to zero (i.e., setting $S_H = E_{H1} =$

$E_{H2} = I_{H1} = I_{H2} = R_{H1} = R_{H2} = \lambda_H = \theta_{HH} = 0$ in (4.5.3)), given by:

$$\begin{aligned}
 \frac{dS_B}{dt} &= \Pi_B - (\lambda_B + \mu_B)S_B, \\
 \frac{dE_{B1}}{dt} &= \lambda_B S_B - (\theta_{EB}\lambda_B + \kappa_1 + \mu_B)E_{B1}, \\
 \frac{dE_{M1}}{dt} &= -(\kappa_2 + \mu_B)E_{M1}, \\
 \frac{dE_{B2}}{dt} &= \kappa_1 E_{B1} - (\theta_{EB}\lambda_B + \sigma_{B2} + \mu_B)E_{B2}, \\
 \frac{dE_{M2}}{dt} &= \kappa_2 E_{M1} - (\sigma_{M2} + \mu_B)E_{M2}, \\
 \frac{dI_{BB}}{dt} &= \sigma_{B2}E_{B2} + (E_{B1} + E_{B2})\theta_{EB}\lambda_B + \theta_{RB}\lambda_B R_{BB} - (\gamma_{B1} + \mu_B + \delta_B)I_{BB}, \\
 \frac{dI_{MB}}{dt} &= \sigma_{M2}E_{M2} - (\gamma_{M1} + \mu_B + \delta_M)I_{MB}, \\
 \frac{dR_{BB}}{dt} &= \gamma_{B1}I_{BB} - (\theta_{RB}\lambda_B + \mu_B)R_{BB}, \\
 \frac{dR_{MB}}{dt} &= \gamma_{M1}I_{MB} - \mu_B R_{MB},
 \end{aligned} \tag{4.5.4}$$

where, now,

$$\lambda_B = \frac{\beta_B}{N_B}(\eta_{B1}E_{B1} + \eta_{B2}E_{B2} + I_{BB}). \tag{4.5.5}$$

It is worth stating that since there are no humans in the dynamics of the buffalo-only model (4.5.4), MTB is not transmitted to susceptible buffalos. Furthermore, it is clear from the third equation in (4.5.4) that

$$E_{M1}(t) \rightarrow 0 \text{ as } t \rightarrow \infty. \tag{4.5.6}$$

Substituting (4.5.6) in the fifth equation in (4.5.4) shows that

$$E_{M2}(t) \rightarrow 0 \text{ as } t \rightarrow \infty.$$

Similarly, by substituting $(E_{M1}, E_{M2}) = (0, 0)$ into the equation for I_{MB} and R_{MB} in (4.5.4), it follows that

$$(I_{MB}(t), R_{MB}(t)) \rightarrow (0, 0) \text{ as } t \rightarrow \infty.$$

Thus, the buffalo-only model reduces to the following (limited) model at steady-state

$$\begin{aligned}
 \frac{dS_B}{dt} &= \Pi_B - (\lambda_B + \mu_B)S_B, \\
 \frac{dE_{B1}}{dt} &= \lambda_B S_B - (\theta_{EB}\lambda_B + \kappa_1 + \mu_B)E_{B1}, \\
 \frac{dE_{B2}}{dt} &= \kappa_1 E_{B1} - (\theta_{EB}\lambda_B + \sigma_{B2} + \mu_B)E_{B2}, \\
 \frac{dI_{BB}}{dt} &= \sigma_{B2}E_{B2} + (E_{B1} + E_{B2})\theta_{EB}\lambda_B + \theta_{RB}\lambda_B R_{BB} - (\gamma_{B1} + \mu_B + \delta_B)I_{BB}, \\
 \frac{dR_{BB}}{dt} &= \gamma_{B1}I_{BB} - (\theta_{RB}\lambda_B + \mu_B)R_{BB}.
 \end{aligned} \tag{4.5.7}$$

Lemma 4.5.1 *The following biologically-feasible region of the buffalo-only model (4.5.7)*

$$\Gamma = \left\{ (S_B, E_{B1}, E_{B2}, I_{BB}, R_{BB}) \in \mathbb{R}_+^5 : S_B + E_{B1} + E_{B2} + I_{BB} + R_{BB} \leq \frac{\Pi_B}{\mu_B} \right\}$$

is positively-invariant and attracting.

Proof. Adding the equations in the buffalo-only model system (4.5.7) gives

$$\frac{dN_B(t)}{dt} = \Pi_B - \mu_B N_B(t) - \delta_B I_{BB}(t), \tag{4.5.8}$$

so that,

$$\frac{dN_B(t)}{dt} \leq \Pi_B - \mu_B N_B(t). \tag{4.5.9}$$

It follows from (4.5.9), and the Gronwall lemma, that

$$N_B(t) \leq N_B(0)e^{-\mu_B t} + \frac{\Pi_B}{\mu_B}[1 - e^{-\mu_B t}].$$

In particular, $N_B(t) \leq \Pi_B/\mu_B$ if $N_B(0) \leq \Pi_B/\mu_B$. Thus, Γ is positively-invariant. Hence, it is sufficient to consider the dynamics of the buffalo-only model (4.5.7) in Γ (where the model can be considered to be epidemiologically and mathematically well-posed [55]). ■

Theorem 4.5.1 *Let the initial data $S_B(0) > 0$, $E_{B1}(0) > 0$, $E_{B2}(0) > 0$, $I_{BB}(0) > 0$, $R_{BB}(0) > 0$. Then, the solutions $S_B(t)$, $E_{B1}(t)$, $E_{B2}(t)$, $I_{BB}(t)$ and $R_{BB}(t)$ of the buffalo-only model (4.5.7) are positive for all $t \geq 0$.*

Proof. It is clear from the first equation of the buffalo-only model (4.5.7) that

$$\frac{dS_B}{dt} \geq -(\lambda_B + \mu_B)S_B,$$

so that,

$$S_B(t) \geq S_B(0) \exp \left[- \int_0^t (\lambda_B + \mu_B) du \right] > 0, \text{ for all } t > 0.$$

Using similar approach, it can be shown that $E_{B1}(t) > 0$, $E_{B2}(t) > 0$, $I_{BB}(t) > 0$ and $R_{BB}(t) > 0$, for all $t > 0$. \square

The buffalo-only model (4.5.4) is fitted using data for the number of infected buffalos with BTB obtained from South Africa's Kruger National Park [28], from the year 2001 to 2005, as shown in Figure 4.3 (from which it is evident that the model mimics the data reasonably well).

4.5.3 Asymptotic stability of disease free equilibrium (DFE)

4.5.3.1 Local asymptotic stability

The DFE of the buffalo-only model (4.5.7) is given by

$$\mathcal{E}_0 = (S_B^*, E_{B1}^*, E_{B2}^*, I_{BB}^*, R_{BB}^*) = \left(\frac{\Pi_B}{\mu_B}, 0, 0, 0, 0 \right). \quad (4.5.10)$$

The linear stability of \mathcal{E}_0 can be established using the next generation operator method on the system (4.5.4) [32, 107]. The matrices F (for the new infection terms) and V (of the transition terms) associated with the system (4.5.7) are given, respectively, by

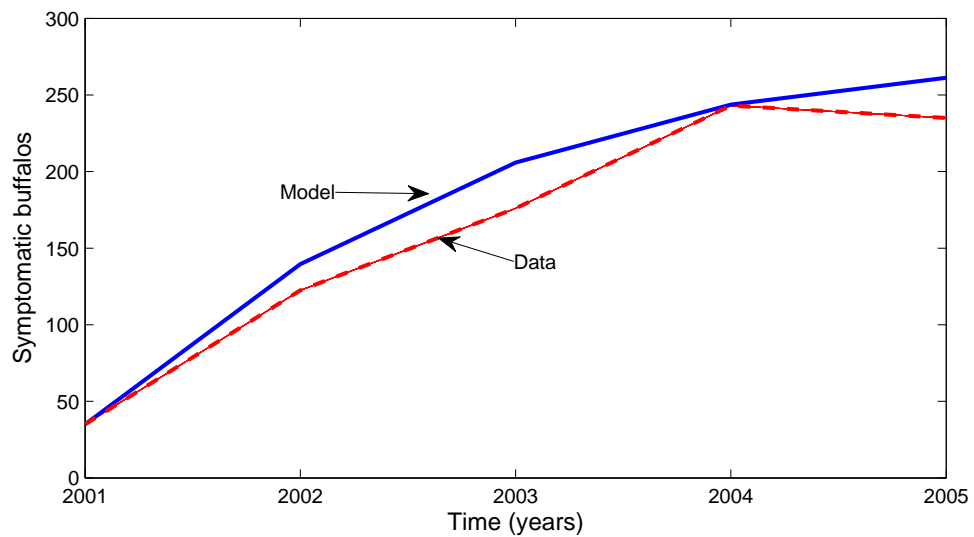


Figure 4.3: Data fit of the simulation of the buffalo-only model (4.5.4), using data obtained from South Africa's Kruger National Park (Table 4.4) [28]. Parameter values used are as given in Table 4.3.

$$F = \begin{bmatrix} \beta_B \eta_{B1} & \beta_B \eta_{B2} & \beta_B \\ 0 & 0 & 0 \\ 0 & 0 & 0 \end{bmatrix}, \quad V = \begin{bmatrix} K_1 & 0 & 0 \\ -\kappa_1 & K_3 & 0 \\ 0 & -\sigma_{B2} & K_5 \end{bmatrix},$$

where, $K_1 = \kappa_1 + \mu_B$, $K_3 = \sigma_{B2} + \mu_B$ and $K_5 = \gamma_{B1} + \mu_B + \delta_B$. It follows that the *basic reproduction number* of the buffalo-only model (4.5.7), denoted by \mathcal{R}_0 , is given by

$$\mathcal{R}_0 = \frac{\beta_B [\eta_{B1} K_3 K_5 + \kappa_1 (\eta_{B2} K_5 + \sigma_{B2})]}{K_1 K_3 K_5}.$$

Hence, using Theorem 2 of [107], the following result is established.

Lemma 4.5.2 *The DFE, \mathcal{E}_0 , of the buffalo-only model (4.5.7) is LAS if $\mathcal{R}_0 < 1$, and unstable if $\mathcal{R}_0 > 1$.*

The threshold quantity, \mathcal{R}_0 , represents the average number of secondary cases of BTB in the buffalo population that one BTB-infected buffalo can generate if introduced into a completely-susceptible buffalo population [3, 4, 55].

Interpretation of \mathcal{R}_0

The threshold quantity, \mathcal{R}_0 , can be interpreted as follows. It is worth recalling, first of all, that susceptible buffalos can acquire BTB infection following effective contact with either early-exposed buffalo with BTB ($E_{B1}(t)$), advanced-exposed buffalo with BTB ($E_{B2}(t)$) or infected buffalo with clinical symptoms of BTB ($I_{BB}(t)$). It follows that, the number of BTB infections generated by an early-exposed buffalo (near the DFE) is given by the product of the infection rate of an early-exposed buffalo ($\frac{\beta_B \eta_{B1}}{N_B^*}$) and the average duration of stay in the early-exposed class ($\frac{1}{K_1}$). Thus, the average number of BTB infections generated by early-exposed buffalos is given by

$$\frac{\beta_B \eta_{B1} S_B^*}{K_1 N_B^*}. \quad (4.5.11)$$

Similarly, the number of BTB infections generated by an advanced-exposed buffalo (near the DFE) is given by the product of the infection rate of

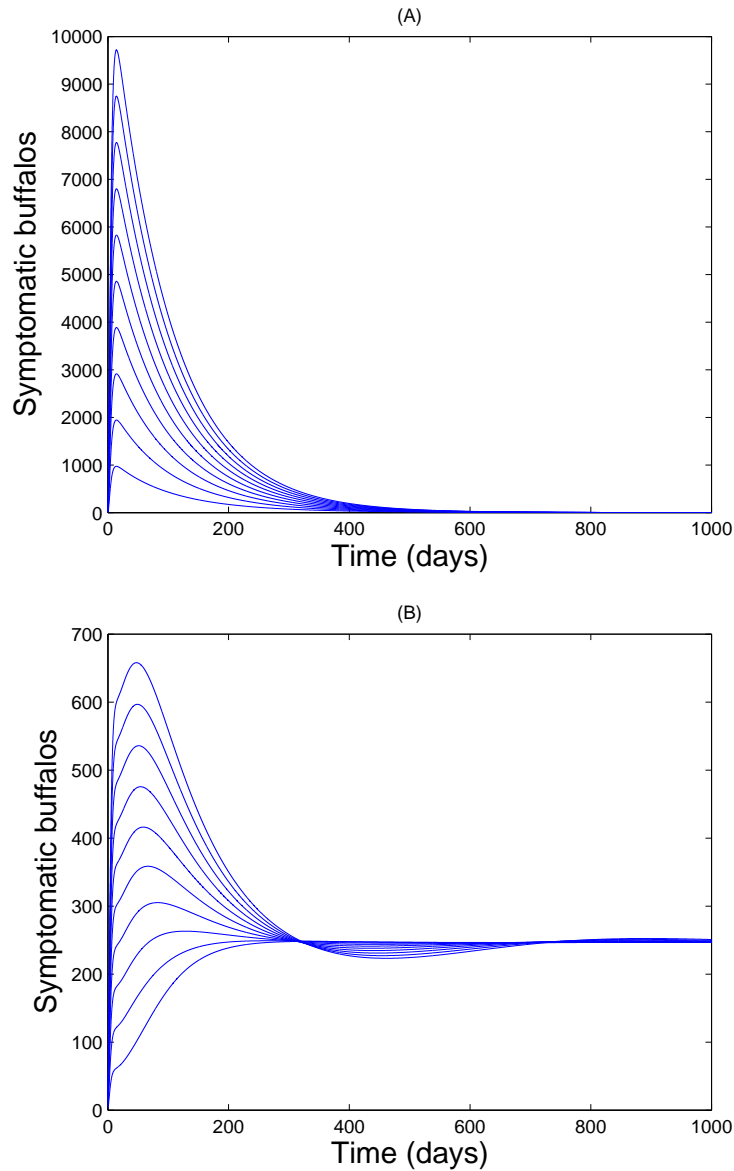


Figure 4.4: Simulations of the buffalo-only model (4.5.7), showing the total number of infected buffalos with clinical symptoms of BTB ($I_{BB}(t)$) at time t as a function of time. Parameter values used are as given in Table 4.3 with (A) $\beta_B = 0.00733$ (so that, $\mathcal{R}_0 = 0.7036 < 1$) and (B) $\beta_B = 0.0733$, $\delta_B = 0$ (so that, $\tilde{\mathcal{R}}_0 = 8.6050 > 1$).

advanced-exposed buffalos ($\frac{\beta_B \eta_{B2}}{N_B^*}$), the probability that early-exposed buffalo survived the early-exposed class and move to the advanced-exposed class ($\frac{\kappa_1}{K_1}$) and the average duration of stay in the advanced-exposed class ($\frac{1}{K_3}$). Thus, the average number of BTB infections generated by advanced-exposed buffalos is given by

$$\frac{\beta_B \eta_{B2} \kappa_1 S_B^*}{K_1 K_3 N_B^*}. \quad (4.5.12)$$

Furthermore, the number of BTB infections generated by an infected buffalo with clinical symptoms of BTB (near the DFE) is given by the product of the infection rate of buffalos with clinical symptoms of BTB ($\frac{\beta_B}{N_B^*}$), the probability that an advanced-exposed buffalo survived the advanced-exposed class and move to the symptomatic class I_{BB} ($\frac{\kappa_1 \sigma_{B2}}{K_1 K_3}$) and the average duration of stay in the symptomatic class I_{BB} ($\frac{1}{K_5}$). Thus, the average number of BTB infections generated by advanced-exposed buffalos is given by

$$\frac{\beta_B \kappa_1 \sigma_{B2} S_B^*}{K_1 K_3 K_5 N_B^*}. \quad (4.5.13)$$

The sum of the terms in (4.5.11), (4.5.12) and (4.5.13) gives \mathcal{R}_0 . That is, the average number of new infections generated by infected buffalos (early-exposed, advanced-exposed or symptomatic) is given by (noting that $S_B^* = \frac{\Pi_B}{\mu_B}$ and $N_B^* = \frac{\Pi_B}{\mu_B}$)

$$\mathcal{R}_0 = \frac{\beta_B [\eta_{B1} K_3 K_5 + \kappa_1 (\eta_{B2} K_5 + \sigma_{B2})]}{K_1 K_3 K_5}.$$

The epidemiological implication of Lemma 4.5.2 is that BTB can be effectively controlled in (or eliminated from) the buffalo population if the initial sizes of the state variables of the buffalo-only model (4.5.7) are in the basin of attraction of the DFE (\mathcal{E}_0). It is worth mentioning, however, that TB models with exogenous re-infection are often shown to exhibit the phenomenon of backward bifurcation (where the stable DFE co-exists with a stable endemic equilibrium when $\mathcal{R}_0 < 1$ [1, 21, 38, 98]). The epidemiological implication of this phenomenon is that the classical requirement of $\mathcal{R}_0 < 1$ is, although necessary, no longer sufficient for diseases elimination [1, 98]. Thus, the presence of backward bifurcation in the transmission dynamics of a disease makes

its effective control in a population more difficult. Hence, it is instructive to explore the possibility of such phenomenon in the buffalo-only model (4.5.4). This is investigated below.

Theorem 4.5.2 *The buffalo-only model (4.5.4) undergoes backward bifurcation at $\mathcal{R}_0 = 1$ whenever the bifurcation coefficient, a , given by (4.5.17) is positive.*

Proof. The proof is based on using centre manifold theory [21, 107]. Consider the buffalo-only model (4.5.4). Let $S_B = x_1$, $E_{B1} = x_2$, $E_{M1} = x_3$, $E_{B2} = x_4$, $E_{M2} = x_5$, $I_{BB} = x_6$, $I_{MB} = x_7$, $R_{BB} = x_8$ and $R_{MB} = x_9$. Thus,

$$N_B = \sum_{i=1}^9 x_i. \text{ Further, by using the vector notation } \mathbf{X} = (x_1, x_2, x_3, x_4, x_5, x_6, x_7, x_8, x_9)^T,$$

the buffalo-only model (4.5.4) can be written in the form

$$\frac{d\mathbf{X}}{dt} = (f_1, f_2, f_3, f_4, f_5, f_6, f_7, f_8, f_9)^T, \text{ as follows}$$

$$\begin{aligned} \frac{dx_1}{dt} &= \Pi_B - (\lambda_B + \mu_B)x_1, \\ \frac{dx_2}{dt} &= \lambda_B x_1 - (\theta_{EB}\lambda_B + \kappa_1 + \mu_B)x_2, \\ \frac{dx_3}{dt} &= -(\kappa_2 + \mu_B)x_3, \\ \frac{dx_4}{dt} &= \kappa_1 x_2 - (\theta_{EB}\lambda_B + \sigma_{B2} + \mu_B)x_4, \\ \frac{dx_5}{dt} &= \kappa_2 x_3 - (\sigma_{M2} + \mu_B)x_5, \\ \frac{dx_6}{dt} &= \sigma_{B2} x_4 + (x_2 + x_4)\theta_{EB}\lambda_B + \theta_{RB}\lambda_B x_8 - (\gamma_{B1} + \mu_B + \delta_B)x_6, \\ \frac{dx_7}{dt} &= \sigma_{M2} x_5 - (\gamma_{M1} + \mu_B + \delta_B)x_7, \\ \frac{dx_8}{dt} &= \gamma_{B1} x_6 - (\theta_{RB}\lambda_B + \mu_B)x_8, \\ \frac{dx_9}{dt} &= \gamma_{M1} x_7 - \mu_B x_9, \end{aligned} \tag{4.5.14}$$

with the associated force of infection given by

$$\lambda_B = \frac{\beta_B(\eta_{B1}x_2 + \eta_{B2}x_4 + x_6)}{\sum_{i=1}^9 x_i}.$$

Consider the case with $\mathcal{R}_0 = 1$. Let β_B^* (obtained by solving for $\beta_B = \beta_B^*$ from $\mathcal{R}_0 = 1$) given by

$$\beta_B = \beta_B^* = \frac{K_1 K_3 K_5}{\eta_{B1} K_3 K_5 + \kappa_1 (\eta_{B2} K_5 + \sigma_{B2})},$$

be chosen as a bifurcation parameter. The Jacobian of the system (4.5.14), evaluated at the DFE (\mathcal{E}_0) with $\beta_B = \beta_B^*$ (denoted by J^*), is given by

$$J^* = \begin{bmatrix} -\mu_B & -\beta_B^* \eta_{B1} & 0 & -\beta_B^* \eta_{B2} & 0 & -\beta_B^* & 0 & 0 & 0 \\ 0 & \beta_B^* \eta_{B1} - K_1 & 0 & \beta_B^* \eta_{B2} & 0 & \beta_B^* & 0 & 0 & 0 \\ 0 & 0 & -K_2 & 0 & 0 & 0 & 0 & 0 & 0 \\ 0 & \kappa_1 & 0 & -K_3 & 0 & 0 & 0 & 0 & 0 \\ 0 & 0 & \kappa_2 & 0 & -K_4 & 0 & 0 & 0 & 0 \\ 0 & 0 & 0 & \sigma_{B2} & 0 & -K_5 & 0 & 0 & 0 \\ 0 & 0 & 0 & 0 & \sigma_{M2} & 0 & -K_6 & 0 & 0 \\ 0 & 0 & 0 & 0 & 0 & \gamma_{B1} & 0 & -\mu_B & 0 \\ 0 & 0 & 0 & 0 & 0 & 0 & \gamma_{M1} & 0 & -\mu_B \end{bmatrix},$$

where K_i ($i = 1, \dots, 6$) are as defined in Section 4.5.2.

The Jacobian (J^*) of the linearized system has a simple zero eigenvalue (with all other eigenvalues having negative real part) obtained through rigorous computations. Hence, the centre manifold theory [21, 107] can be used to analyze the dynamics of the system (4.5.14) around $\beta_B = \beta_B^*$. Using the notation in [21], the following computations are carried out.

Eigenvectors of J^* $\Big|_{\beta_B=\beta_B^*}$

For the case when $\mathcal{R}_0 = 1$, it can be shown that the Jacobian, J^* , has a right eigenvector (corresponding to the simple zero eigenvalue), given by $\mathbf{w} = [w_1, w_2, w_3, w_4, w_5, w_6, w_7, w_8, w_9]^T$, where,

$$\begin{aligned} w_1 &= \frac{-\beta_B^*(\eta_{B1}w_2 + \eta_{B2}w_4 + w_6)}{\mu}, \quad w_2 = w_2, \quad w_3 = 0, \\ w_4 &= \frac{K_5w_6}{\sigma_{B2}}, \quad w_5 = \frac{K_6w_7}{\sigma_{M2}}, \quad w_6 = w_6, \quad w_7 = w_7, \quad w_8 = \frac{\gamma_{B1}w_6}{\mu_B}, \quad w_9 = \frac{\gamma_{M1}w_7}{\mu_B}. \end{aligned} \quad (4.5.15)$$

Similarly, the components of the left eigenvector of J^* (corresponding to the simple zero eigenvalue), denoted by $\mathbf{v} = [v_1, v_2, v_3, v_4, v_5, v_6, v_7, v_8, v_9]$, are given by,

$$\begin{aligned} v_3 &= \frac{\kappa_2\sigma_{M2}v_7}{K_2K_4}, \quad v_4 = \frac{(K_1 - \beta_B^*\eta_{B1})v_2}{\kappa_1} = \frac{1}{K_3K_5}[\beta_B^*v_2(\eta_{B2}K_5 + \sigma_{B2}) + \sigma_{B2}\gamma_{B1}v_8], \\ v_5 &= \frac{\sigma_{M2}v_7}{K_4}, \quad v_6 = \frac{\beta_B^*v_2 + \gamma_{B1}v_8}{K_5}, \quad v_9 = \frac{K_6v_7}{\gamma_{M1}}, \quad v_1 = 0, \quad v_2 > 0, \quad v_7 > 0, \quad v_8 > 0. \end{aligned} \quad (4.5.16)$$

It is worth mentioning that the free right eigenvectors, w_2, w_6 and w_7 and left eigenvectors, v_2, v_7 and v_8 , are chosen to be

$$v_2 = 1, \quad v_7 = \frac{1}{K_6}, \quad v_8 = 1, \quad w_2 = \frac{1}{3}, \quad w_6 = \frac{1}{3A_1} \quad \text{and} \quad w_7 = \frac{1}{3A_2},$$

where,

$$A_1 = \frac{[\beta_B^*(\eta_{B2}K_5 + \sigma_{B2}) + \gamma_{B1}\sigma_{B2}]}{K_3\sigma_{B2}} + \frac{\mu_B(\beta_B^* + \gamma_{B1}) + \gamma_{B1}K_5}{K_5\mu_B},$$

and,

$$A_2 = \frac{K_2[\mu_B(K_4 + K_6) + K_4K_6]}{K_2K_4K_6\mu_B},$$

so that $\mathbf{v} \cdot \mathbf{w} = 1$ (in line with [21]).

It can be shown, by computing the non-zero partial derivatives of the right-hand side functions, $f_i (i = 1, \dots, 9)$, that the associated backward bifurcation coefficients, a and b , are given, respectively, by (see Theorem 4.1 in [21]):

$$\begin{aligned} a &= \sum_{k,i,j=1}^8 v_k w_i w_j \frac{\partial^2 f_k}{\partial x_i \partial x_j}(0,0), \\ &= \frac{2\beta_B^* \mu_B}{\Pi_B} \{ \theta_{EB} [w_2(v_6 - v_2) + w_4(v_6 - v_4)] + \theta_{RB} w_8(v_6 - v_8) \\ &\quad - v_2(w_2 + w_3 + w_4 + w_5 + w_6 + w_7 + w_8 + w_9) \}, \\ &= \frac{2\beta_B^* \mu_B}{3\Pi_B} \left\{ \theta_{EB} \left(\frac{\beta_B^* + \gamma_{B1} - K_5}{K_5} + A_3 \right) + \frac{\theta_{RB}}{A_1} \left(\frac{\beta_B^* + \gamma_{B1} - K_5}{K_5} \right) \right. \\ &\quad \left. - \left[1 + \frac{\mu_B K_5 + \sigma_{B1}}{A_1 \mu_B \sigma_{B2}} + \frac{\gamma_{M1} \sigma_{M2} K_2 + K_2 \mu_B K_6 + \sigma_{B2}}{A_2 K_2 \mu_B \sigma_{M2}} \right] \right\}, \end{aligned} \quad (4.5.17)$$

and,

$$\begin{aligned} b &= \sum_{k,i=1}^9 v_k w_i \frac{\partial^2 f_k}{\partial x_i \partial \beta_B^*}(0,0) = v_2(\eta_{B1} w_2 + \eta_{B2} w_4 + w_6), \\ &= \frac{1}{3} \left[\eta_{B1} + \frac{1}{A_1 \sigma_{B2}} (\eta_{B2} K_5 + \sigma_{B2}) \right], \end{aligned}$$

where,

$$A_3 = \frac{1}{A_1 \sigma_{B2} K_3} [K_3(\beta_B^* + \gamma_{B1}) - \beta_B^*(\eta_{B2} K_5 + \sigma_{B2}) + \sigma_{B2} \gamma_{B1}].$$

Since the bifurcation coefficient, b , is automatically positive, it follows from Theorem 4.1 in [21] that the buffalo-only model (4.5.4) (or its transformed

equivalent (4.5.14)) will undergo backward bifurcation if the bifurcation coefficient, a , given by (4.5.17), is positive. ■

This result is consistent with that in [1, 21, 98], on the transmission dynamics of mycobacterium tuberculosis in human populations. This result is summarized below.

Lemma 4.5.3 *The buffalo-only model (4.5.4) does not undergo backward bifurcation at $\mathcal{R}_0 = 1$ in the absence of re-infection of exposed and recovered buffalos ($\theta_{EB} = \theta_{RB} = 0$).*

Hence, this study shows that the re-infection of exposed and recovered buffalos causes the phenomenon of backward bifurcation in the transmission dynamics of BTB and MTB in a buffalo-only population. To further confirm the absence of backward bifurcation in this case, a global asymptotic stability result is established for the DFE (\mathcal{E}_0) of the buffalo-only model (4.5.7) in the absence of re-infection (i.e., $\theta_{EB} = \theta_{RB} = 0$) below.

4.5.3.2 Global asymptotic stability of the DFE

Consider the buffalo-only model (4.5.7) in the absence of re-infection of exposed ($\theta_{EB} = 0$) and recovered ($\theta_{RB} = 0$) buffalos.

Theorem 4.5.3 *The DFE, \mathcal{E}_0 , of the buffalo-only model (4.5.7) with $\theta_{EB} = \theta_{RB} = 0$ is GAS in Γ if $\mathcal{R}_0 \leq 1$.*

Proof. Consider the buffalo-only model (4.5.7) in the absence of re-infection ($\theta_{EB} = \theta_{RB} = 0$). Furthermore, let $\mathcal{R}_0 \leq 1$. Consider the following linear Lyapunov function $\mathcal{F} = a_0 E_{B1} + a_1 E_{B2} + a_2 I_{BB}$, where,

$$a_0 = \mathcal{R}_0, a_1 = \frac{\beta_B(\eta_{B2}K_5 + \sigma_{B2})}{K_3K_5}, a_2 = \frac{\beta_B}{K_5},$$

with Lyapunov derivative given by

$$\begin{aligned}
 \dot{\mathcal{F}} &= a_0 \dot{E}_{B1} + a_1 \dot{E}_{B2} + a_2 \dot{I}_{BB}, \\
 &= a_0 \left[\frac{\beta_B}{N_B} (\eta_{B1} E_{B1} + \eta_{B2} E_{B2} + I_{BB}) S_B - K_1 E_{B1} \right] + a_1 (\kappa_1 E_{B1} - K_3 E_{B2}) \\
 &\quad + a_2 (\sigma_{B2} E_{B2} - K_5 I_{BB}), \\
 &= \left(a_0 \frac{\beta_B \eta_{B1} S_B}{N_B} - a_0 K_1 + a_1 \kappa_1 \right) E_{B1} + \left(a_0 \frac{\beta_B \eta_{B2} S_B}{N_B} - a_1 K_3 + a_2 \sigma_{B2} \right) E_{B2} \\
 &\quad + \left(a_0 \frac{\beta_B S_B}{N_B} - a_2 K_5 \right) I_{BB}, \\
 &\leq \beta_B (\eta_{B1} E_{B1} + \eta_{B2} E_{B2} + I_{BB}) (\mathcal{R}_0 - 1) \text{ since } S_B(t) \leq N_B(t) \text{ for all } t \text{ in } \Gamma, \\
 &\leq 0 \text{ if } \mathcal{R}_0 \leq 1.
 \end{aligned}$$

Since all the parameters and variables of the model (4.5.7) are non-negative (Theorem 4.5.1), it follows that $\dot{\mathcal{F}} \leq 0$ for $\mathcal{R}_0 \leq 1$ with $\dot{\mathcal{F}} = 0$ if and only if $E_{B1} = E_{B2} = I_{BB} = 0$. Thus, it follows, by LaSalle's Invariance Principle [70], that

$$(E_{B1}(t), E_{B2}(t), I_{BB}(t)) \rightarrow (0, 0, 0) \text{ as } t \rightarrow \infty. \quad (4.5.18)$$

Since $\limsup_{t \rightarrow \infty} I_{BB}(t) = 0$ (from (4.5.18)), it follows that, for sufficiently small $\varpi^* > 0$, there exists a constant $M > 0$, such that, $\limsup_{t \rightarrow \infty} I_{BB}(t) \leq \varpi^*$ for all $t > M$. Hence, it follows from the fifth equation of the buffalo-only model (4.5.7) that, for $t > M$, $\dot{R}_{BB} \leq \gamma_{B1} \varpi^* - \mu_B R_{BB}$. Thus, by comparison theorem [99], $R_{BB}^\infty = \limsup_{t \rightarrow \infty} R_{BB} \leq \frac{\gamma_{B1} \varpi^*}{\mu_B}$, so that, by letting, $\varpi^* \rightarrow 0$,

$$R_{BB}^\infty = \limsup_{t \rightarrow \infty} R_{BB}(t) \leq 0. \quad (4.5.19)$$

Similarly, it can be shown that

$$R_{BB\infty} = \liminf_{t \rightarrow \infty} R_{BB}(t) \geq 0. \quad (4.5.20)$$

Thus, it follows from (4.5.19) and (4.5.20), that $R_{BB\infty} \geq 0 \geq R_{BB}^\infty$. Hence,

$$\lim_{t \rightarrow \infty} R_{BB}(t) = 0. \quad (4.5.21)$$

Furthermore, substituting (4.5.18) in the first equation of (4.5.7) show that

$$S_B(t) \rightarrow \frac{\Pi_B}{\mu_B} \text{ as } t \rightarrow \infty. \quad (4.5.22)$$

Thus, by combining equations (4.5.18), (4.5.21) and (4.5.22), it follows that every solution of the equations of the buffalo-only model (4.5.7), with $\theta_{EB} = \theta_{RB} = 0$ and initial conditions in Γ , approaches \mathcal{E}_0 , as $t \rightarrow \infty$ (whenever $\mathcal{R}_0 \leq 1$). ■

Theorem 4.5.3 shows that, in the absence of the re-infection of exposed and recovered buffalos (i.e., $\theta_{EB} = \theta_{RB} = 0$), BTB can be eliminated from the buffalo-only population if the reproduction number of the model (\mathcal{R}_0) can be brought to (and maintained at) a value less than unity. Figure 4.4A depicts the solution profiles of the buffalo-only model (4.5.7), generated using various initial conditions, showing convergence to the DFE \mathcal{E}_0 when $\mathcal{R}_0 < 1$ (in line with Theorem 4.5.3).

4.5.4 Existence of endemic equilibria: Special case

In this section, the existence of non-trivial (endemic) equilibria (where the components of the infected variables of the model are non-zero) of the buffalo-only model (4.5.7) is explored for the special case without re-infection (i.e., $\theta_{EB} = \theta_{RB} = 0$). Solving the equations of the buffalo-only model (4.5.7) at steady-state gives the following general form of the EE (denoted by \mathcal{E}_1)

$$\mathcal{E}_1 = \left(S_B^{**}, E_{B1}^{**}, E_{B2}^{**}, I_{BB}^{**}, R_{BB}^{**} \right),$$

where,

$$\begin{aligned}
S_B^{**} &= \frac{\Pi_B}{\lambda_B^{**} + \mu_B}, \quad E_{B1}^{**} = \frac{\lambda_B^{**} \Pi_B}{K_1(\lambda_B^{**} + \mu_B)}, \quad E_{B2}^{**} = \frac{\kappa_1 \lambda_B^{**} \Pi_B}{K_1 K_3 (\lambda_B^{**} + \mu_B)}, \\
I_{BB}^{**} &= \frac{\sigma_{B2} \kappa_1 \lambda_B^{**} \Pi_B}{K_1 K_3 K_5 (\lambda_B^{**} + \mu_B)}, \quad R_{BB}^{**} = \frac{\gamma_{B1} \sigma_{B2} \kappa_1 \lambda_B^{**} \Pi_B}{K_1 K_3 K_5 \mu_B \lambda_B^{**} + \mu_B},
\end{aligned} \tag{4.5.23}$$

with the force of infection at steady-state (λ_B^{**}) given by

$$\lambda_B^{**} = \frac{\beta_B}{N_B^{**}} (\eta_{B1} E_{B1}^{**} + \eta_{B2} E_{B2}^{**} + I_{BB}^{**}). \tag{4.5.24}$$

Using (4.5.23) in the expression for λ_B^{**} in (4.5.24) shows that the non-zero equilibrium of the model (4.5.4) satisfy the linear equation

$$b_1 \lambda_B^{**} + b_2 = 0, \tag{4.5.25}$$

where, $b_1 = K_5 \mu_B (K_3 + \kappa_1) + \sigma_{B2} \kappa_1 (\mu_B + \gamma_{B2})$ and $b_2 = K_1 K_3 K_5 \mu_B (1 - \mathcal{R}_0)$. Clearly, the coefficient b_1 is always positive, and b_2 is positive (negative) if \mathcal{R}_0 is less than (greater than) unity, respectively. Thus, the linear system (4.5.25) has a unique positive solution, given by $\lambda_B^{**} = -b_2/b_1$, whenever $\mathcal{R}_0 > 1$. Further, the force of infection for buffalos (λ_B^{**}) is negative whenever $\mathcal{R}_0 < 1$ (which is biologically meaningless). Hence, the buffalo-only model (4.5.4) has no positive equilibrium in this case. These results are summarized below.

Theorem 4.5.4 *The buffalo-only model (4.5.7), with $\theta_{EB} = \theta_{RB} = 0$, has a unique EE, \mathcal{E}_1 , whenever $\mathcal{R}_0 > 1$, and no EE otherwise.*

4.5.4.1 Global asymptotic stability of endemic equilibrium

The global asymptotic stability of the unique EE (\mathcal{E}_1) of the buffalo-only model is explored for the special case without re-infection ($\theta_{EB} = \theta_{RB} = 0$) and BTB-induced death in buffalos ($\delta_B = 0$). It is convenient to define

$$\Gamma_1 = \{(S_B, E_{B1}, E_{B2}, I_{BB}, R_{BB}) \in \Gamma : E_{B1} = E_{B2} = I_{BB} = R_{BB} = 0\},$$

the stable manifold of the DFE (\mathcal{E}_0) of the buffalo-only model (4.5.7).

Theorem 4.5.5 *The unique EE (\mathcal{E}_1) of the buffalo-only model (4.5.7), with $\theta_{EB} = \theta_{RB} = \delta_B = 0$, is GAS in $\Gamma \setminus \Gamma_1$ if $\tilde{\mathcal{R}}_0 = \mathcal{R}_0|_{\delta_B=0} > 1$.*

Proof. Consider the buffalo-only model (4.5.7) with $\theta_{EB} = \theta_{RB} = \delta_B = 0$. For this case, it follows from Theorem 4.5.4 that the buffalo-only model (4.5.7) has a unique EE whenever $\tilde{\mathcal{R}}_0 > 1$. Furthermore, setting $\delta_B = 0$ in the model (4.5.7) shows that $N_B(t) \rightarrow \Pi_B/\mu_B$ as $t \rightarrow \infty$. Consider the following non-linear Lyapunov function (of Goh-Volterra type) for the subsystem of the model (4.5.7) involving the state variables S_B , E_{B1} , E_{B2} and I_{BB} (noting that $N_B(t)$ is now replaced by its limiting value Π_B/μ_B):

$$\begin{aligned} \mathcal{F} = & S_B - S_B^{**} - S_B^{**} \ln \left(\frac{S_B}{S_B^{**}} \right) + E_{B1} - E_{B1}^{**} - E_{B1}^{**} \ln \left(\frac{E_{B1}}{E_{B1}^{**}} \right) \\ & + \left(\frac{\tilde{\beta}_B \eta_{B2} S_B^{**} E_{B2}^{**} + \tilde{\beta}_B S_B^{**} I_{BB}^{**}}{\kappa_1 E_{B1}^{**}} \right) \left[E_{B2} - E_{B2}^{**} - E_{B2}^{**} \ln \left(\frac{E_{B2}}{E_{B2}^{**}} \right) \right] \\ & + \frac{\tilde{\beta}_B S_B^{**} I_{BB}^{**}}{\sigma_{B2} E_{B2}^{**}} \left[I_{BB} - I_{BB}^{**} - I_{BB}^{**} \ln \left(\frac{I_{BB}}{I_{BB}^{**}} \right) \right], \end{aligned}$$

where, $\tilde{\beta}_B = \frac{\mu_B \beta_B}{\Pi_B}$. The Lyapunov derivative of \mathcal{F} is given by

$$\begin{aligned}
 \dot{\mathcal{F}} &= \dot{S}_B - \frac{S_B^{**}}{S_B} \dot{S}_B + \dot{E}_{B1} - \frac{E_{B1}^{**}}{E_{B1}} \dot{E}_{B1} \\
 &+ \left(\frac{\tilde{\beta}_B \eta_{B2} S_B^{**} E_{B2}^{**} + \tilde{\beta}_B S_B^{**} I_{BB}^{**}}{\kappa_1 E_{B1}^{**}} \right) \left(\dot{E}_{B2} - \frac{E_{B2}^{**}}{E_{B2}} \dot{E}_{B2} \right) \\
 &+ \frac{\tilde{\beta}_B S_B^{**} I_{BB}^{**}}{\sigma_{B2} E_{B2}^{**}} \left(\dot{I}_{BB} - \frac{I_{BB}^{**}}{I_{BB}} \dot{I}_{BB} \right), \\
 &= \Pi_B - \tilde{\beta}_B (\eta_{B1} E_{B1} + \eta_{B2} E_{B2} + I_{BB}) S_B - \mu_B S_B \\
 &- \frac{S_B^{**}}{S_B} \left[\Pi_B - \tilde{\beta}_B (\eta_{B1} E_{B1} + \eta_{B2} E_{B2} + I_{BB}) S_B - \mu_B S_B \right] \\
 &+ \tilde{\beta}_B (\eta_{B1} E_{B1} + \eta_{B2} E_{B2} + I_{BB}) S_B \\
 &- K_1 E_{B1} - \frac{E_{B1}^{**}}{E_{B1}} \left[\tilde{\beta}_B (\eta_{B1} E_{B1} + \eta_{B2} E_{B2} + I_{BB}) S_B - K_1 E_{B1} \right] \\
 &+ \left(\frac{\tilde{\beta}_B \eta_{B2} S_B^{**} E_{B2}^{**} + \tilde{\beta}_B S_B^{**} I_{BB}^{**}}{\kappa_1 E_{B1}^{**}} \right) \left[\kappa_1 E_{B1} - K_3 E_{B2} - \frac{E_{B2}^{**}}{E_{B2}} (\kappa_1 E_{B1} - K_3 E_{B2}) \right] \\
 &+ \frac{\tilde{\beta}_B S_B^{**} I_{BB}^{**}}{\sigma_{B2} E_{B2}^{**}} \left[\sigma_{B2} E_{B2} - K_5 I_{BB} - \frac{I_{BB}^{**}}{I_{BB}} (\sigma_{B2} E_{B2} - K_5 I_{BB}) \right].
 \end{aligned} \tag{4.5.26}$$

Using the following steady-state relations (obtained from (4.5.7)),

$$\begin{aligned}
 \Pi_B &= \tilde{\beta}_B (\eta_{B1} E_{B1}^{**} + \eta_{B2} E_{B2}^{**} + I_{BB}^{**}) S_B^{**} + \mu_B S_B^{**}, \quad \kappa_1 E_{B1}^{**} = K_3 E_{B2}^{**}, \\
 \tilde{\beta}_B (\eta_{B1} E_{B1}^{**} + \eta_{B2} E_{B2}^{**} + I_{BB}^{**}) S_B^{**} &= K_1 E_{B1}^{**}, \quad \sigma_{B2} E_{B2}^{**} = K_5 I_{BB}^{**}, \quad \gamma_{B1} I_{BB}^{**} = \mu_B R_{BB}^{**},
 \end{aligned} \tag{4.5.27}$$

the Lyapunov derivative can be simplified to

$$\begin{aligned}
\dot{\mathcal{F}} &= \tilde{\beta}_B(\eta_{B1}E_{B1}^{**} + \eta_{B2}E_{B2}^{**} + I_{BB}^{**})S_B^{**} + \mu_B S_B^{**} - \mu_B S_B \\
&\quad - \frac{S_B^{**}}{S_B} \left[\tilde{\beta}_B(\eta_{B1}E_{B1}^{**} + \eta_{B2}E_{B2}^{**} + I_{BB}^{**})S_B^{**} + \mu_B S_B^{**} - \tilde{\beta}_B(\eta_{B1}E_{B1} + \eta_{B2}E_{B2} + I_{BB})S_B \right. \\
&\quad \left. - \mu_B S_B \right] - K_1 E_{B1} - \frac{E_{B1}^{**}}{E_{B1}} \left[\tilde{\beta}_B(\eta_{B1}E_{B1} + \eta_{B2}E_{B2} + I_{BB})S_B - K_1 E_{B1} \right] \\
&\quad + \left(\frac{\tilde{\beta}_B \eta_{B2} S_B^{**} E_{B2}^{**} + \tilde{\beta}_B S_B^{**} I_{BB}^{**}}{\kappa_1 E_{B1}^{**}} \right) \left[\kappa_1 E_{B1} - K_3 E_{B2} - \frac{E_{B2}^{**}}{E_{B2}} (\kappa_1 E_{B1} - K_3 E_{B2}) \right] \\
&\quad + \frac{\tilde{\beta}_B S_B^{**} I_{BB}^{**}}{\sigma_{B2} E_{B2}^{**}} \left[\sigma_{B2} E_{B2} - K_5 I_{BB} - \frac{I_{BB}^{**}}{I_{BB}} (\sigma_{B2} E_{B2} - K_5 I_{BB}) \right], \\
&= \mu_B S_B^{**} \left(2 - \frac{S_B^{**}}{S_B} - \frac{S_B}{S_B^{**}} \right) \\
&\quad + \tilde{\beta}_B I_{BB}^{**} S_B^{**} \left(4 - \frac{S_B^{**}}{S_B} - \frac{E_{B2} I_{BB}^{**}}{E_{B2}^{**} I_{BB}} - \frac{E_{B1} E_{B2}^{**}}{E_{B1}^{**} E_{B2}} - \frac{I_{BB} S_B E_{B1}^{**}}{I_{BB}^{**} S_B^{**} E_{B1}} \right) \\
&\quad + \tilde{\beta}_B \eta_{B1} E_{B1}^{**} S_B^{**} \left(2 - \frac{S_B^{**}}{S_B} - \frac{S_B}{S_B^{**}} \right) \\
&\quad + \tilde{\beta}_B \eta_{B2} E_{B2}^{**} S_B^{**} \left(3 - \frac{S_B^{**}}{S_B} - \frac{E_{B1} E_{B2}^{**}}{E_{B1}^{**} E_{B2}} - \frac{E_{B2} S_B E_{B1}^{**}}{E_{B2}^{**} S_B^{**} E_{B1}} \right).
\end{aligned}$$

Finally, since the arithmetic mean exceeds the geometric mean, it follows then that

$$\begin{aligned}
\mu_B S_B^{**} \left(2 - \frac{S_B^{**}}{S_B} - \frac{S_B}{S_B^{**}} \right) &\leq 0, \\
\tilde{\beta}_B I_{BB}^{**} S_B^{**} \left(4 - \frac{S_B^{**}}{S_B} - \frac{E_{B2} I_{BB}^{**}}{E_{B2}^{**} I_{BB}} - \frac{E_{B1} E_{B2}^{**}}{E_{B1}^{**} E_{B2}} - \frac{I_{BB} S_B E_{B1}^{**}}{I_{BB}^{**} S_B^{**} E_{B1}} \right) &\leq 0, \\
\tilde{\beta}_B \eta_{B1} E_{B1}^{**} S_B^{**} \left(2 - \frac{S_B^{**}}{S_B} - \frac{S_B}{S_B^{**}} \right) &\leq 0, \\
\tilde{\beta}_B \eta_{B2} E_{B2}^{**} S_B^{**} \left(3 - \frac{S_B^{**}}{S_B} - \frac{E_{B1} E_{B2}^{**}}{E_{B1}^{**} E_{B2}} - \frac{E_{B2} S_B E_{B1}^{**}}{E_{B2}^{**} S_B^{**} E_{B1}} \right) &\leq 0.
\end{aligned}$$

Furthermore, since all the model parameters are non-negative, it follows that $\dot{\mathcal{F}} \leq 0$ for $\tilde{\mathcal{R}}_0 > 1$. Thus, \mathcal{F} is a Lyapunov function for the sub-system of the model (4.5.4) on $\Gamma \setminus \Gamma_1$. Therefore, it follows, by LaSalle's Invariance Principle [70], that

$$\lim_{t \rightarrow \infty} S_B(t) = S_B^{**}, \lim_{t \rightarrow \infty} E_{B1}(t) = E_{B1}^{**}, \lim_{t \rightarrow \infty} E_{B2}(t) = E_{B2}^{**}, \lim_{t \rightarrow \infty} I_{BB}(t) = I_{BB}^{**}.$$

Since $I_{BB}(t) \rightarrow I_{BB}^{**}$ as $t \rightarrow \infty$, it follows from the equation for dR_{BB}/dt in (4.5.4) that, $R_{BB}(t) \rightarrow \frac{\gamma_{B1} I_{BB}^{**}}{\mu_B} = R_{BB}^{**}$, as $t \rightarrow \infty$. The proof is concluded using similar arguments as in the proof of Theorem 4.5.3. ■

The epidemiological implication of Theorem 4.5.5 is that BTB will be endemic in the buffalo population if $\tilde{\mathcal{R}}_0 > 1$ (and $\theta_{EB} = \theta_{RB} = \delta_B = 0$). Figure 4.4 B depicts the solutions of the model (4.5.7) for the case when $\tilde{\mathcal{R}}_0 > 1$ and $\theta_{EB} = \theta_{RB} = \delta_B = 0$, showing convergence of the initial solutions to the unique EE (in line with Theorem 4.5.5). In general, the dynamics of the buffalo-only model have shown that it exhibit the phenomenon of backward bifurcation, where an asymptotically-stable disease free equilibrium (DFE) co-exists with an asymptotically-stable EE when the associated reproduction number is less than unity. This phenomenon is shown to arise due to the exogenous re-infection of exposed and recovered buffalos. In the absence of such re-infection, it is shown, using a linear Lyapunov function, that the DFE of the model is GAS whenever the associated reproduction number is less than unity. Moreover, the model has a unique EE for a special case, which is shown, using a non-linear Lyapunov function, to be GAS.

4.5.5 Sensitivity and uncertainty analyses

In this section, sensitivity and uncertainty analyses will be carried out, using Latin Hypercube Sampling (LHS) and Partial Correlation Coefficient (PRCC) [62, 63, 64], to assess the effect of uncertainty in the estimate of the parameter values used to simulate the buffalo-only model (on the simulation results obtained) and to determine the key parameters that drive the dynamics of the disease in the buffalo-human population. The ranges and baseline

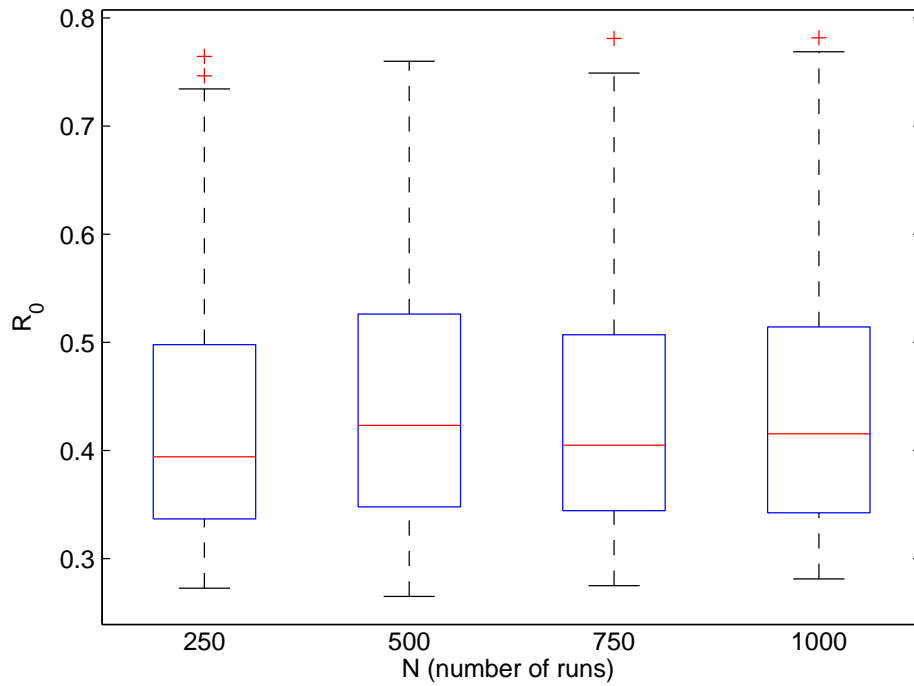


Figure 4.5: Box plot of \mathcal{R}_0 as a function of the number of LHS runs carried out for the buffalo-only model (4.5.4), using parameter values and ranges given in Table 3.

values of the parameters of the buffalo-only model, given in Table 4.3, will be used in these analyses. Each parameter of the buffalo-only model (4.5.4) is assumed to obey a uniform distribution [15]. Following [15], a total of 1000 LHS runs ($N=1000$) are carried out. Furthermore, the following initial conditions (which are consistent with the dynamics of African buffalo in the Kruger National Park [28]): $(S_B(0), E_{B1}(0), E_{M1}(0), E_{B2}(0), E_{M2}(0), I_{BB}(0), I_{MB}(0), R_{BB}(0), R_{MB}(0)) = (28000, 100, 100, 20, 20, 10, 10, 100, 100)$ are used in the simulations.

Figure 4.5 depicts a box plot of \mathcal{R}_0 , as a function of the number of LHS

Epidemic model

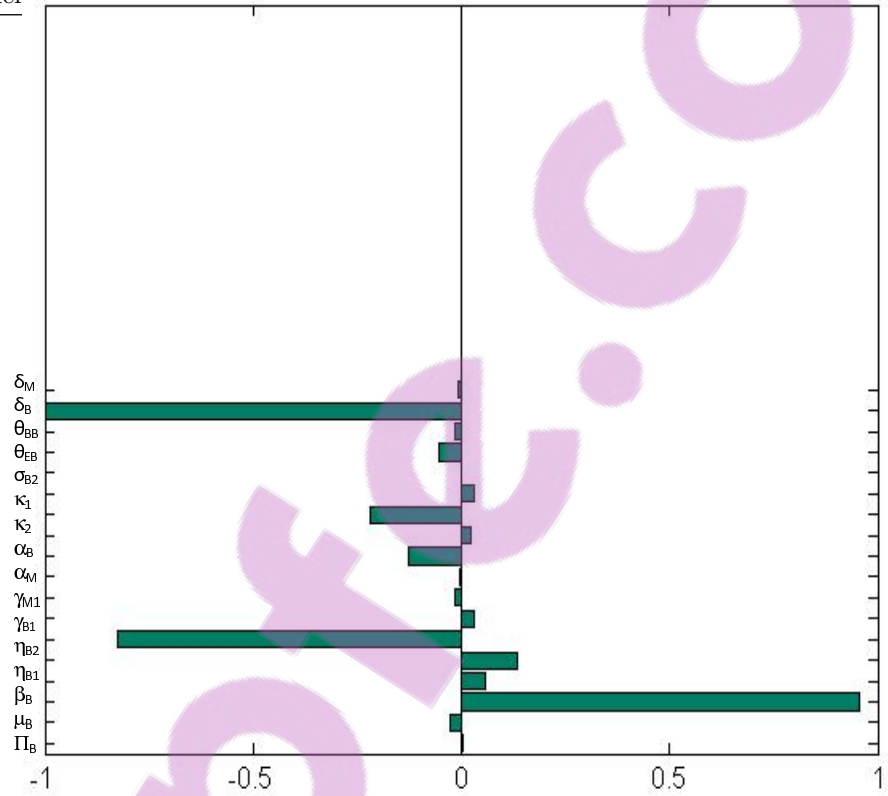


Figure 4.6: PRCC values of the parameters of the buffalo-only model (4.5.4), using \mathcal{R}_0 as the output function. Parameter values used are as given in Table 4.3.

runs carried out ($N = 1000$), from which it is evident that the distribution of \mathcal{R}_0 lie in the range $\mathcal{R}_0 \in [0.34, 0.55]$ (each box plot displays the upper and lower quartile ranges of \mathcal{R}_0 . A horizontal line within the box is the median value, and values of \mathcal{R}_0 beyond the whiskers are outliers [78]). Thus, since the distribution of the reproduction number of the buffalo-only model is less than unity, it follows (from Lemma 4.5.2 and Theorem 4.5.3) that the BTB outbreaks (in the buffalo-human population) will die out with time (in other words, the disease will be effectively controlled). The PRCC values of the parameters of the buffalo-only model (4.5.4), using \mathcal{R}_0 as the response function, are depicted in Figure 4.6. It follows from Figure 4.6 that the top

three parameters that most influences the value of \mathcal{R}_0 (hence the disease dynamics) are the BTB transmission rate (β_B), the recovery rate of buffalos (γ_{B1}) and the BTB-induced mortality in buffalos (δ_B).

Similarly, Figure 4.7 depicts the box plot of the buffalo-only model (4.5.4) using total number of symptomatic buffalos ($I_{BB} + I_{MB}$) as the response function. This figure shows a distribution of the number of symptomatic buffalos lying in the range [42, 118]. Hence, this study shows that, using the parameter values and ranges relevant to BTB-MTB dynamics at the Kruger National Park, a BTB outbreak could cause no more than 120 confirmed cases (of BTB and MTB) in the park. The associated PRCC values (with the total number of symptomatic buffalos as the output) are depicted in Figure 4.8, from which it is evident that, in this scenario, the top three parameters (that most influences the output) are the buffalo recruitment rate (Π_B), the natural (μ_B) and the disease-induced (δ_B) death rate of buffalos. Hence, this study shows variability in the top-ranked PRCC values on the chosen response/output function.

Therefore, in this section, the detailed sensitivity analysis reveals that the parameters that most influence the dynamics of the buffalo-only model (using the reproduction number as the response/output function) are the BTB transmission rate, the recovery rate of buffalos and the BTB-induced death rate of buffalos. For the case where the response function is the total number of symptomatic buffalos (with BTB or MTB), the buffalo demographic parameters were found to be the most influential. Furthermore, it is shown, using an uncertainty analysis, the distribution of the reproduction number of the buffalo-only model is shown to be less than unity (hence, the disease outbreak will not persist in the buffalo-human population). It is shown that both the buffalo-only model and the full BTB-MTB model have essentially the same qualitative dynamics with respect to the asymptotic local- and global- of the disease free equilibrium and the backward bifurcation phenomenon established in the transmission dynamics of BTB and BTB-MTB in a buffalo-human population; which, in both cases, is shown to arise due to the re-infection of exposed and recovered host(s) (buffalos or both buffalos and humans).

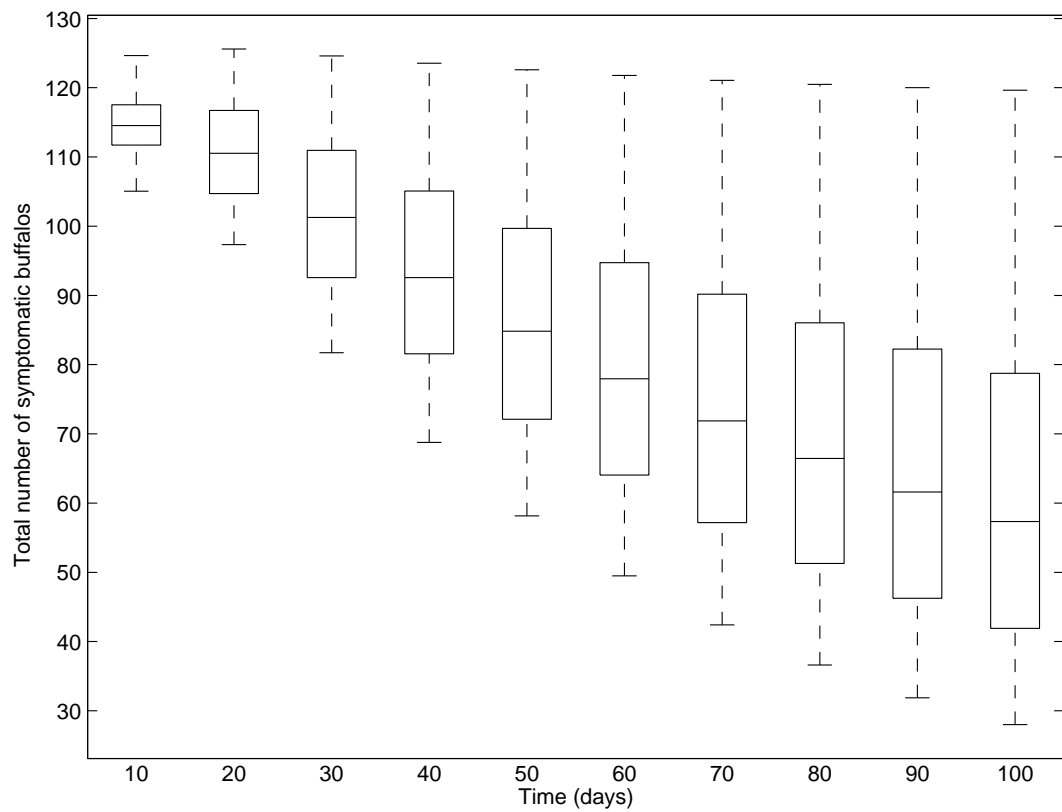


Figure 4.7: Box plot of the total number of symptomatic buffalos ($I_{BB} + I_{MB}$) as a function of the number of LHS runs for the buffalo-only model (4.5.4), using parameter values and ranges given in Table 3.

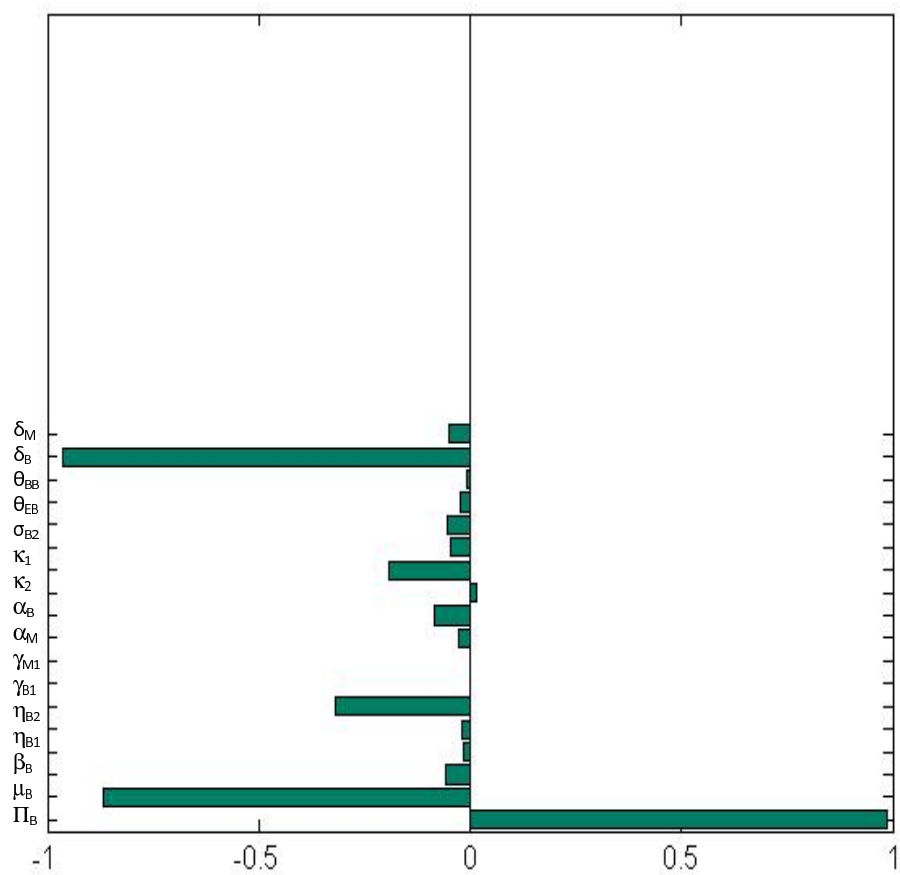


Figure 4.8: PRCC values of the parameters of the buffalo-only model (4.5.4), using total number of symptomatic buffalos ($I_{BB} + I_{MB}$) as the output function. Parameter values used are as given in Table 4.3.

Having fully studied the dynamics of the buffalo-only model (4.5.4), the full BTB-MTB model (4.5.3) will now be analyzed.

4.6 Analysis of the BTB-MTB model

It can be shown, using the approach in Section 4.5.2, that the following biologically-feasible region,

$$\Omega = \left\{ (S_H, E_{H1}, E_{H2}, I_{H1}, I_{H2}, R_{H1}, R_{H2}, S_B, E_{B1}, E_{M1}, E_{B2}, E_{M2}, I_{BB}, I_{MB}, R_{BB}, R_{MB}) \in \mathbb{R}_+^{16} : N_H \leq \frac{\Pi_H}{\mu_H}, N_B \leq \frac{\Pi_B}{\mu_B} \right\},$$

is positively-invariant and attracting for the BTB-MTB model (4.5.3).

4.6.1 Local stability of DFE

The analyses in this section will be carried out for the special case of the BTB-MTB model (4.5.3) with $\theta_{MM} = \theta_{BB} = 0$. The justification for this assumption is based on the fact that contact between humans and buffalos in the Kruger National Park are tightly controlled (hence, it is reasonable to assume that buffalo-to-human or human-to-buffalo transmission of BTB is negligible). The DFE of the BTB-MTB model (4.5.3) is given by

$$\begin{aligned} \mathcal{E}_{0f} &= (S_H^*, E_{H1}^*, E_{H2}^*, I_{H1}^*, I_{H2}^*, R_{H1}^*, R_{H2}^*, S_B^*, E_{B1}^*, E_{M1}^*, E_{B2}^*, E_{M2}^*, \\ &\quad I_{BB}^*, I_{MB}^*, R_{BB}^*, R_{MB}^*) \\ &= \left(\frac{\Pi_H}{\mu_H}, 0, 0, 0, 0, 0, 0, \frac{\Pi_B}{\mu_B}, 0, 0, 0, 0, 0, 0, 0 \right). \end{aligned} \quad (4.6.1)$$

The associated next generation matrices of the BTB-MTB model (4.5.3), denoted by F_f and V_f are given, respectively, by

$$F_f = \begin{bmatrix} \beta_H \eta_{H1} & 0 & \beta_H & 0 & 0 & 0 & 0 & 0 & 0 & 0 \\ 0 & \beta_H \eta_{H2} & 0 & \beta_H & 0 & 0 & 0 & 0 & 0 & 0 \\ 0 & 0 & 0 & 0 & 0 & 0 & 0 & 0 & 0 & 0 \\ 0 & 0 & 0 & 0 & 0 & 0 & 0 & 0 & 0 & 0 \\ 0 & 0 & 0 & 0 & \beta_B \eta_{B1} & 0 & \beta_B \eta_{B2} & 0 & \beta_B & 0 \\ 0 & 0 & 0 & 0 & 0 & 0 & 0 & 0 & 0 & 0 \\ 0 & 0 & 0 & 0 & 0 & 0 & 0 & 0 & 0 & 0 \\ 0 & 0 & 0 & 0 & 0 & 0 & 0 & 0 & 0 & 0 \\ 0 & 0 & 0 & 0 & 0 & 0 & 0 & 0 & 0 & 0 \\ 0 & 0 & 0 & 0 & 0 & 0 & 0 & 0 & 0 & 0 \end{bmatrix},$$

$$V_f = \begin{bmatrix} Q_1 & 0 & 0 & 0 & 0 & 0 & 0 & 0 & 0 & 0 \\ 0 & Q_2 & 0 & 0 & 0 & 0 & 0 & 0 & 0 & 0 \\ -\sigma_1 & 0 & Q_3 & 0 & 0 & 0 & 0 & 0 & 0 & 0 \\ 0 & -\sigma_2 & 0 & Q_4 & 0 & 0 & 0 & 0 & 0 & 0 \\ 0 & 0 & 0 & 0 & K_1 & 0 & 0 & 0 & 0 & 0 \\ 0 & 0 & 0 & 0 & 0 & K_2 & 0 & 0 & 0 & 0 \\ 0 & 0 & 0 & 0 & -\kappa_1 & 0 & K_3 & 0 & 0 & 0 \\ 0 & 0 & 0 & 0 & 0 & 0 & -\kappa_2 & K_4 & 0 & 0 \\ 0 & 0 & 0 & 0 & 0 & 0 & -\sigma_{B2} & 0 & K_5 & 0 \\ 0 & 0 & 0 & 0 & 0 & 0 & 0 & -\sigma_{M2} & 0 & K_6 \end{bmatrix}.$$

It follows then that the *reproduction number* of the BTB-MTB model (4.5.3), denoted by \mathcal{R}_f , is given by

$$\mathcal{R}_f = \rho(F_f V_f^{-1}) = \max\{\mathcal{R}_{HM}, \mathcal{R}_{HB}, \mathcal{R}_0\},$$

where \mathcal{R}_{HM} and \mathcal{R}_{HB} are the associated *reproduction numbers* for humans infected with MTB and with BTB, respectively, given by

$$\mathcal{R}_{HM} = \frac{\beta_H(\eta_{H1}Q_3 + \sigma_1)}{Q_1Q_3} \text{ and } \mathcal{R}_{HB} = \frac{\beta_H(\eta_{H2}Q_4 + \sigma_2)}{Q_2Q_4}, \quad (4.6.2)$$

where $Q_1 = \sigma_1 + \mu_H$, $Q_2 = \sigma_2 + \mu_H$, $Q_3 = \gamma_1 + \mu_H + \delta_{H1}$ and $Q_4 = \gamma_2 + \mu_H + \delta_{H2}$,

and \mathcal{R}_0 is as defined in Section 4.5.2. Thus, using the approach in Section 4.5.3, the following result can be established for the BTB-MTB model (4.5.3).

Lemma 4.6.1 *The DFE, \mathcal{E}_{0f} , of the model (4.5.3), with $\theta_{MM} = \theta_{BB} = 0$, is LAS in Ω if $\mathcal{R}_f < 1$, and unstable if $\mathcal{R}_f > 1$.*

It can be shown, as in Section 4.5.2, that the BTB-MTB model (4.5.3) also undergoes backward bifurcation. Unlike in the buffalo-only model (4.5.4), however, this phenomenon persists even if the bovine-associated re-infection terms (θ_{RB} and θ_{EB}) are set to zero. This is due to the re-infection of exposed and recovered humans (i.e., $\theta_{H1} \neq 0$ and $\theta_{H2} \neq 0$). To illustrate this fact, it is shown that the DFE (\mathcal{E}_{0f}) of the BTB-MTB model (4.5.3) is GAS in Ω in the absence of re-infection of exposed and recovered buffalos and humans, whenever the associated reproduction number (\mathcal{R}_f) is less than unity.

4.6.2 Global asymptotic stability of DFE

Theorem 4.6.1 *The DFE, \mathcal{E}_{0f} , of the BTB-MTB model (4.5.3) with $\theta_{H1} = \theta_{H2} = \theta_{RB} = \theta_{RH} = \theta_{BB} = \theta_{MM} = \theta_{EB} = \theta_{RB} = 0$, is GAS in Ω if $\mathcal{R}_f < 1$.*

Proof. Consider BTB-MTB model (4.5.4) with $\theta_{H1} = \theta_{H2} = \theta_{RB} = \theta_{RH} = \theta_{BB} = \theta_{MM} = \theta_{EB} = \theta_{RB} = 0$. The proof is based on using a comparison theorem [71]. It should be noted, first of all, that the equations for the infected components in the BTB-MTB model (4.5.3) can be re-written in the following matrix form

$$\frac{d\tilde{\mathbf{x}}}{dt} = \left[(F_f - V_f) - \left(1 - \frac{S_H}{N_H}\right) M_1 - \left(1 - \frac{S_B}{N_B}\right) M_2 \right] \tilde{\mathbf{x}}, \quad (4.6.3)$$

where $\tilde{\mathbf{x}} = [E_{H1}, E_{H2}, I_{H1}, I_{H2}, E_{B1}, E_{M1}, E_{B2}, E_{M2}, I_{BB}, I_{MB}]^T$, the matrices F_f and V_f are as given in Section 4.6.1, and

$$M_1 = \begin{bmatrix} \beta_H \eta_{H1} & 0 & \beta_H & 0 & 0 & 0 & 0 & 0 & 0 & 0 \\ 0 & \beta_H \eta_{H2} & 0 & \beta_H & 0 & 0 & 0 & 0 & 0 & 0 \\ 0 & 0 & 0 & 0 & 0 & 0 & 0 & 0 & 0 & 0 \\ 0 & 0 & 0 & 0 & 0 & 0 & 0 & 0 & 0 & 0 \\ 0 & 0 & 0 & 0 & 0 & 0 & 0 & 0 & 0 & 0 \\ 0 & 0 & 0 & 0 & 0 & 0 & 0 & 0 & 0 & 0 \\ 0 & 0 & 0 & 0 & 0 & 0 & 0 & 0 & 0 & 0 \\ 0 & 0 & 0 & 0 & 0 & 0 & 0 & 0 & 0 & 0 \\ 0 & 0 & 0 & 0 & 0 & 0 & 0 & 0 & 0 & 0 \\ 0 & 0 & 0 & 0 & 0 & 0 & 0 & 0 & 0 & 0 \end{bmatrix},$$

$$M_2 = \begin{bmatrix} 0 & 0 & 0 & 0 & 0 & 0 & 0 & 0 & 0 & 0 \\ 0 & 0 & 0 & 0 & 0 & 0 & 0 & 0 & 0 & 0 \\ 0 & 0 & 0 & 0 & 0 & 0 & 0 & 0 & 0 & 0 \\ 0 & 0 & 0 & 0 & 0 & 0 & 0 & 0 & 0 & 0 \\ 0 & 0 & 0 & 0 & \beta_B \eta_{B1} & 0 & \beta_B \eta_{B2} & 0 & \beta_B & 0 \\ 0 & 0 & 0 & 0 & 0 & 0 & 0 & 0 & 0 & 0 \\ 0 & 0 & 0 & 0 & 0 & 0 & 0 & 0 & 0 & 0 \\ 0 & 0 & 0 & 0 & 0 & 0 & 0 & 0 & 0 & 0 \\ 0 & 0 & 0 & 0 & 0 & 0 & 0 & 0 & 0 & 0 \\ 0 & 0 & 0 & 0 & 0 & 0 & 0 & 0 & 0 & 0 \end{bmatrix}.$$

It follows, since $S_H(t) < N_H(t)$ and $S_B(t) < N_B(t)$ for all $t \geq 0$ in Ω , that

$$\frac{d\tilde{\mathbf{x}}}{dt} \leq (F_f - V_f) \tilde{\mathbf{x}}. \quad (4.6.4)$$

Using the fact that the eigenvalues of the matrix $F_f - V_f$ all have negative real parts (where $\rho(F_f V_f^{-1}) < 1$ if $\mathcal{R}_f < 1$, which is equivalent to $F_f - V_f$ having eigenvalues with negative real parts when $\mathcal{R}_f < 1$ of [107]). Consequently, the linearized differential inequality system (4.6.4) is stable whenever $\mathcal{R}_f < 1$. Thus,

$(E_{H1}(t), E_{H2}(t), I_{H1}(t), I_{H2}(t), E_{B1}(t), E_{M1}(t), E_{B2}(t), E_{M2}(t), I_{BB}(t), I_{MB}(t)) \rightarrow$
 $(0, 0, 0, 0, 0, 0, 0, 0, 0, 0)$ as $t \rightarrow \infty$. It follows, by comparison theorem (see [71], pp 31), that

$(E_{H1}(t), E_{H2}(t), I_{H1}(t), I_{H2}(t), E_{B1}(t), E_{M1}(t), E_{B2}(t), E_{M2}(t), I_{BB}(t), I_{MB}(t)) \rightarrow$
 $(0, 0, 0, 0, 0, 0, 0, 0, 0, 0)$. Substituting $E_{H1}(t) = E_{H2}(t) = I_{H1}(t) = I_{H2}(t) =$
 $E_{B1}(t) = E_{M1}(t) = E_{B2}(t) = E_{M2}(t) = I_{BB}(t) = I_{MB}(t) = 0$ in the suscep-
 tible and the recovered compartments of (4.5.3) gives, $S_H(t) \rightarrow S_H^*, R_{H1} \rightarrow$
 $0, R_{H2} \rightarrow 0, S_B(t) \rightarrow S_B^*, R_{BB} \rightarrow 0$ and $R_{MB} \rightarrow 0$ as $t \rightarrow \infty$. Thus, the
 DFE (\mathcal{E}_{0f}) of the BTB-MTB model (4.5.3) is GAS in Ω if $\mathcal{R}_f < 1$ and with
 $\theta_{H1} = \theta_{H2} = \theta_{RB} = \theta_{RH} = \theta_{BB} = \theta_{MM} = \theta_{EB} = \theta_{RB} = 0$. ■

Hence, the analyses in this section show that the buffalo-only model and the full BTB-MTB model (4.5.3) have essentially the same qualitative dynamics with respect to the local- and global-asymptotic stability of the associated disease free equilibrium (in the absence of re-infection) as well as the backward bifurcation property established in the transmission dynamics of BTB and BTB-MTB in a buffalo-human population. In both cases, the backward bifurcation phenomenon is shown to arise due to the re-infection of the exposed and recovered host(s) (buffalos for the buffalo-only model (4.5.4), and buffalos and humans for the BTB-MTB model). Numerical simulations of the BTB-MTB model show that the cumulative number of MTB cases in humans (buffalos) decreases with increasing number of BTB infections in humans (buffalos).

4.6.3 Numerical simulations

The BTB-MTB model (4.5.3) is simulated, using the baseline values tabulated in Table 4.3 (unless otherwise stated), to assess the effect of the dynamics of BTB (MTB) on the spread of MTB (BTB) in the human (buffalo) population.

4.6.3.1 Effect of BTB on MTB

The effect of BTB (in the human-buffalo population within the Kruger National Park) on the spread of MTB in the human population (within the park) is assessed by simulating the BTB-MTB model (4.5.3) using parameter values in Table 4.3, subject to the following four effectiveness levels of BTB transmission likelihood from buffalos to humans (i.e., choosing four different values of the parameter θ_{MM} , for the reduced likelihood of humans acquiring BTB infection from buffalos):

- (I) No transmission of BTB from buffalos to humans: $\theta_{MM} = 0$;
- (II) Low rate of transmission of BTB from buffalos to humans: $\theta_{MM} = 0.25$;
- (III) Moderate rate of transmission of BTB from buffalos to humans: $\theta_{MM} = 0.50$;
- (IV) High rate of transmission of BTB from buffalos to humans: $\theta_{MM} = 0.75$.

The simulation results obtained, depicted in Figure 4.9A, show that the cumulative number of new MTB cases in humans decreases with increasing rate of BTB transmission to humans by buffalos (θ_{MM}).

4.6.3.2 Effect of MTB on BTB

Similar plot is generated to assess the effect of MTB (in the human-buffalo population) on the spread of BTB in the buffalo population. Here, too, four transmission levels of the associated parameter (θ_{HH}) are considered, namely: none ($\theta_{HH} = 0$), low ($\theta_{HH} = 0.25$), moderate ($\theta_{HH} = 0.50$) and high ($\theta_{HH} = 0.75$). The results obtained, depicted in Figure 4.9B, show that the cumulative number of new BTB infections in buffalos decreases with increasing rate of MTB transmission to buffalos by humans.

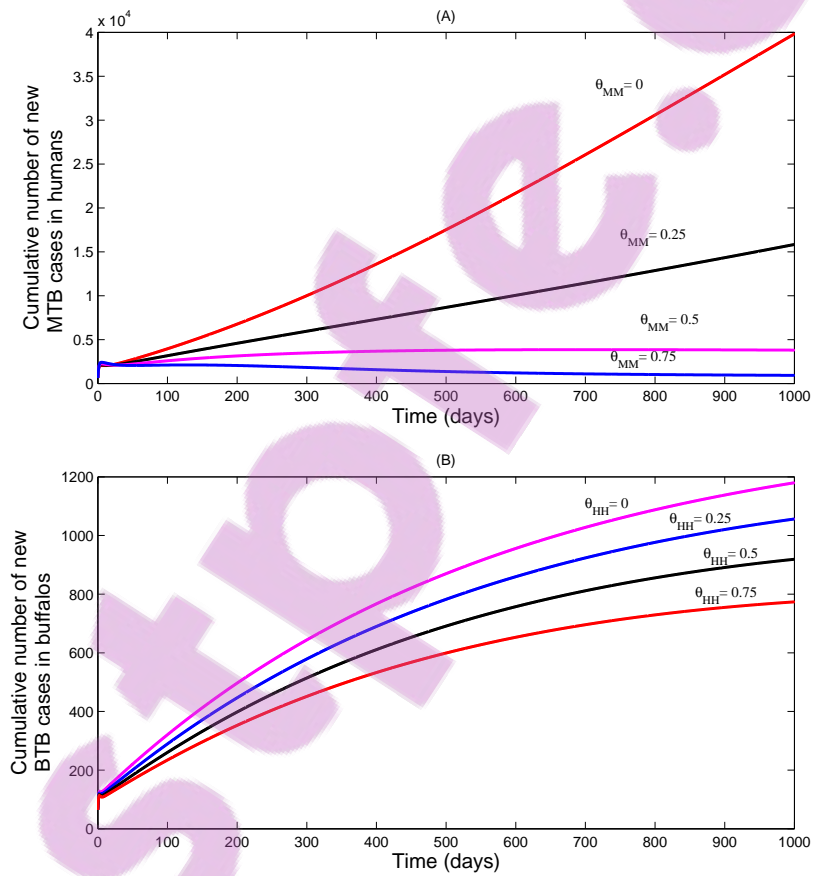


Figure 4.9: Cumulative number of new cases of (A) MTB infection in humans. (B) BTB infection in buffalos. Parameter values used are as given in Table 4.3, with various values of θ_{MM} (A) or θ_{HH} (B).

Table 4.2: Description of parameters of the BTB-MTB model (4.5.3).

Parameter	Interpretation
Π_H	Recruitment rate of humans
Π_B	Recruitment rate of buffalos
μ_H	Natural death rate of humans
μ_B	Natural death rate of buffalos
β_H	Transmission rate of MTB
β_B	Transmission rate of BTB
η_{H1}	Modification parameter for the reduction in infectiousness of exposed humans in comparison to humans with clinical symptoms of MTB
η_{H2}	Modification parameter for the reduction in infectiousness of exposed humans in comparison to humans with clinical symptoms of BTB
η_{B1}, η_{B2}	Modification parameters for the reduction in infectiousness of exposed buffalos in comparison to buffalos with clinical symptoms of BTB
θ_{HH}, θ_{BB}	Modification parameters for the reduction in transmissibility of MTB to buffalos in comparison to humans
θ_{MM}	Modification parameters for the reduction in transmissibility of BTB to humans in comparison to buffalos
γ_i ($i = 1, 2$)	Recovery rate of humans
γ_{B1}, γ_{M1}	Recovery rate of buffalos
σ_i ($i = 1, 2$)	Progression rate from E_{Hi} to I_{Hi} class
κ_1	Progression rate from E_{B1} to E_{B2} class
κ_2	Progression rate from E_{M1} to E_{M2} class
σ_{B2}	Progression rate from E_{B2} to I_{BB} class
σ_{M2}	Progression rate from E_{M2} to I_{MB} class
θ_{Hi} ($i = 1, 2$)	Exogenous re-infection rate for humans in the E_{Hi} class
θ_{RB}, θ_{RH}	Exogenous re-infection rate for recovered humans
θ_{EB}	Exogenous re-infection rate for buffalos in the exposed and recovered classes, respectively
δ_{H1}, δ_{H2}	Disease-induced death rate for humans
δ_B, δ_M	Disease-induced death rate for buffalos

Table 4.3: Ranges and baseline values for parameters of the BTB-MTB model (4.5.3).

Parameter	Range (day ⁻¹)	Baseline Value (day ⁻¹)	Reference
Π_H	[26,80]	53	[96]
Π_B	[2,4]	3	[79, 87, 96]
μ_H	[0.0000274,0.0000549]	0.000047	[13, 22, 34, 38]
μ_B	(0.00009477,0.00011583)	0.0001053	[26, 87]
β_H	[0.00011,0.000959]	0.000535	[13, 21]
β_B	(0.006597,0.008063)	0.00733	[27]
η_{H1}	[0,1)	0.5	Fitted
η_{H2}	[0,1)	0.5	Fitted
η_{B1}	(0.4455,0.5045)	0.45	Fitted
η_{B2}	(0.495,0.605)	0.55	Fitted
θ_{BB}	[0,1)	0.5	Fitted
θ_{MM}	[0,1]	0.5	Assumed
θ_{HH}	[0,1)	0.5	Assumed
γ_i ($i = 1, 2$)	(0.0000823,0.000823)	0.000453	[13, 22]
γ_{B1}	(0.00774,0.00946)	0.0086	[27]
γ_{M1}	(0.13374,0.160086)	0.1486	[1]
σ_i ($i = 1, 2$)	(0.0000822,0.00247)	0.001	[22, 93]
κ_1	(0.45,0.55)	0.5	[93]
κ_2	(0.45,0.55)	0.5	[93]
σ_{B2}	(0.25,0.35)	0.3	[93]
σ_{M2}	(0.36,0.44)	0.4	[93]
θ_{Hi} ($i = 1, 2$)	[0,0.1]	0.00271	[22]
θ_{RB}, θ_{RH}	[0.002439,0.002981]	0.00271	[22]
θ_{EB}	[0.002439,0.002981]	0.00271	[22]
δ_{H1}, δ_{H2}	[0.000115,0.000822]	0.0002	[13, 22, 21, 38]
δ_B	[0.0018,0.0022]	0.002	[29]
δ_M	[0.0018,0.0022]	0.002	[13, 22]

Table 4.4: Number of symptomatic buffalos with BTB at Kruger National Park [28].

Year	Number of Symptomatic Buffalos [28]
2001	35
2002	135
2003	185
2004	238
2005	230

CHAPTER 5

CONCLUSION AND FUTURE WORK

This thesis consists of two main parts that deals with two ways of considering the delay process in epidemiological models. The first approach, which constitutes the first part of the thesis, deals with the SIS model, which takes the form of a deterministic system of nonlinear differential equations with (discrete) time delay. The main motivation of this part is the need to construct a robust nonstandard finite difference scheme for this model. Despite the simplicity of the SIS model, the presence of delay is a challenge from the numerical point of view as observed in the literature [9, 35, 76]. For this reason, and given also the importance of the linearization process in the qualitative and constructive analysis of dynamical systems in general and epidemiological models in particular, we start with a linear delay differential equation (LDDE) for which we construct an innovative Exact-NSFD scheme. The second part of the thesis deals with the second way of considering delay in epidemiological models. That is by introducing one or several exposed classes. In this part, we do a thorough quantitative, qualitative and statistical analyses of two new models for bovine tuberculosis (BTB) and mycobacterium tuberculosis (MTB) in a buffalo-human population. The models which are

gradually built from basic SEIR models, extends numerous other models for the transmission dynamics of one or both diseases in the literature.

The specific contributions of the thesis are summarized below:

5.1 Contributions of the thesis

5.1.1 Nonstandard finite difference for SIS delay model

As stated earlier, one of the main contributions of the thesis is the design of a novel NSFD for solving linear delay differential equation model (which is associated with an SIS delay model for disease transmission). Some of the main findings and contributions for the linear delay differential equation are as follows:

- (i) The combined Exact-NSFD scheme is dynamically consistent with the LDDE in many respects.
 - It preserves all the properties of the solution at the earlier time evolution.
 - It has no spurious fixed-point and it replicates the asymptotic stability property of the trivial equilibrium of the continuous model. These facts are verified both theoretically (under some conditions on the coefficients of the delay differential equation) and computationally when the conditions are not satisfied.
 - The profile of the solutions for the combined Exact-NSFD scheme with delay shows oscillations in accordance with the trajectories of the continuous model, while such phenomenon is absent in the same scheme without delay. Furthermore, the better performance (convergence of order 2) of the trapezoidal NSFD scheme is observed.
 - When the delay coefficient is positive, it is shown that the NSFD scheme preserves positivity of solutions at all times irrespective of the step size value Δt , whenever the initial conditions are positive.

- (ii) The robustness of the NSFD scheme is shown in which the fixed point is asymptotically stable irrespective of the large step sizes used, while in the case of classical theta-method, the fixed point is shown to be unstable.
- (iii) The relevance of the exact scheme at the early stage of the process is seen in numerical simulations specifically when the delay is longer. On the other hand, for Euler scheme, the delay has effect on the stability of the fixed-point with regards to the smaller step sizes used. For Euler scheme with no delay, the solution profiles converge to the fixed point for these step sizes while in Euler scheme with delay, the solution profiles diverge for the same smaller step sizes.

As for the SIS model with delay, our primary goal, we design a NSFD scheme whose linearized part corresponds to the NSFD scheme obtained above. It is illustrated that this NSFD scheme preserves the complex dynamics of the continuous SIS delay model that is rigourously analyzed in an effort to put together results that are scattered in the literature [58, 59, 91, 108].

5.1.2 Mathematical modeling of BTB-MTB dynamics

A new model, which takes the forms of deterministic systems of 16-dimensional nonlinear differential equations is designed and used to gain the qualitative and quantitative insight into the transmission dynamics of BTB and MTB in a given buffalo-human population (using Kruger National Park, South Africa). The model extends numerous other models for the transmission dynamics of one or both diseases in the previous studies by, *inter alia*,

- (a) Including the dynamics of early- and advanced- exposed buffalos. Exposed buffalo classes were not considered in [1, 6, 21, 31, 67].
- (b) Allowing for BTB and MTB transmission by exposed buffalos and humans. This was not considered in [1, 6, 21, 31, 67, 105].
- (c) Including the dynamics of humans. This was not considered in [2, 31, 67, 105].

- (d) Allowing for the re-infection of exposed and recovered buffalos and humans (this was not considered in [1, 2, 6, 31, 67]).
- (e) Allowing for the transmission of both BTB and MTB in both the buffalo and human populations (this was not considered in [1, 2, 6, 21, 31, 67]).

From this part of the study, some of the main findings are:

- (i) The buffalo-only model undergoes the phenomenon of backward bifurcation. This phenomenon is caused by the exogenous reinfection of exposed and infected buffalos (this finding is consistent with the well-known presence of this phenomenon in MTB dynamics in human populations). This finding is crucial in terms of public health since its presence makes effort to effectively control the two diseases difficult.
- (ii) In the absence of re-infection of recovered and exposed buffalos, it is shown, using Lyapunov function theory and La Salle's Invariance Principle that the disease free equilibrium of the buffalo-only model is shown to be globally asymptotically stable whenever the associated reproduction number of the model is less than unity. The epidemiological implication of this result is that, in the absence of backward bifurcation, BTB can be effectively controlled in (or eliminated from) the buffalo population if the associated reproduction threshold can be brought to (and maintained at) a value less than unity.
- (iii) In the absence of the re-infection of exposed and recovered buffalos, the buffalo-only model is shown to have unique endemic equilibrium whenever its reproduction number exceeds unity. This equilibrium is shown to be globally-asymptotically stable for the special case where the disease-induced mortality in buffalos is negligible.
- (iv) Detailed uncertainty analysis, using Latin Hyper Cube Sampling, of the buffalo-only model, using a reasonable set of parameter values and ranges (relevant to BTB dynamics in the Kruger National Park), shows that the distribution of the associated reproduction number of

the buffalo-only model is less than unity (hence, BTB outbreaks will not persist in the Park). Furthermore, such outbreak would cause no more than 120 confirmed (symptomatic) cases of BTB within the Park. Sensitivity analysis, using Partial Rank Correlation Coefficient, for the case when the reproduction number is chosen as the response/output function, reveals that the three main parameters that govern the disease dynamics are the BTB transmission rate, recovery rate of buffalos and BTB-induced mortality rate. Similarly, three parameters (recruitment rate of buffalos, natural and BTB-induced death rates in buffalos) are identified as the main influential parameters for the case where the number of symptomatic buffalos (with BTB) is the chosen output function.

- (v) It is shown, rigorously, that the full BTB-MTB model has the same dynamics as the buffalo-only model with respect to the (local and global) asymptotic dynamics of the respective disease free equilibrium and the backward bifurcation property. However, unlike in the buffalo-only model, the phenomenon of backward bifurcation persists even if the bovine-associated re-infection terms are set to zero. This is due to the reinfection of exposed and recovered humans. It is shown that this model does not undergo backward bifurcation in the absence of reinfection of exposed and recovered host(s) (buffalos and humans). For this case, it is shown that the DFE of the BTB-MTB model is globally-asymptotically stable, whenever the associated reproduction number is less than unity.
- (vi) Numerical simulations of the BTB-MTB model, using MATLAB ODE45, show that an increase in the cumulative number of BTB infection leads to a marked reduction in the cumulative number of new MTB cases in humans. Similarly, an increase in the cumulative number of MTB infection leads to a significant decrease in the cumulative number of new BTB cases in buffalos.

5.2 Future work

Along the lines of this thesis, there remains number of issues and extensions that will be addressed in future work. These include:

- Investigating the dynamic consistency of the combined Exact-NSFD scheme for the SIS delay model with disease induced death rate.
- Extending the NSFD approach to more challenging delay epidemiological models.
- Designing reliable NSFD schemes for the new tuberculosis models.
- Testing the complete BTB-MTB model using data relevant to Kruger National Park and incorporating control strategies.
- Incorporating seasonality in the full BTB-MTB model to ascertain the variation and impact of the two diseases in the community.

BIBLIOGRAPHY

- [1] S. O. Adewale, C. N. Podder, and A. B. Gumel. Mathematical analysis of a TB transmission model with DOTS. *The Canadian Applied Mathematics Quarterly*, **17**(1):1–36, 2009.
- [2] F. B. Augusto, S. Lenhart, A. B. Gumel, and A. Odoi. Mathematical analysis of a model for the transmission dynamics of bovine tuberculosis. *Mathematical Methods in the Applied Sciences*, **34**(15):1873–1887, 2011.
- [3] R. M. Anderson and R. M. May. Population biology of infectious diseases. In *[Report of the Dahlem Workshop, Berlin, 14th-19th March 1982]*. Springer-Verlag, 1982.
- [4] R. M. Anderson and R. M. May. *Infectious diseases of humans*, volume 1. Oxford university press Oxford, 1991.
- [5] R. Anguelov, P. Kama, and J. M.-S. Lubuma. On non-standard finite difference models of reaction–diffusion equations. *Journal of Computational and Applied Mathematics*, **175**(1):11–29, 2005.
- [6] R. Anguelov and H. Kojouharov. Continuous age-structured model for bovine tuberculosis in african buffalo. In *1st International Conference*

On Applications Of Mathematics In Technical And Natural Sciences, volume **1186**, pages 443–450. AIP Publishing, 2009.

- [7] R. Anguelov and J. M.-S. Lubuma. Contributions to the mathematics of the nonstandard finite difference method and applications. *Numerical Methods for Partial Differential Equations*, **17**(5):518–543, 2001.
- [8] W. Y. Ayele, S. D. Neill, J. Zinsstag, M. G. Weiss, and I. Pavlik. Bovine tuberculosis: an old disease but a new threat to Africa. *The International Journal of Tuberculosis and Lung Disease*, **8**(8):924–937, 2004.
- [9] Christopher TH Baker. Retarded differential equations. *Journal of Computational and Applied Mathematics*, **125**(1):309–335, 2000.
- [10] R. E. Bellman and K. L. Cooke. *Differential-difference equations*. Rand Corporation, 1963.
- [11] E. Beretta and Y. Kuang. Geometric stability switch criteria in delay differential systems with delay dependent parameters. *SIAM Journal on Mathematical Analysis*, **33**(5):1144–1165, 2002.
- [12] A. Berman and R. J. Plemmons. *Nonnegative Matrices in the Mathematical Sciences*. SIAM, 1994.
- [13] C. P. Bhunu, W. Garira, Z. Mukandavire, and M. Zimba. Tuberculosis transmission model with chemoprophylaxis and treatment. *Bulletin of Mathematical Biology*, **70**(4):1163–1191, 2008.
- [14] W. R. Bishai, N. M. H. Graham, S. Harrington, Hooper N. Pope, D. S., J. Astemborski, L. Sheely, D. Vlahov, G. E. Glass, and R. E. Chaisson. Molecular and geographic patterns of tuberculosis transmission after 15 years of directly observed therapy. *Jama*, **280**(19):1679–1684, 1998.
- [15] S. M. Blower and H. Dowlatabadi. Sensitivity and uncertainty analysis of complex models of disease transmission: an HIV model, as an example. *International Statistical Review/Revue Internationale de Statistique*, pages 229–243, 1994.

- [16] F. Brauer. Backward bifurcations in simple vaccination models. *Journal of Mathematical Analysis and Applications*, **298**(2):418–431, 2004.
- [17] F. Brauer and C. Castillo-Chavez. *Mathematical models in population biology and epidemiology*, volume 1. Springer, 2001.
- [18] F. Brauer and C. Castillo-Chavez. *Mathematical models in population biology and epidemiology*. Springer, 2011.
- [19] S. Campbell, R. Edwards, and P. van den Driessche. Delayed coupling between two neural network loops. *SIAM Journal of Applied Mathematics*, **65**(1):316–335, 2004.
- [20] C. Castillo-Chavez and Z. Feng. To treat or not to treat: the case of tuberculosis. *Journal of Mathematical Biology*, **35**(6):629–656, 1997.
- [21] C. Castillo-Chavez and B. Song. Dynamical models of tuberculosis and their applications. *Mathematical Biosciences and Engineering: MBE*, (1):361–404, 2004.
- [22] T. Cohen, C. Colijn, B. Finklea, and M. Murray. Exogenous re-infection and the dynamics of tuberculosis epidemics: local effects in a network model of transmission. *Journal of The Royal Society Interface*, **4**(14):523–531, 2007.
- [23] K. Cooke, P. van den Driessche, and X. Zou. Interaction of maturation delay and nonlinear birth in population and epidemic models. *Journal of Mathematical Biology*, **39**(4):332–352, 1999.
- [24] K. L. Cooke and P. van den Driessche. On zeroes of some transcendental equations. *Funkcialaj Ekvacioj*, **29**(1):77–90, 1986.
- [25] K. L. Cooke and J. A. Yorke. Some equations modelling growth processes and gonorrhea epidemics. *Mathematical Biosciences*, **16**(1):75–101, 1973.



- [26] H.P. Cronje, B.K. Reilly, and I.D. MacFadyen. Natural mortality among four common ungulate species on Letaba ranch, Limpopo province, South Africa. *Koedoe*, **45**(1):79–86, 2002.
- [27] P. C. Cross and W. M. Getz. Assessing vaccination as a control strategy in an ongoing epidemic: Bovine tuberculosis in African buffalo. *Ecological Modelling*, **196**(3):494–504, 2006.
- [28] P. C. Cross, Heisey, D. M., J. A. Bowers, C. T. Hay, J. Wolhuter, P. Buss, M. Hofmeyr, A. L. Michel, R. G. Bengis, and T. L. F. Bird. Disease, predation and demography: assessing the impacts of bovine tuberculosis on African buffalo by monitoring at individual and population levels. *Journal of Applied Ecology*, **46**(2):467–475, 2009.
- [29] P. C. Cross, J. O. Lloyd-Smith, J. A. Bowers, C. T. Hay, M. Hofmeyr, and W. M. Getz. Integrating association data and disease dynamics in a social ungulate: bovine tuberculosis in African buffalo in the Kruger National Park. In *Annales Zoologici Fennici*, pages 879–892. JSTOR, 2004.
- [30] G. W. de Lisle, C. G. Mackintosh, and R. G. Bengis. Mycobacterium bovis in free-living and captive wildlife, including farmed deer. *Revue scientifique et technique (International Office of Epizootics)*, **20**(1):86–111, 2001.
- [31] V. De Vos, R. G. Bengis, N. P. J. Kriek, A. L. Michel, D. F. Keet, J. P. Raath, and H.F.A.K. Huchzermeyer. The epidemiology of tuberculosis in free-ranging African buffalo (*Syncerus caffer*) in the Kruger National Park, South Africa. 2001.
- [32] O. Diekmann, J. A. P. Heesterbeek, and J. A. J. Metz. On the definition and the computation of the basic reproduction ratio R_0 in models for infectious diseases in heterogeneous populations. *Journal of Mathematical Biology*, **28**(4):365–382, 1990.

- [33] J. Dushoff, W. Huang, and C. Castillo-Chavez. Backwards bifurcations and catastrophe in simple models of fatal diseases. *Journal of Mathematical Biology*, **36**(3):227–248, 1998.
- [34] C. Dye and B. G. Williams. Eliminating human tuberculosis in the twenty-first century. *Journal of the Royal Society Interface*, **5**(23):653–662, 2008.
- [35] K. Engelborghs, T. Luzyanina, and D. Roose. Numerical bifurcation analysis of delay differential equations. *Journal of Computational and Applied Mathematics*, **125**(1):265–275, 2000.
- [36] E. Etter, P. Donado, F. Jori, A. Caron, F. Goutard, and F. Roger. Risk analysis and bovine tuberculosis, a re-emerging zoonosis. *Annals of the New York Academy of Sciences*, **1081**(1):61–73, 2006.
- [37] G. Fan, J. Liu, P. van den Driessche, J. Wu, and H. Zhu. The impact of maturation delay of mosquitoes on the transmission of West Nile virus. *Mathematical Biosciences*, **228**(2):119–126, 2010.
- [38] Z. Feng, C. Castillo-Chavez, and A. F. Capurro. A model for tuberculosis with exogenous reinfection. *Theoretical Population Biology*, **57**(3):235–247, 2000.
- [39] Centers for Disease Control. *Mycobacterium bovis* (Bovine Tuberculosis) in Humans. <http://www.cdc.gov/tb/publications/factsheets/general/mbovis.pdf>, 2014. [Online; accessed March 2014].
- [40] The Centre for Food Security and Iowa State University Public Health. Bovine Tuberculosis. http://www.cfsph.iastate.edu/Factsheets/pdfs/bovine_tuberculosis.pdf, 2014. [Online; accessed April 2014].
- [41] G. Frye. Bovine tuberculosis eradication. In C. O. Thoen and J. H. Steele, editors, *Mycobacterium bovis Infection in Animals and Humans*. Iowa State University Press, 1994.

- [42] S. M. Garba, A. B. Gumel, and M.R. A. Bakar. Backward bifurcations in dengue transmission dynamics. *Mathematical Biosciences*, **215**(1):11–25, 2008.
- [43] S. M. Garba, A. B. Gumel, and J. M.-S. Lubuma. Dynamically-consistent non-standard finite difference method for an epidemic model. *Mathematical and Computer Modelling*, **53**(1):131–150, 2011.
- [44] S. M. Garba, A.B. Gumel, A.S. Hassan, and J. M.-S. Lubuma. Switching from exact scheme to nonstandard finite difference scheme for linear delay differential equation. *Applied Mathematics and Computation*, **258**:388–403, 2015.
- [45] J. M. Grange and C. H. Collins. Bovine tubercle bacilli and disease in animals and man. *Epidemiology and Infection*, **99**(02):221–234, 1987.
- [46] D. Greenhalgh. Some results for an SEIR epidemic model with density dependence in the death rate. *Mathematical Medicine and Biology*, **9**(2):67–106, 1992.
- [47] D. Greenhalgh. Hopf bifurcation in epidemic models with a latent period and nonpermanent immunity. *Mathematical and Computer Modelling*, **25**(2):85–107, 1997.
- [48] T. H. Gronwall. Note on the derivatives with respect to a parameter of the solutions of a system of differential equations. *Annals of Mathematics*, pages 292–296, 1919.
- [49] A. B. Gumel, K. C. Patidar, and R. J. Spiteri. Asymptotically consistent nonstandard finite difference methods for solving mathematical models arising in population biology. In R. E. Mickens, editor, *Advances in the Applications of Nonstandard Finite Difference Schemes*, pages 385–421. World Scientific, Singapore, 2005.
- [50] A.B. Gumel. Causes of backward bifurcations in some epidemiological models. *Journal of Mathematical Analysis and Applications*, **395**(1):355–365, 2012.

- [51] J. K. Hale. *Introduction to functional differential equations*, volume 99. Springer Science & Business Media, 1993.
- [52] A. S. Hassan, S. M. Garba, A. B. Gumel, and J. M.-S. Lubuma. Dynamics of mycobacterium and bovine tuberculosis in a human-buffalo population. *Computational and Mathematical Methods in Medicine*, **2014**, 2014.
- [53] J. A. P. Heesterbeek. *Mathematical epidemiology of infectious diseases: model building, analysis and interpretation*, volume 5. John Wiley & Sons, 2000.
- [54] H. W. Hethcote. Qualitative analyses of communicable disease models. *Mathematical Biosciences*, **28**(3):335–356, 1976.
- [55] H. W. Hethcote. The mathematics of infectious diseases. *SIAM review*, **42**(4):599–653, 2000.
- [56] H. W. Hethcote. The basic epidemiology models: Models, expressions for R_0 , parameter estimation, and applications. *Mathematical Understanding of Infectious Disease Dynamics*, **16**:1–61, 2009.
- [57] H. W. Hethcote, H. W. Stech, and P. Van Den Driessche. Nonlinear oscillations in epidemic models. *SIAM Journal on Applied Mathematics*, **40**(1):1–9, 1981.
- [58] H. W. Hethcote, H. W. Stech, and P. van den Driessche. Periodicity and stability in epidemic models: a survey. *Differential Equations and Applications in Ecology, Epidemics and Population Problems (SN Busenberg and KL Cooke, eds.)*, pages 65–82, 1981.
- [59] H. W. Hethcote and P. van den Driessche. An SIS epidemic model with variable population size and a delay. *Journal of Mathematical Biology*, **34**(2):177–194, 1995.
- [60] H. W. Hethcote and P. van den Driessche. Two SIS epidemiologic models with delays. *Journal of Mathematical Biology*, **40**(1):3–26, 2000.

- [61] G. Huang and Y. Takeuchi. Global analysis on delay epidemiological dynamic models with nonlinear incidence. *Journal of Mathematical Biology*, **63**(1):125–139, 2011.
- [62] R. L. Iman and W. J. Conover. Small sample sensitivity analysis techniques for computer models. with an application to risk assessment. *Communications in Statistics-theory and Methods*, **9**(17):1749–1842, 1980.
- [63] R. L. Iman and J. C. Helton. An investigation of uncertainty and sensitivity analysis techniques for computer models. *Risk analysis*, **8**(1):71–90, 1988.
- [64] R. L. Inman, J. C. Helson, and J. E. Campbell. An approach to sensitivity analysis of computer models: Part ii-ranking of input variables, response surface validation, distribution effect and technique synopsis. *Journal of Quality Technology*, **13**(4), 1981.
- [65] E. I. Jury. *Theory and Application of the z-Transform Method*, volume 3. Wiley New York, 1964.
- [66] P. Kama. *Non-standard finite difference methods in dynamical systems*. PhD thesis, University of Pretoria, 2009.
- [67] R. R. Kao, M. G. Roberts, and T. J. Ryan. A model of bovine tuberculosis control in domesticated cattle herds. *Proceedings of the Royal Society of London. Series B: Biological Sciences*, **264**(1384):1069–1076, 1997.
- [68] W. O. Kermack and A. G. McKendrick. A contribution to the mathematical theory of epidemics. In *Proceedings of the Royal Society of London A: Mathematical, Physical and Engineering Sciences*, volume **115**, pages 700–721. The Royal Society, 1927.
- [69] Q. J. A. Khan and D. Greenhalgh. Hopf bifurcation in epidemic models with a time delay in vaccination. *Mathematical Medicine and Biology*, **16**(2):113–142, 1999.

- [70] J. P. La Salle. The stability of dynamical systems. 1976.
- [71] V. Lakshmikantham, S. Leela, and A. A. Martynyuk. *Stability analysis of nonlinear systems*. Marcel Dekker, Inc., NewYork and Basel, 1989.
- [72] G. Lay, Y. Poquet, P. Salek-Peyron, M.-P. Puissegur, C. Botanch, H. Bon, F. Levillain, J.-L. Duteyrat, J.-F. Emile, and F. Altare. Langhans giant cells from m. tuberculosis-induced human granulomas cannot mediate mycobacterial uptake. *The Journal of pathology*, **211**(1):76–85, 2007.
- [73] J. M.-S. Lubuma, E. W. Mureithi, and Y. A. Terefe. Nonstandard discretizations of the SIS epidemiological model with and without diffusion. *Second Order Elliptic Equations and Elliptic Systems: Contemporary Mathematics*, **618**:113, 2014.
- [74] J. M.-S. Lubuma and A. Roux. An improved theta-method for systems of ordinary differential equations. *The Journal of Difference Equations and Applications*, **9**(11):1023–1035, 2003.
- [75] T. Luzyanina and D. Roose. Numerical stability analysis and computation of hopf bifurcation points for delay differential equations. *Journal of Computational and Applied Mathematics*, **72**(2):379–392, 1996.
- [76] Tatyana Luzyanina and Dirk Roose. Numerical stability analysis and computation of hopf bifurcation points for delay differential equations. *Journal of Computational and Applied Mathematics*, **72**(2):379–392, 1996.
- [77] M. Martcheva and O. Prosper. Unstable dynamics of vector-borne diseases: Modeling through delay-differential equations. In *Dynamic Models of Infectious Diseases*, pages 43–75. Springer, 2013.
- [78] R. G. McLeod, J. F. Brewster, A. B. Gumel, and A. Slonowsky. Sensitivity and uncertainty analyses for a SARS model with time-varying inputs and outputs. *Mathematical Biosciences and Engineering*, **3**(3):527, 2006.

- [79] A. L. Michel, R. G. Bengis, D. F. Keet, M. Hofmeyr, L. M. De Klerk, P. C. Cross, A. E. Jolles, D. Cooper, I. J. Whyte, and P. Buss. Wildlife tuberculosis in South African conservation areas: implications and challenges. *Veterinary Microbiology*, **112**(2):91–100, 2006.
- [80] R. E. Mickens. *Nonstandard finite difference models of differential equations*. World Scientific, 1994.
- [81] R. E. Mickens. *Advances in the Applications of Nonstandard Finite Difference Schemes*. World Scientific, 2005.
- [82] R. E. Mickens. Calculation of denominator functions for nonstandard finite difference schemes for differential equations satisfying a positivity condition. *Numerical Methods for Partial Differential Equations*, **23**(3):672–691, 2007.
- [83] J. D. Murray. *Mathematical Biology I: An Introduction*, vol. 17 of *Interdisciplinary Applied Mathematics*. Springer, New York, NY, USA,, 2002.
- [84] J. D. Murray. Mathematical biology i: An introduction, vol. 17 of interdisciplinary applied mathematics, 2002.
- [85] K. E. Nelson and C. F. Williams. Early history of infectious disease. In S. Ma and Y. Xia, editors, *Early history of infectious disease: epidemiology and control of infectious diseases.*, volume Ed. 2, pages 3–23. Jones and Bartlett Publishers, 2007.
- [86] G. A. Ngwa, A. M. Niger, and A. B. Gumel. Mathematical assessment of the role of non-linear birth and maturation delay in the population dynamics of the malaria vector. *Applied Mathematics and Computation*, **217**(7):3286–3313, 2010.
- [87] W. C. Oosthuizen. *Chemical immobilization of African buffalo (Syncerus caffer) in Kruger National Park: evaluating effects on survival and reproduction*. PhD thesis, University of Pretoria, 2006.

- [88] World Health Organization. The global hiv/aids epidemic. <https://www.aids.gov/hiv-aids-basics/hiv-aids-101/global-statistics/>, 2015. [Online; accessed June 2015].
- [89] Kruger National Park. Herd of Cape Buffalo. http://www.krugerpark.co.za/africa_african_buffalo.html, 2014. [Online; accessed April 2014].
- [90] K. C. Patidar. On the use of nonstandard finite difference methods. *Journal of Difference Equations and Applications*, **11**(8):735–758, 2005.
- [91] C. Paulhus and X.-S. Wang. Global stability analysis of a delayed susceptible–infected–susceptible epidemic model. *Journal of Biological Dynamics*, (ahead-of-print):1–6, 2014.
- [92] A. Quarteroni, R. Sacco, and F. Saleri. *Numerical mathematics*, volume 37. Springer Science & Business Media, 2010.
- [93] S. C. Resch, J. A. Salomon, M. Murray, and M. C. Weinstein. Cost-effectiveness of treating multidrug-resistant tuberculosis. *PLoS Medicine*, **3**(7):e241, 2006.
- [94] G. Rosen. *A history of public health*. Johns Hopkins University Press, 2015.
- [95] M. A. Safi. *Mathematical Analysis of The Role of Quarantine and Isolation in Epidemiology*. PhD thesis, University of Manitoba, 2010.
- [96] South African National Parks (SANParks). Annual Report 2012. <http://www.sanparks.co.za/assets/docs/general/annual-report-2012.pdf>, 2012. [Online; accessed March 2014].
- [97] O. Sharomi and A.B. Gumel. Re-infection-induced backward bifurcation in the transmission dynamics of Chlamydia trachomatis. *Journal of Mathematical Analysis and Applications*, **356**(1):96–118, 2009.
- [98] O. Sharomi, C. Podder, A. B. Gumel, and B. Song. Mathematical analysis of the transmission dynamics of HIV/TB coinfection in the

- presence of treatment. *Mathematical Biosciences and Engineering*, **5**(1):145, 2008.
- [99] H. L. Smith. *The theory of the chemostat: dynamics of microbial competition*, volume 13. Cambridge university press, 1995.
- [100] H. L. Smith. Monotone dynamical systems. an introduction to the theory of competitive and cooperative systems. *American Mathematical Society, Providence, Rhode Island*, 1996.
- [101] X.u Song, S. Wang, and J. Dong. Stability properties and hopf bifurcation of a delayed viral infection model with lytic immune response. *Journal of Mathematical Analysis and Applications*, **373**(2):345–355, 2011.
- [102] A. Stuart and A. R. Humphries. *Dynamical systems and numerical analysis*. Cambridge University Press, 1998.
- [103] Y. A. Terefe. Bifurcation analysis and nonstandard finite difference schemes for Kermack and McKendrick type epidemiological models. Master’s thesis, University of Pretoria, 2012.
- [104] P. van den Driessche. Some epidemiological models with delays. In *Differential Equations and Applications to Biology and Industry*, pages 507–520. World Scientific, 1996.
- [105] P. van den Driessche, L. Wang, and X. Zou. Modeling diseases with latency and relapse. *Mathematical Biosciences and Engineering*, **4**(2):205, 2007.
- [106] P. van den Driessche and J. Watmough. A simple SIS epidemic model with a backward bifurcation. *Journal of Mathematical Biology*, **40**(6):525–540, 2000.
- [107] P. van den Driessche and J. Watmough. Reproduction numbers and sub-threshold endemic equilibria for compartmental models of disease transmission. *Mathematical Biosciences*, **180**(1):29–48, 2002.

- [108] C. Vargas-De-León. Stability analysis of a SIS epidemic model with standard incidence. *Foro RED-Mat*, **28**, 2011.
- [109] B. Vielle and G. Chauvet. Delay equation analysis of human respiratory stability. *Mathematical Biosciences*, **152**(2):105–122, 1998.
- [110] M. Villasana and A. Radunskaya. A delay differential equation model for tumor growth. *Journal of Mathematical Biology*, **47**(3):270–294, 2003.
- [111] J. G. Villavicencio-Pulido, I. Barradas, and J. C. Hernández-Gómez. A basic backward bifurcation model in epidemiology. *Applied Mathematical Sciences*, **7**(107):5327–5340, 2013.
- [112] V. Volterra. Sur la théorie mathématique des phénomènes héréditaires. *Journal de Mathématiques pures et Appliquées*, pages 249–298, 1928.
- [113] W. Wang and S. Ruan. Bifurcations in an epidemic model with constant removal rate of the infectives. *Journal of Mathematical Analysis and Applications*, **291**(2):775–793, 2004.
- [114] Z. Wang and R. Xu. Stability and hopf bifurcation in a viral infection model with nonlinear incidence rate and delayed immune response. *Communications in Nonlinear Science and Numerical Simulation*, **17**(2):964–978, 2012.
- [115] WHO. Global Tuberculosis Report 2013. http://www.who.int/tb/publications/global_report/en/, 2014. [Online; accessed March 2014].
- [116] S. Wiggins. *Introduction to applied nonlinear dynamical systems and chaos*, volume 2. Springer Science & Business Media, 2003.
- [117] E. Zeidler. *Applied functional analysis*, volume 108. Springer, 1995.
- [118] T. Zhao. Global periodic-solutions for a differential delay system modeling a microbial population in the chemostat. *Journal of Mathematical Analysis and Applications*, **193**(1):329–352, 1995.

- [119] J. Zhou and H. W. Hethcote. Population size dependent incidence in models for diseases without immunity. *Journal of Mathematical Biology*, **32**(8):809–834, 1994.